TECHNISCHE UNIVERSITÄT MÜNCHEN
Lehrstuhl für Bauchemie

Wirkmechanismus verschiedener Celluloseether als Wasserretentionsmittel in der Tiefbohrzementierung und in Trockenmörtelsystemen

Daniel Bülichen

Vollständiger Abdruck der von der Fakultät für Chemie der Technischen Universität München zur Erlangung des akademischen Grades eines

Doktors der Naturwissenschaften (Dr. rer. nat.)

genehmigten Dissertation.

Vorsitzender:	Univ.-Prof. Dr. Michael Schuster
Prüfer der Dissertation:	1. Univ.-Prof. Dr. Johann P. Plank 2. Univ.-Prof. Dr. Cordt Zollfrank

Die Dissertation wurde am 02.01.2013 bei der Technischen Universität München eingereicht und durch die Fakultät für Chemie am 14.02.2013 angenommen.

„Nichts kann geduldige Ausdauer ersetzen. Das Talent
nicht: es gibt zahllose erfolglose Menschen mit Talent.
Das Genie nicht: verkannte Genies sind fast sprichwörtlich.
Bildung nicht: die Welt wimmelt von gescheiterten Gebildeten.
Beharrlichkeit und Entschlossenheit sind beinahe allmächtig.“

CALVIN COOLIDGE, 1872-1933

Amerikanischer Politiker, 30. Präsident der USA

Die vorliegende Arbeit entstand in der Zeit von September 2009 bis Januar 2013 unter Anleitung von **Herrn Prof. Dr. Johann Plank** am Lehrstuhl für Bauchemie der Technischen Universität München.

Besonderer Dank gilt meinem geschätzten akademischen Lehrer

Herrn Prof. Dr. Johann Plank

für die anspruchsvolle und interessante Themenstellung, die hervorragende Unterstützung und Zusammenarbeit während der gesamten Promotionszeit, die wissenschaftlichen Diskussionen und das Interesse am Gelingen dieser Arbeit.

Danksagung

Unschätzbar wertvoll für das Gelingen dieser Arbeit waren meine „Ölfeld-Freunde“ Constantin Tiemeyer, Oyewole Taye Salami und Timon Echt. Es hat riesigen Spaß gemacht, mit diesen hochmotivierten, engagierten jungen Forschern und Kollegen zu arbeiten. Auch einige Diskussionen über die aktuellsten Fußballergebnisse werden mir sicher in Erinnerung bleiben. Ich wünsche Euch allen beruflich wie privat viel Erfolg und Glück in der Zukunft!

Ebenso danke ich meinen Vorgängern Dr. Nils Recalde Lummer und Dr. Fatima Dugonjić-Bilić. Durch die beiden habe ich das interessante Forschungsgebiet entdeckt und konnte zu Beginn viel von ihrem Wissen profitieren. Ihr wart eine sehr große Hilfe und habt mir vorgelebt, wie man sich als Doktorand durch den wissenschaftlichen Alltag kämpft.

Ein besonderer Dank geht an Richard Beiderbeck und Dagmar Lettrich für die Übernahme wichtiger Messungen sowie an Daniela Michler und Tim Dannemann im Sekretariat. Spezieller Dank zudem an Tom Pavlitschek für seine Hilfe bei Soft- und Hardwareproblemen sowie an Dr. Oksana Storcheva und Dr. Roland Sieber für zahlreiche Diskussionen und ihre Hilfe bei verschiedenen Fragestellungen. Aber auch allen anderen Kollegeninnen und Kollegen des Lehrstuhls (Stefan Baueregger, Dr. Hang Bian, Xiao Xiao Du, Dr. Elina Dubina, Michael Glanzer-Heinrich, Dr. Markus Gretz, Dr. Mirko Gruber, Yu Jin, Dr. Ahmad Habbaba, Friedrich von Hoessle, Dr. Helena Keller, Somruedee Klaithong, Tobias Kornprobst, Alex Lange, Lei Lei, Matthias Lesti, Markus Meier, Maike Müller, Dr. Vera Nilles, Dr. Geok Bee Serina Ng, Julia Pickelmann, Johanna de Reese, Dr. Christof Schröfl, Dr. Birgit Wienecke, Bin Yang, Fan Yang, Nan Zou, Dr. Nadia Zouaoui) danke ich für die herzliche, kollegiale und konstruktive Atmosphäre.

Meinen Praktikantinnen/Praktikanten Nadine Feichtmeier, Alex Kronast, Franziska Mandl und dem Bachelorstudenten Johannes Kainz möchte ich für ihr Interesse und Engagement während ihrer Mitarbeit danken.

Bei den Firmen Dyckerhoff AG, SE Tylose GmbH, Hasit Trockenmörtel GmbH und BASF SE bedanke ich mich für die Bereitstellung von Bindemitteln und Chemikalien.

Außerdem möchte ich meinen Eltern Bernhard und Renate sowie meinem Bruder Sascha danken, die mich immer bestmöglich bei der Erreichung meiner Ziele unterstützt haben. Besonders bedanke ich mich zuletzt bei meiner Partnerin Andrea Schöttner, die immer für mich da war und mich stets motiviert hat.

Abkürzungen

AFS	Aceton-Formaldehyd-Sulfit
AHPS	Allyloxy-2-hydroxypropansulfonsäure
AMPS®	2-Acrylamido-2-methylpropansulfonsäure
API	American Petroleum Institute
CMHEC	Carboxymethylhydroxyethylcellulose
DS	degree of substitution
ESEM	environmental scanning electron microscope
FLA	Fluid Loss Additiv
GPC	Gelpermeationschromatographie
HEC	Hydroxyethylcellulose
MC	Methylcellulose
MFS	Melamin-Formaldehyd-Sulfit
MHEC	Methylhydroxyethylcellulose
MHPC	Methylhydroxypropylcellulose
MS	molar degree of substitution
M_w	gewichtsmittlere Molmasse
NMR	nuclear magnetic resonance (Kernspinresonanz)
NNDMA	N,N-Dimethylacrylamid
NSF	β-Naphthalinsulfonsäure-Formaldehyd
PEI	Polyethylenimin
PVA	Polyvinylalkohol
RFA	Röntgenfluoreszenzanalyse
w/z-Wert	Wasser-zu-Zement-Wert
WRM	Wasserretentionsmittel
XRD	x-ray diffraction (Röntgenpulverdiffraktometrie)

Publikationen

Diese Arbeit beinhaltet folgende Publikationen:

[1] D. Bülichen, J. Plank

"Role of Colloidal Polymer Associates for the Effectiveness of Hydroxyethyl Cellulose as a Fluid Loss Control Additive in Oil Well Cement"

Journal of Applied Polymer Science (2012), Volume 126 (S1), Special Issue: Polysaccharides, p. E25

[2] D. Bülichen, J. Plank

"*Mechanistic Study on Carboxymethyl Hydroxyethyl Cellulose as Fluid Loss Control Additive in Oil Well Cement"*

Journal of Applied Polymer Science (2012), Volume 124 (3), p. 2340

[3] D. Bülichen, J. Kainz, J. Plank

"Working Mechanism of Methyl Hydroxyethyl Cellulose (MHEC) as Water Retention Agent"

Cement and Concrete Research (2012), Volume 42 (7), p. 953

[4] D. Bülichen, J. Plank

"Water Retention Capacity and Working Mechanism of Methyl Hydroxypropyl Cellulose (MHPC) in Gypsum Plaster – Which Impact has Sulfate?"

Cement and Concrete Research, accepted on 29th of January 2013

Des Weiteren wurden nachfolgende Tagungsbeiträge veröffentlicht / eingereicht:

[1] J. Plank, C. Tiemeyer, D. Bülichen, N. Recalde Lummer

"*A Review of Synergistic and Antagonistic Effects Between Oilwell Cement Additives"*

SPE - International Symposium on Oilfield Chemistry, The Woodlands, TX/USA; SPE paper 164103 (2013), accepted on 5th of October 2012

[2] C. Tiemeyer, D. Bülichen, J. Plank

"*CO_2-Beständigkeit von Zementsystemen unter den Bedingungen einer geologischen Endlagerung von CO_2 (CCS-Technologie)"*

18. Ibausil, Bauhaus-Universität Weimar, Tagungsbericht Band 2 (2012), p.419

[3] D. Bülichen, J. Plank

"*Formation Of Colloidal Polymer Associates From Hydroxyethyl Cellulose (HEC) And Their Role To Achieve Fluid Loss Control In Oil Well Cement"*

SPE - International Symposium on Oilfield Chemistry, The Woodlands, TX/USA; SPE paper 141182 (2011)

[4] J. Plank, D. Bülichen, C. Tiemeyer

"*Der Unfall auf der Ölbohrung von BP - Welche Rolle spielte die Zementierung"*

GDCh Monographie Band 42 (2010), p. 59

[5] N. Recalde Lummer, F. Dugonjić-Bilić, D. Bülichen, J. Plank

"Wichtige Zusatzmittel für die Tiefbohrzementierung"

GDCh Monographie Band 41 (2009), p. 181

Inhaltsverzeichnis

1 Einleitung und Aufgabenstellung

1.1 Einleitung

Cellulosederivate (sog. Celluloseether) sind seit Mitte des 20. Jahrhunderts ein fester Bestandteil der bauchemischen Industrie und werden zudem bei Ölbohrungen (in Bohrspülungen und bei Zementierungen) eingesetzt [1-3]. In zwei Voruntersuchungen am Lehrstuhl konnten bereits erste Eindrücke zum Wirkmechanismus dieser faszinierenden Additive gewonnen werden [4, 5]. Aufbauend auf diesen Voruntersuchungen zu den Eigenschaften und Effekten dieser Hochleistungsadditive beschäftigt sich die hier vorliegende Arbeit intensiv mit den Wirkmechanismen der Wasserrückhaltung (auch als Wasserretention bezeichnet) in zementären Systemen (Tiefbohrzementierung, Putze, Fliesenkleber, etc.) und Gips-gebundenen Baustoffen (Leichtgipsputz).

Celluloseether sind ungiftig, meist wasserlöslich und weiß bis gelblich gefärbte Pulver oder Granulate [6]. Eine erste Beschreibung der Herstellung findet sich im Jahr 1905 bei *Suida* [7]. Des Weiteren gehören die Patente von *Lilienfeld*, *Leuchs* und *Dreyfus* [8-10] über die Herstellung von nicht-ionischen Alkylethern zu den Pionierarbeiten. Die stark anionische Carboxymethylcellulose wurde 1918 von *Jansen* dargestellt, Hydroxyethylcellulose war erstmals 1920 Bestandteil eines Patents von *Hubert* [11, 12]. Basierend auf dieser Grundlage begann die Produktion von Celluloseethern in Deutschland bereits in den frühen 1920er Jahren, gefolgt von den USA 1937 / 38. Eine Liste der verschiedenen, heute üblicherweise im Baubereich und in Tiefbohrungen eingesetzten Produkte mit den dazugehörigen Abkürzungen ist in **Tabelle 1** gezeigt [13].

Tabelle 1 – Großtechnisch produzierte und häufig eingesetzte Celluloseether [13].

Celluloseether	Kurzbezeichnung
Methylcellulose	MC
Methylhydroxyethylcellulose	MHEC
Methylhydroxypropylcellulose	MHPC
Hydroxyethylcellulose	HEC
Hydroxypropylcellulose	HPC
Carboxymethylcellulose	CMC
Carboxymethylhydroxyethylcellulose	CMHEC
Ethylcellulose	EC
Ethylhydroxyethylcellulose	EHEC

Nach ihrer weltweiten wirtschaftlichen Bedeutung geordnet steht die Carboxymethylcellulose mit ~ 230.000 t / Jahr an erster Stelle, gefolgt von Methyl- beziehungsweise Hydroxyalkylcellulosen (~ 120.000 t / Jahr). Weiter schließen sich in geringerer Menge Hydroxyethylcellulose (~ 60.000 t / Jahr) sowie Hydroxypropylcellulose (< 10.000 t / Jahr) an [6].

Im Allgemeinen werden Celluloseether in der modernen Baustoffindustrie eingesetzt, um Wasserretention zu gewährleisten und die Viskosität eines Systems zu optimieren [14]. Ebenso erfordern Ölbohrungen aufgrund der herrschenden extremen Bedingungen (Temperaturen bis 250 °C, Drücke bis 150 MPa und Wegstrecken über 20 km) den Zusatz sogenannter Fluid Loss Additive (FLAs), wie Wasserretentionsmittel dort branchenüblich bezeichnet werden [15]. Die Hauptfunktion der hochwirksamen Celluloseether liegt bei allen Anwendungen darin, einen unkontrollierten Wasserverlust des Bindemittelsystems an poröse Materialien wie Ziegel, Kalkstein, Luftporenbeton, Gipskartonplatten (Bauanwendungen) beziehungsweise an hochpermeable Gesteinsformationen (Tiefbohrungen) zu verhindern oder zu minimieren. Ein Nebeneffekt dieser polymeren Additive ist die stark verzögernde Wirkung auf die Hydratation des Zements. In einigen Anwendungen kann dies von Vorteil sein, sie führt allerdings bei höheren Dosierungen auch zu unerwünscht langen Abbindezeiten [16, 17].

Der frühe Einsatz von Celluloseethern in der Tiefbohrtechnologie hat diese revolutioniert. Erst damit wurde es möglich, Bohrlöcher in größerer Tiefe erfolgreich herzustellen und gegen äußere Einflüsse abzusichern. Besonders zu erwähnen ist, dass die wasserrückhaltenden Eigenschaften anfänglich nur von der Ölfeldbranche beobachtet und ausgenutzt wurden. 1948 wurde Carboxymethylcellulose erstmals einer wasserbasierten, Bentonit-haltigen Bohrflüssigkeit („Spülung“) zugegeben. Die Spülung, welche beim Bohren zirkuliert, dient dazu den Bohrmeißel zu kühlen und das entstehende Bohrklein (sog. „cuttings“) aus dem Bohrloch zu transportieren [15]. Durch die mit Celluloseethern möglich gewordene Filtratkontrolle konnten wesentlich längere Bohrstrecken am Stück abgeteuft werden. Zehn Jahre später (1958) wurden Hydroxyethylcellulose und Carboxymethylhydroxyethylcellulose erstmals auch in der Tiefbohrzementierung verwendet und sind dort heute noch in Gebrauch [13, 18, 19].

Die weitaus größeren Mengen an Celluloseether werden allerdings außerhalb von Tiefbohrungen ein- und umgesetzt. In der Trockenmörtelindustrie (sog. „dry-mix mortars“) waren 2010 nahezu ausschließlich Methylhydroxyethyl- und Methylhydroxypropylcellulosen

als Wasserretentionsmittel in Verwendung und wiesen einen Marktanteil von ~ 90 % auf. Umgangssprachlich werden beide Additive auch heute noch als „Methylcellulose“ (MC) bezeichnet, obwohl dieses Produkt in Reinform kaum noch Verwendung findet [20]. Weitere wichtige Einsatzgebiete von Celluloseethern sind Maschinenputze, Spachtelmassen, Fliesenkleber, Fließestriche und Selbstverlaufsmassen. Die zugesetzten Dosierungen bewegen sich typischerweise zwischen 0,02 und 1,0 %, bezogen auf die verwendete Bindemittelmenge [1, 21]. Aufgrund ihres günstigen Preis-Leistungsverhältnisses und ihrer Umweltverträglichkeit sind Celluloseether im Bausektor unangefochten marktführend [22].

1.2 Aufgabenstellung und Motivation

Ziel dieser Arbeit war es zunächst, die Wirkmechanismen der gängigsten Celluloseether im Bereich der Tiefbohrzementierung (HEC, CMHEC) zu untersuchen. Trotz einiger Voruntersuchung (siehe Kapitel 2.3.3) zu den Mechanismen der Wasserretention war bisher nicht eindeutig geklärt beziehungsweise kontrovers diskutiert worden, wie Celluloseether als Wasserretentionsmittel wirken. In diesen Studien sollte daher herausgefunden werden, wie diese Additive funktionieren, um ein besseres Verständnis für die Optimierung der Polymere (z.B. eine Wirksamkeit auch bei höheren Temperaturen durch chemische Modifizierung) oder für die Wechselwirkung mit anderen Additiven zu entwickeln.

Hierfür wurde eine Voruntersuchung zu HEC im Rahmen der eigenen Masterarbeit [5] weitergeführt sowie die Erkenntnisse anschließend mit einem stark anionischen Celluloseether (CMHEC) verglichen und Unterschiede herausgearbeitet. Da es sich bei beiden Derivaten um ein nicht-ionisches (HEC) und ein anionisches (CMHEC) Polymer handelte wurde erwartet, dass sich die Mechanismen deutlich unterscheiden. Methodisch wurde bei beiden Polymeren zunächst das Wasserrückhaltevermögen der Celluloseether mit Hilfe spezieller Hochdruck (70 bar)-Stahlzellen bestimmt. Dabei findet eine Druckfiltration statt, welche die Vorgänge in einer realen Zementschlämme im Bohrloch nachstellt. Anschließend wurden die verschiedenen, theoretisch denkbaren Wirkmechanismen analytisch überprüft. Hierfür konnten die charakteristischen Eigenschaften der untersuchten Proben sowie ihr Verhalten in Zementporenlösung – eine durch Filtration der Zementschlämme gewonnene alkalische Salzlösung – ermittelt werden.

Des Weiteren sollte der Einfluss anderer gängiger Additive (hier: Fließmittel) auf das Verhalten und den Mechanismus der Celluloseether betrachtet werden. Aus anderen Arbeiten des

Lehrstuhls war bereits bekannt, dass einige Additiv-Additiv-Kombinationen unverträglich (antagonistisch) beziehungsweise sich gegenseitig verstärkend (synergistisch) sein können. Sollten derartige Effekte auftreten, galt es die Hintergründe dafür zu klären. Bei einer tatsächlichen Anwendung im Feld können derartige Additiv-Additiv-Wechselwirkungen zu Problemen bei der Zementierung und damit später zu Undichtigkeiten des Bohrlochs führen. Es ist daher unbedingt nötig zu verstehen, wieso Interaktionen auftreten. Gegebenenfalls müssten schädliche Kombinationen vermieden werden, oder – im Falle eines Synergismus – könnten sich eventuell Kosteneinsparungen durch niedrigere Dosierungen ergeben.

Im zweiten Teil der Dissertation wurden die Wirkmechanismen von typischen Vertretern der Celluloseether in zementären Baustoffsystemen (MHEC und MHPC) erforscht. Neben der speziellen Anwendung von Celluloseethern in der Tiefbohrzementierung ist der Einsatz in Fliesenklebern, Mörteln oder Putzen sehr bedeutend. Diese Unterscheidung ist wichtig, da Methylcellulosen im Baubereich bei gemäßigten Temperaturen und ohne äußere Druckeinwirkung eingesetzt werden. Daher können unter Umständen andere Eigenschaften zu guter Wasserretentionswirkung führen. Das hier übliche Testverfahren der Wasserretention unterscheidet sich im Vergleich zu dem in der Tiefbohrzementierung ebenfalls. So wurde in dieser Arbeit mittels eines einfach konzipierten Papiertuchtests die Wasserrückhaltung simuliert, wobei mehrere Lagen von Papiertüchern den wassersaugenden Untergrund bildeten. Allerdings konnten ähnliche mechanistische Konzepte zur Filtration wie im Tiefbohrbereich angewendet werden, da auch hier eine Filtration an einem porösen Untergrund stattfindet. Weiterhin halfen Untersuchungen zum Lösungsverhalten sowie anderer charakteristischer Eigenschaften des Celluloseethers, den Mechanismus genauer zu verstehen.

In der letzten Studie wurde die Effektivität von MHPC (ein Celluloseether, welcher typischerweise in Putzen verwendet wird) in Gips-basierten Baustoffen näher untersucht. Die Motivation hierfür lag darin, dass von Gips-gebundenen Systemen wie beispielsweise Leichtgipsputz bekannt ist, dass dort im Vergleich zum Zement höhere Dosierungen für eine ausreichende Wasserretention benötigt werden. Die Ursache hierfür war bisher unbekannt. Zur Untersuchung wurde der Einfluss eines erhöhten Sulfatgehalts in der Porenlösung auf die vorher erarbeiteten, dem Wirkmechanismus zugrundliegenden Effekte hin studiert. Besonders die Entwicklung der dynamischen Viskosität sowie die Bildung von Assoziaten in Sulfat-reicher Umgebung wurden analysiert.

2 Theorie und Methoden

2.1 Celluloseether

In den vergangen Jahren wurden in Deutschland stetig steigende Mengen (2009: 165.000 t, 2010: 180.000 t, 2011: 205.000 t) Cellulose und deren Derivate produziert [23]. Für Tiefbohrzementierungen und moderne bauchemische Anwendungen sind spezielle Celluloseether längst unverzichtbar geworden. Erst durch ihren Einsatz wurde der Wasseraustrag bei Tiefbohrungen kontrollierbar und Maschinenputz konnte die konventionelle Handputztechnik fast vollständig verdrängen [13, 24]. Diese Arbeit beschäftigt sich mit Hydroxyethyl- und Carboxymethylhydroxyethylcellulose für Tiefbohranwendungen sowie Methylcellulosen (konkret Methylhydroxyethyl- und Methylhydroxypropylcellulose) für den Einsatz in zementären und Gips-gebundenen Baustoffen (z.B. Trockenmörtel oder Leichtgipsputz). Die generellen Strukturen der genannten Celluloseether sind in **Abbildung 1** dargestellt.

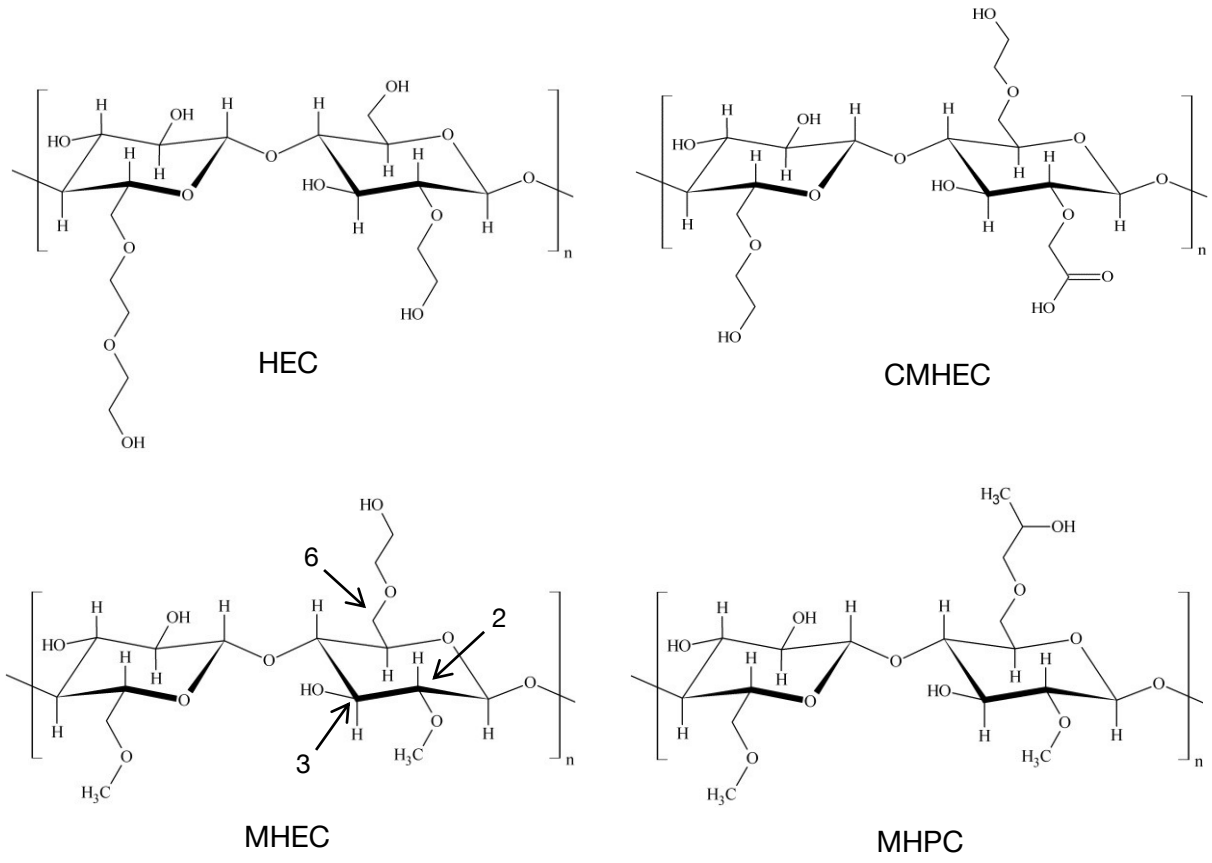

Abbildung 1 – Strukturen von in dieser Studie verwendeten Celluloseethern.

2.1.1 Industrielle Herstellung

Die Herstellung von Celluloseethern erfolgt in einem verfahrenstechnisch aufwendigen heterogenen Prozess [25]. Um die Cellulose einer chemischen Reaktion zugänglich zu machen, wird sie zunächst fein aufgemahlen (Zellstoffmahlung) und mit ~ 18 – 50 %iger Natronlauge im Tauch- oder Maisch-Verfahren zu Alkalicellulose umgesetzt. Die Alkalibehandlung führt unter anderem zu Aufweitungen und Umwandlungen der kristallinen Struktur in den geordneten Bereichen der Cellulose. Die resultierende, alkali-behandelte Cellulose ist reaktiver als unbehandelte Cellulose und kann deshalb mit verschiedenen Veretherungsmitteln (z.B. Monochlormethan, Ethylenoxid oder Propylenoxid) umgesetzt werden, wodurch wasserlösliche Celluloseether entstehen. Die dabei ablaufende Sauerstoff-Alkylierung mit Halogenalkanen wird als *Williamson*'sche Ethersynthese bezeichnet und ist die häufigste Umsetzungsart der Alkalicellulosen [26, 27].

Bei der Veretherung werden statistisch Wasserstoffatome der Hydroxylgruppen der Anhydroglucose-Einheiten ersetzt. Im Fall einer Methylierung von Alkalicellulose mit Methylchlorid wird die Position C-2 bevorzugt angegriffen, gefolgt von C-6 und der unreaktivsten Position C-3 (siehe **Abbildung 1**). Bei einer Alkoxylierung (z.B. mit Ethylenoxid) können sich längere Oligo- oder Polyethylenoxid-Seitenketten bilden, denn die primären Hydroxylgruppen der Seitengruppen haben stets eine höhere Affinität zu Epoxiden als die ringständigen sekundären Hydroxylgruppen. An den ringständigen Hydroxylgruppen hingegen können sich die Reaktivitäten je nach Alkalität relativ zueinander verschieben, so dass auch Position C-6 bevorzugt substituiert werden kann [1, 28, 29].

Die Ethersynthese läuft in einem Temperaturbereich von 50 – 140 °C bei Reaktionszeiten von wenigen Minuten bis einigen Stunden ab und wird in der Regel bis zum vollständigen Verbrauch des eingesetzten Veretherungsmittels durchgeführt. Als weitere wichtige Umsetzungen sind noch die *Michael*-Addition von Reagentien an aktivierte Doppelbindungen sowie die Umsetzung mit Dialkylsulfaten zu nennen [2, 30].

Nach Beendigung der Veretherungsreaktion werden die als Feststoff vorliegenden Roh-Celluloseether durch Filtration oder Zentrifugation abgetrennt. Eventuell ist vorher eine Neutralisation der unverbrauchten Natronlauge notwendig. Nach der Abtrennung müssen noch enthaltene Verunreinigungen durch Waschen der Celluloseether entfernt werden. Im Detail handelt es sich hierbei um organische Reaktionsnebenprodukte wie Methanol, Ethanol, Glykolate (Alkylierungsreaktionen) beziehungsweise Diglykolate (Carboxymethylierungsreaktionen) sowie Alkalimetall-Salze. Celluloseether, die bei höherer

Temperatur wasserunlöslich sind, können problemlos durch Waschen mit Heißwasserdampf gereinigt werden. Ist dies auf Grund einer Löslichkeit bis 100 °C (z.B. Hydroxyethylcellulose) nicht möglich, wird mit wassermischbaren, organischen Lösungsmitteln wie Ethanol oder Isopropanol gereinigt. Nach der Reinigung werden die Celluloseether getrocknet und durch Mahlen beziehungsweise Sichten in die gewünschte Form (Pulver oder Granulat mit definierter Partikelgröße) gebracht [3, 25, 30]. Eine Übersicht über die Herstellung der in dieser Arbeit verwendeten sowie der häufigsten kommerziellen Celluloseether ist in **Abbildung 2** gegeben.

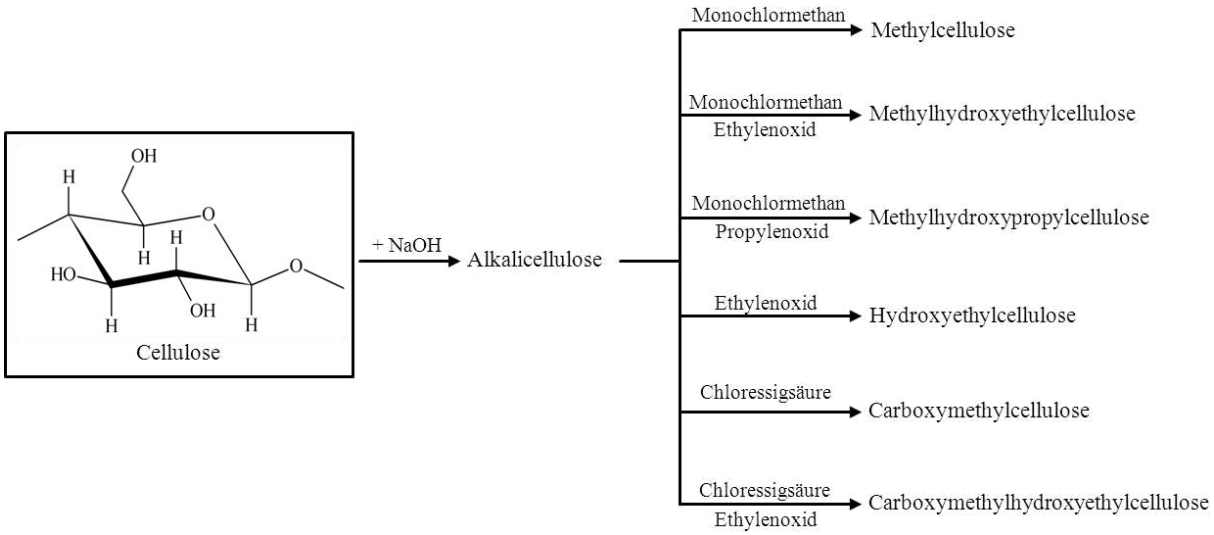

Abbildung 2 – Übersicht zur Herstellung wichtiger kommerzieller Celluloseether [26].

2.1.2 Typische Eigenschaften

2.1.2.1 Veretherungsgrad

Neben der Auswahl der Substituenten bestimmt der Grad der Substitution die Eigenschaften des Celluloseethers. Hierbei wird zwischen degree of substitution (DS) und molar degree of substitution (MS) unterschieden. Die DS- und MS-Werte sowie die Position der Substituenten in der Anhydroglucose-Einheit der Cellulose sind mittels NMR-Spektroskopie bestimmbar [6].

- **DS-Wert (degree of substitution):** Er gibt an, wie viele der drei reaktionsfähigen OH-Gruppen der Anhydroglucose-Einheit der Cellulose verethert sind. Es handelt sich dabei um einen statistischen Mittelwert, der maximal den Wert 3 annehmen kann.

- **MS-Wert (molar degree of substitution):** Er gibt die durchschnittliche Anzahl angelagerter Moleküle (z.B. von Ethylenoxid) pro Anhydroglucose-Einheit der Cellulose an. Damit kann die Länge der aufgepfropften Seitenkette abgeschätzt werden.

In der Industrie bezeichnet man allerdings zur Vereinfachung den Gehalt an Methyl-, Ethyl- oder Carboxymethylgruppen als DS und denjenigen von Hydroxyethyl- sowie Hydroxypropylgruppen als MS, was wissenschaftlich nicht korrekt ist.

Die wichtigste Eigenschaft, welche über den Substitutionsgrad eingestellt werden kann, ist die Löslichkeit. Hierbei durchläuft die Löslichkeit mit zunehmender Substituierung verschiedene Stadien. So variiert z.B. die Löslichkeit von Methylcellulosen mit dem DS-Wert. Bei einem DS bis ~ 1,0 sind sie nur in alkalischen Lösungen, bei einem DS von etwa 1,2 bis 2,5 in Wasser löslich. Schon in diesem Bereich kommt der hydrophobe Charakter der CH_3O-Gruppe dadurch zum Ausdruck, dass Methylcellulosen mit einem DS von über 2,5 sehr gut in organischen Lösemitteln löslich sind, wobei die Übergänge fließend sind [1, 31]. An dieser Stelle soll auch erwähnt sein, dass Celluloseether in Lösung gehen beziehungsweise anquellen müssen, um ihre Wirkung optimal entfalten zu können. Der Zeitpunkt und die Dauer des Kontakts mit Wasser spielt daher eine wichtige Rolle bei einer Wirkungsbetrachtung. In allen bauchemischen Anwendungen sowie im Rahmen dieser Arbeit wird der Celluloseether trocken mit dem Bindemittel vermischt und in Kontakt mit Wasser gebracht.

Des Weiteren ist aufgrund der gleichzeitigen Anwesenheit hydrophiler und hydrophober Gruppen bei Celluloseethern stets eine gewisse Grenzflächenaktivität zu erwarten [32]. MHPC ist besonders oberflächenaktiv, seine wässrige Lösung schäumt beim Schütteln. MHEC und HEC zeigen schwächere Oberflächenaktivität und schäumen in Lösung daher auch weniger stark [33].

2.1.2.2 Temperaturbedingte Flockung

Eine weitere besondere Eigenschaft von Celluloseethern mit hydrophoben Substituenten ist die Abhängigkeit ihrer Löslichkeit von der Temperatur. Hydroxyethylcellulose zeigt keine temperaturabhängige Flockung. Hingegen ist Methylcellulose in kaltem Wasser noch löslich, flockt bei erhöhten Temperaturen jedoch aus [34]. Dieser Prozess ist reversibel und so kann durch Abkühlung ein erneutes Auflösen der Methylcellulose erreicht werden.

Reine Methylcellulose flockt beispielsweise zwischen 55 und 65 °C aus. Durch Mischveretherung und die Einführung von hydrophilen Substituenten (wie bei MHEC oder MHPC) ist es möglich, den sogenannten Flockungspunkt auf der Temperaturskala weiter nach oben zu verschieben. Genügend hoch mischveretherte Typen flocken aus wässriger Lösung im Bereich von 65 bis 80 °C aus. Die Ausflockung ist allerdings wie in einigen Studien bereits gezeigt wurde von der Konzentration der Celluloseetherlösung, der Homogenität der Substitution sowie dem Substitutionsgrad abhängig [1, 6, 35].

2.1.2.3 Viskosität und Molekulargewicht

Celluloseether lösen sich kolloidal und polydispers in kaltem Wasser. Die Lösungen enthalten hydratisierte Makromoleküle und verhalten sich häufig scherverdünnend. Bei sonst gleichbleibenden Parametern (z.B. Substitutionsgrad, Konzentration) erhöht sich die Viskosität einer 2 %igen wässrigen Lösung von Celluloseethern bei 20 °C mit steigendem Polymerisationsgrad (vgl. **Abbildung 3**) [36, 37].

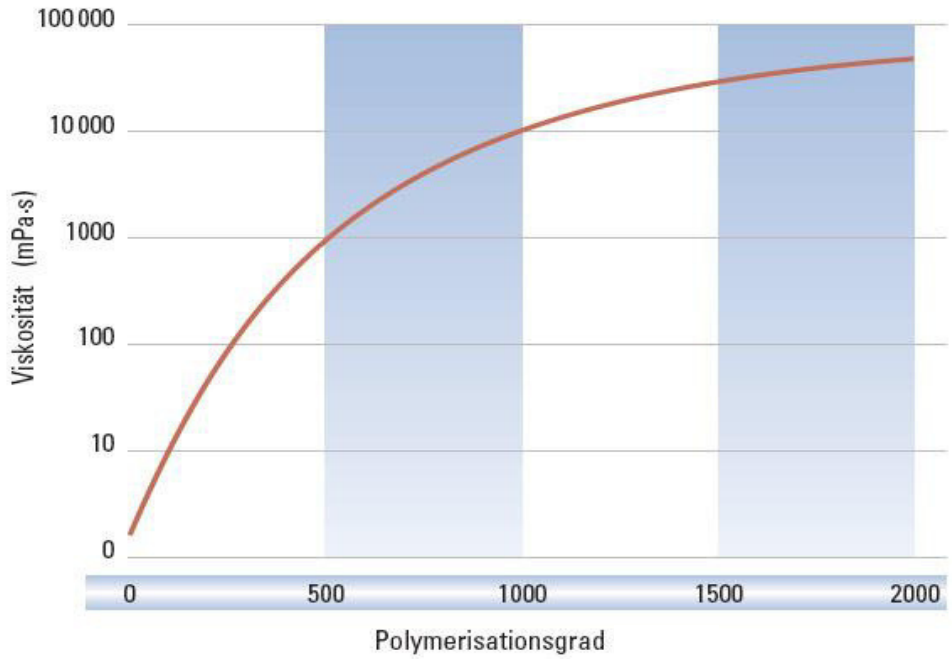

Abbildung 3 – Verdickungswirkung (Viskosität) einer 2%igen wässrigen Celluloseether-Lösung in Abhängigkeit des Polymerisationsgrads [36].

In bauchemischen Anwendungen finden sich hauptsächlich Produkte mit einer Viskosität zwischen 300 und 100.000 mPa·s. Die Viskositäten der in dieser Arbeit verwendeten Derivate liegen bei ~ 200 mPa·s (HEC), ~ 50 mPa·s (CMHEC), ~ 10.000 mPa·s (MHEC) sowie ~ 60.000 mPa·s (MHPC), wobei die Molekulargewichte mittels Gelpermeations-chromatographie (GPC) zwischen 200.000 und 500.000 g/mol bestimmt wurden.

2.1.2.4 Festkörper- und Lösungsstruktur

Die Festkörperstruktur der Rohcellulose besteht aus kristallinen Bereichen, die über Wasserstoffbrückenbindungen der Hydroxylgruppen hierarchisch aufgebaut sind. Neben den kristallinen existieren auch wenig geordnete (amorphe) Abschnitte. Die kristallinen Domänen können z.B. röntgendiffraktometrisch nachgewiesen werden. Eine detaillierte Übersicht über die Struktur und Eigenschaften der nativen Cellulose im Festkörper und in Lösung kann der Literatur entnommen werden [2, 38].

Durch Veretherung werden die Wasserstoffbrückenbindungen der Rohcellulose teilweise zerstört, die Molekülstränge leichter beweglich und damit auch solvatisierbar. Die Veretherung ist in der Regel jedoch nicht gleichmäßig und es entstehen vollständig veretherte bis unsubstituierte Domänen. In wässriger Lösung kommt es deshalb zu einer ungleichmäßigen lateralen Aggregation, die durch ein Fransenmizellen-Modell nach *Burchard* (vgl. **Abbildung 4**) sinnvoll beschrieben wird [38, 39].

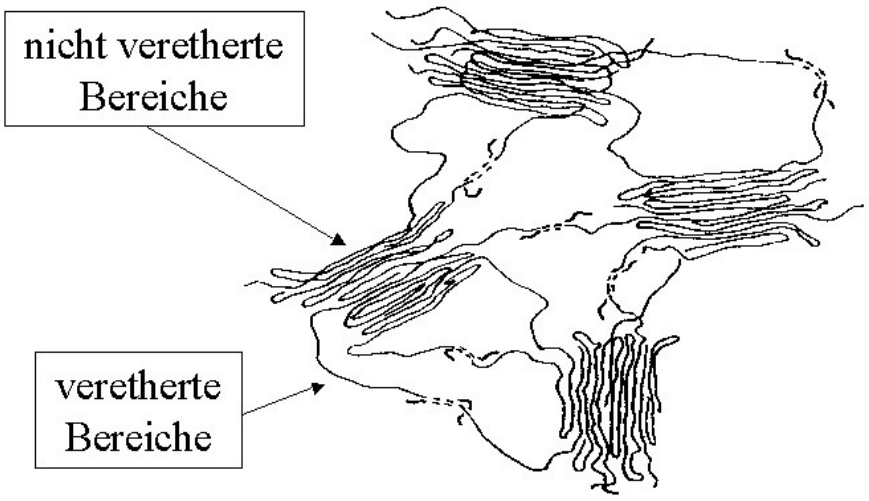

Abbildung 4 – Modell einer Fransenmizelle aus Celluloseethern, nach *Burchard* [39, 40].

Die hauptsächlich im Inneren zu findenden, nicht veretherten Abschnitte des Moleküls behalten ihre Kristallinität und damit auch ihren starken Zusammenhalt über Wasserstoffbrückenbindungen bei. Im oberflächennahen Bereich sind die Anhydroglucose-Einheiten nahezu vollständig substituiert. Bisher ist kein Lösemittel bekannt, das diese ungleichmäßig aufgebauten Fransenmizellen vollständig aufbrechen kann [39, 41].

Celluloseether können aufgrund ihrer Löslichkeit mit statischer und dynamischer Lichtstreuung untersucht werden. Allerdings treten in Lösung häufig gleichzeitig verschiedene Wechselwirkungen (Wasserstoffbrückenbindungen, hydrophobe Wechselwirkungen oder Komplexbildungen) auf und es werden polymere Überstrukturen gebildet. Diese Wechselwirkungen können die Charakterisierung der in Lösung befindlichen Celluloseether erschweren [42].

2.1.2.5 Verzögernde Wirkung auf die Zementhydratation

Eine weitere Eigenschaft von Celluloseethern, die in dieser Arbeit nicht genauer untersucht wurde aber eine wichtige Rolle spielt, ist die meist verzögernde Wirkung auf die Zementhydratation. Das bedeutet, dass die Hydratation des Zements und damit die Abbindegeschwindigkeit des Bindemittels verlangsamt werden. Dieser Effekt wurde bereits in zahlreichen Publikationen beschrieben [17, 43-46]. Am deutlichsten erkennbar wird die Verzögerung durch Messung des Wärmeflusses eines hydratisierenden Zements ohne Zusatzmittel und in Anwesenheit von Celluloseethern. Die verschiedenen Typen zeigen unterschiedlich starke Effekte, unter anderem abhängig vom Veretherungsgrad sowie der Art der Veretherung (vgl. **Abbildung 5**).

Man erkennt, dass die verschiedenen Typen die Zementhydratation um bis zu 10 Stunden verzögern können. Die möglichen Ursachen hierfür sind sehr vielfältig. So kann eine Inhibierung des Kristallwachstums von Zementhydratphasen (speziell eine Änderung der Morphologie von Portlandit [43]), eine Komplexierung der Alkali- und Erdalkalimetalle oder einer Erniedrigung der Ionenmobilität Grund für die verzögernde Wirkung sein. Auch der Einfluss des DS-Wertes von Celluloseethern und damit der Anteil der Hydroxylgruppen wird diskutiert [17].

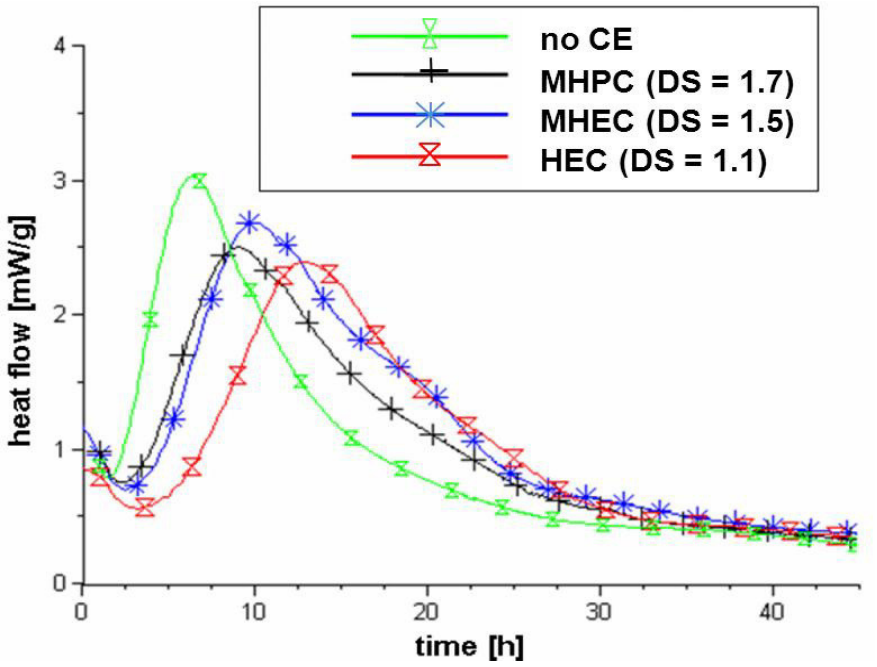

Abbildung 5 – Messung der Verzögerungswirkung von Celluloseethern (MHPC, MHEC und HEC) auf Zement durch Wärmeflusskalorimetrie, nach *Hucko / Zwanzig*, *Hercules GmbH* [16, 47].

Generell muss eine mögliche verzögernde Wirkung bedacht werden, wenn Celluloseether in zementären Systemen als Wasserretentionsmittel verwendet werden. Mit steigenden Dosierungen kann die Verzögerung ein unerwünscht hohes Maß annehmen. Da die Verzögerung durch Celluloseether in zahlreichen Baustoffsystemen sehr stört, wurde im Jahr 2007 bereits ein weniger stark verzögerndes Produkt der Firma Hercules GmbH vorgestellt. Dort wird durch Variation des Herstellungsprozesses eines Celluloseethers mit gleichem DS- und MS-Wert die verzögernde Wirkung auf die Zementhydratation um etwa 5 Stunden verringert [47].

Im Folgenden wird nun auf die Wasserretention / Wasserrückhaltewirkung als wichtigste Funktion von Celluloseethern in der Bauchemie eingegangen.

2.2 Anwendungsgebiete von Celluloseethern als Wasserretentionsmittel

2.2.1 Tiefbohrzementierung

In diesem Kapitel soll ein Einblick in die Technologie der Tiefbohrzementierung gegeben werden. Dieses Feld stellt ein sehr wichtiges Einsatzgebiet von Celluloseethern als

Zusatzmittel (Wasserretention und gegebenenfalls Verzögerung) in einem zementären System dar. Die in dieser Arbeit gezeigten Vertreter HEC sowie CMHEC sind auf Grund ihrer Temperaturstabilität im Vergleich zu anderen Celluloseethern die am häufigsten angewandten Produkte. Generell werden Celluloseether bis ~ 100 °C verwendet. Sie stellen dort auch die wichtigste Klasse an Wasserretentionsmitteln dar (hier als „Fluid Loss Additive“ bezeichnet). Bei höheren Temperaturen nimmt ihre Wirksamkeit hingegen deutlich ab [15, 48].

Für Temperaturen bis 150 °C kommen vollsynthetische, temperaturstabile Copolymere auf Basis von 2-Acrylamido-2-methylpropansulfonsäure (AMPS®) zum Einsatz. Patentiert wurde ein solches Polymer, bestehend aus AMPS® und N,N-Dimethylacrylamid (NNDMA), erstmals 1985 von der Firma Halliburton [49]. Für Temperaturen bis 200 °C und höher wurden synthetische Copolymere auf Basis von Allyloxy-2-hydroxypropansulfonsäure (AHPS) vorgeschlagen [50].

2.2.1.1 Technologie

Das Hauptziel der Zementation eines Bohrlochs ist die sogenannte „zonal isolation“. Diese dient dazu, öl- und gasführende Schichten gegeneinander und gegen wasserführende Schichten abzudichten. Das am meisten angewandte Verfahren bei der Erstellung eines Bohrlochs ist das Prinzip der Ringraumzementierung (vgl. **Abbildung 6**). Nach dem Betonieren einer Plattform wird mit einem rotierenden Bohrmeißel bis zur gewünschten Teufe gebohrt und Futterrohre (sog. „casings“) in das Bohrloch bis zur Bohrlochsohle platziert.

Durch Verpressen einer individuell auf die Tiefe, die Temperatur und die jeweilige Formation abgestimmten Zementschlämme hinter den „casings“ wird der Ringraum zwischen Gesteinsformation und Verrohrung von unten mit Zement gefüllt. Das Verfahren des Bohrens und Zementierens wird mit nach unten kleiner werdenden Rohrdurchmessern (teleskopartig) bis zur Erreichung der Endteufe wiederholt [15, 51].

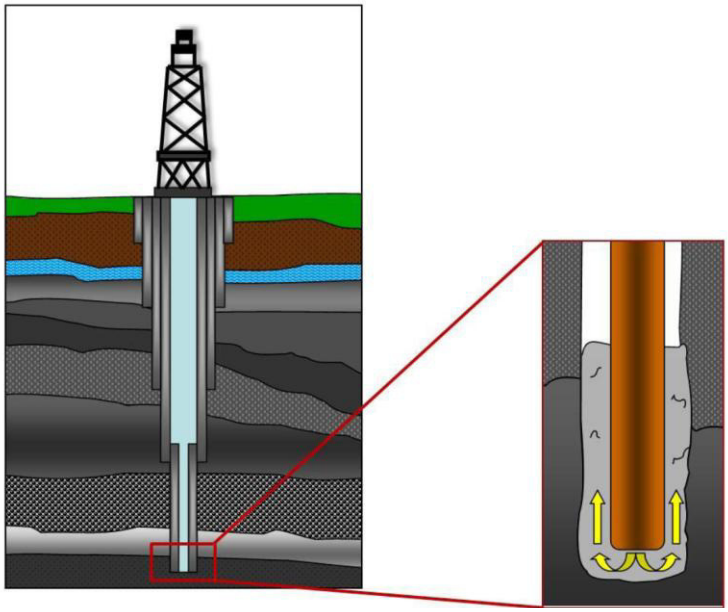

Abbildung 6 – Schematische Darstellung der Tiefbohrzementierung [52].

2.2.1.2 Wasserretentionsmittel (Fluid Loss Additive)

Zementschlämmen, welche bei Tiefbohrungen verpumpt werden, beinhalten stets mehrere Additive, wobei Fluid Loss Additive nach Verzögerern, Beschleunigern und Fließmitteln eine wichtige Gruppe darstellen. Da durch Kapillarsaugkräfte des umgebenden Gesteins und den hydrostatischen Druck der Zementschlämme stets Wasserverlust auftritt, werden Hochleistungsadditive zugegeben, um dies zu verhindern. Bei übermäßiger Wasserabgabe im Bohrloch besteht zudem die Gefahr, dass die Zementschlämme frühzeitig eindickt und die Dichte erhöht wird. Auch das Eindringen von Filtrat in die Gesteinsformation kann sehr schädlich für die spätere Förderung sein.

Der Vorgang der Druckfiltration an einer porösen Gesteinswand ist in **Abbildung 7** dargestellt. Durch den Wasserverlust kann die vollständige Hydratation des Zements nicht mehr gewährleistet werden [53]. Außerdem wird der Ringraum in diesem Fall nicht mehr vollständig durch einen gasdichten Zementmantel ausgekleidet. Wird Wasserretentionsmittel (WRM) zugegeben, so kann eine übermäßige Wasserabgabe verhindert werden (vgl. **Abbildung 7**). In der Regel entsteht ein wesentlich dünnerer und homogener Filterkuchen, welcher ein gleichmäßiges Aushärten des Zementmantels ermöglicht [15, 18, 51].

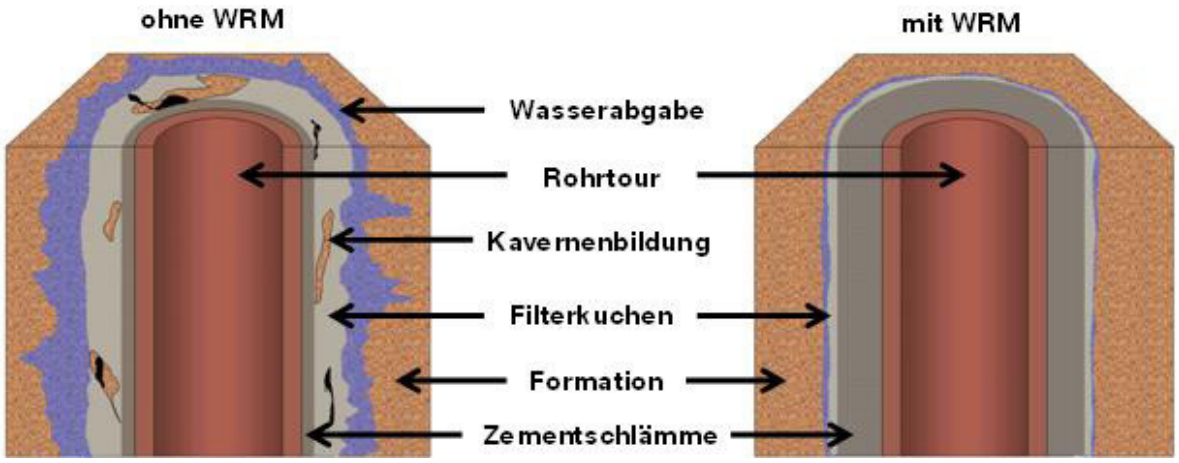

Abbildung 7 – Querschnitt durch die einzementierte Rohrtour einer Erdölbohrung. Links: Bei starker Wasserabgabe der Zementschlämme an der porösen Gesteinswand entsteht ein dicker Filterkuchen. Rechts: Wasserretentionsmittel reduzieren die Wasserabgabe – dadurch bildet sich ein dünner Filterkuchen.

2.2.1.3 Druckfiltration nach API

Die Wirksamkeit eines Fluid Loss Additives wird nach der Norm des American Petroleum Institutes (API) bestimmt [54]. Hierfür wird nach dem Einstellen der Temperatur und dem Anlegen eines Differenzdrucks (Δp = 70 bar) das Bodenventil geöffnet und das austretende Filtrat gesammelt (vgl. **Abbildung 8**). Die Zementpartikel setzen sich zu Beginn der Filtration am Maschensieb ab und bilden einen Filterkuchen.

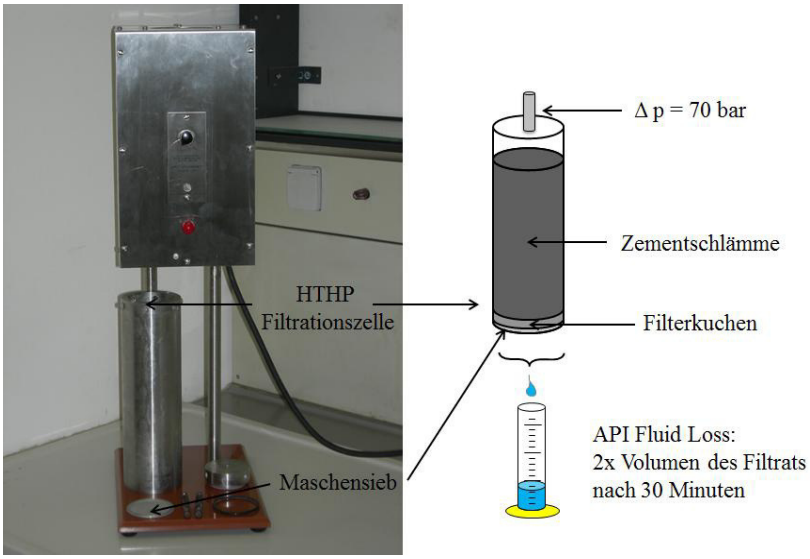

Abbildung 8 – High temperature/high pressure (HTHP)-Filtrationszelle zur Bestimmung der Wirksamkeit eines Fluid Loss Additives in der Tiefbohrzementierung [55, 56].

Nach 30 Minuten kann mit einem Messzylinder das Volumen des Filtrats (API Fluid Loss = 2 x Filtratvolumen) bestimmt werden. Je weniger Filtrat in der vorgegebenen Zeit austritt, desto wirksamer ist das Additiv.

2.2.2 Baustoffsysteme

In der Trockenmörtelindustrie werden die in dieser Arbeit untersuchten Celluloseether MHEC und MHPC hauptsächlich in Spachtelmassen, Fliesenklebern und Maschinenputzen eingesetzt. Im Folgenden werden diese Baustoffsysteme und die Rolle von Celluloseethern dabei kurz vorgestellt.

2.2.2.1 Trockenmörtel (dry-mix mortars)

Die Einführung der Trockenmörteltechnologie erbrachte zwischen 1960 und 1995 eine Steigerung des Mörtel- und Putzumsatzes in Deutschland um 600 %, während die Zahl der Bauhandwerker in diesem Sektor gleichzeitig um 25 % sank. Dies entspricht einer Steigerung der Produktivität um 800 %. Der Grund dafür liegt darin, dass moderne Trockenmörtel im Gegensatz zu konventionellem Baustellenmörtel im Werk vorgemischt werden. Sie enthalten bereits alle nötigen Bestandteile wie Bindemittel, Aggregate (Füller) und chemische Additive. Diese werden in Silos gelagert und dann automatisiert abgemischt. Auf diese Weise lassen sich definierte Produkte produzieren, welche eine hohe Qualität und sehr gute Konsistenz aufweisen [20, 57, 58].

Ohne den Zusatz von Additiven wären moderne Trockenmörtel jedoch nicht denkbar und einige technische Eigenschaften dieser Produkte nicht erzielbar. Bezogen auf den Anteil an mineralischen Bestandteilen bestehen Trockenmörtel lediglich zu 0,1 – 5 Gew.-% aus Additiven. Diese verbessern unter anderem die Mischbarkeit mit Wasser, die rheologischen Eigenschaften, die Verarbeitbarkeit und das Abbindeverhalten (Festigkeitsentwicklung) des Produkts [20].

2.2.2.2 Maschinenputz

Wandputze können entweder per Hand aufgetragen oder als Maschinenputz an die Wand gespritzt werden (vgl. **Abbildung 9**). Seit den 1970er Jahren ist das maschinelle Anspritzverfahren am weitesten verbreitet. Da lediglich zwei Handwerker nötig sind, um einen Maschinenputz zu applizieren, konnte die Flächenleistung pro Arbeitskraft und Stunde von weniger als 20 m^2 auf ~ 50 m^2 gesteigert werden [13].

Abbildung 9 – Auftragen eines Gips-basierten Maschinenputzes an die Wand mittels *Knauf PFT G5 Verputzmaschine* und anschließendes Glattziehen [59].

Tabelle 2 zeigt die typische Zusammensetzung von auf verschiedenen Bindemitteln basierenden Maschinenputzen. Es gilt zu beachten, dass Gips-basierte Putze höhere Dosierungen an Celluloseether benötigen, um ausreichend gute Eigenschaften zu erzielen. Mögliche Ursachen dieses Effektes wurden in dieser Arbeit untersucht.

Tabelle 2 – Rezepturen von Zement-, Zement/Kalk- und Gips-Maschinenputz [13].

Rohstoff	Art des Putzes		
	Zement	Zement/Kalk	Gips
Portlandzement	15-20 %	10-15 %	-
Mehrphasengips	-	-	85-98 %
Kalk	0 - 2 %	5-10 %	0-3 %
$CaCO_3$ oder Quarz < 1mm	65-78 %	65-75 %	0-10 %
$CaCO_3$ Pulver < 0,1 mm	5-10 %	5-10 %	-
Perlit < 1 mm	0-2 %	0-2 %	0-1 %
WRM (z.B. Celluloseether)	0,08-0,15 %	0,10-0,15 %	0,18-0,23 %
Stellmittel	0-0,03 %	0-0,03 %	0-0,05 %
Schäumer	0,01-0,03 %	0,01-0,03 %	0,01-0,03 %
Gips-Verzögerer	-	-	0,05-0,15 %

2.2.2.3 Wasserretentionsmittel

Erst durch den Einsatz von Celluloseethern wurden die notwendige Wasserretention, Verarbeitung, Nasshaftung und das Standvermögen in den beschriebenen Baustoffanwendungen erzielt. MHEC ist hierbei das Produkt der Wahl für Selbstverlaufsmassen und Fliesenkleber, während MHPC auf Grund der hydrophoberen Hydroxypropylgruppen mehr Luft einführen kann und verstärkt in Putzen Einsatz findet [20].

Nötig sind Celluloseether in diesen Baustoffsystemen, da das aus hochporösen Materialien (z.B. Ziegel, Kalkstein, Gasbeton) bestehende Mauerwerk dem Bindemittelsystem sehr viel Wasser entziehen würde und so ein vollständiges Abbinden des Bindemittels nicht mehr möglich ist. Rissbildung und Abplatzungen wären die Folge. Erst durch den Einsatz von Wasserretentionsmittel konnte das früher übliche und nötige Tränken der Mauer mit Wasser vor dem Auftragen des Putzes entfallen und maschinelle Anwendungen realisiert werden [1, 6, 21].

2.2.2.4 Papiertuchtest

Das Wasserretentionsvermögen in Baustoffsystemen kann im Labor mit Hilfe einer modifizierten Version der Filterpapiermethode nach EN 495-2 (früher DIN-18555-7), dem

sogenannten „Papiertuchtest“, untersucht werden [60, 61]. Hierbei werden 15 Papiertücher (240 x 105 mm) halbiert und mit einer Lage eines Taschentuchs bedeckt. Darauf wird ein Vicat-Ring (konisch, 70 x 80 x 40 mm) mit dem kleineren Durchmesser nach unten zeigend platziert (vgl. **Abbildung 10,** links).

Abbildung 10 – „Papiertuchtest“ zur Bestimmung der Wasserretention. Links: zu Beginn wird ein Vicat-Ring auf einem Papierstapel platziert und mit der Baustoffsuspension gefüllt; Mitte: Papierstapel zeigt eine große Menge sorbierten Wassers nach dem Test. Rechts: Wassermenge unter Zusatz von Wasserretentionsmittel (hier: 0.8 % MHEC, bezogen auf Zementanteil)

Zur Messung der Wasserretention wird der Vicat-Ring mit dem zu untersuchenden Bindemittelleim bis an den Rand gefüllt und 7,5 Minuten stehen gelassen. Während dieser Zeit nimmt das Filterpapier, welches den saugenden Untergrund repräsentiert, eine bestimmte Menge Wasser auf. Je besser die Wasserretentionswirkung im System, desto weniger Wasser wird an den Papiertuchstapel abgegeben (vgl. **Abbildung 10**, Mitte und rechts). Die Menge des absorbierten Wassers wird aus dem Differenzgewicht des Papiertuchstapels vor und nach der Messung gemäß **Gleichung 1** bestimmt.

$$\text{Wasserretention}\ (\%) \quad = \quad \left(1 \; - \; \frac{w_{abs}}{w_0}\right) \cdot 100$$

Gleichung 1 – Berechnung der prozentualen Wasserretention. w_{abs} = absorbierte Wassermenge, w_0 = Gesamtwassergehalt der Bindemittelsuspension im Vicatring.

2.3 Wirkmechanismen von Wasserretentionsmitteln

Die Wirkmechanismen von Wasserretentionsmitteln sind bisher nur teilweise bekannt. Eine gute Übersicht für Fluid Loss Additive in der Tiefbohrzementierung bietet das Buch „Well Cementing: Second Edition“ von *Nelson* [15], in welchem Wasserretentionsmittel in zwei Gruppen eingeteilt werden. Einerseits werden Feststoffe wie beispielsweise Bentonite beschrieben und andererseits wasserlösliche Polymere. Einige Fluid Loss Additive weisen einen adsorptiven Wirkmechanismus auf, während andere die Wasserretention durch physikalische Effekte (Porenverstopfung) hervorrufen.

Auch zum Wirkmechanismus von Methylcellulosen im Baubereich existieren einige frühere Untersuchungen. In den folgenden Abschnitten wird genauer auf die theoretischen Konzepte zu möglichen Mechanismen wie auch auf bisherige experimentelle Ansätze eingegangen.

2.3.1 Mechanismus der Wasserretention nach *Desbrières*

Im Bereich der Tiefbohrzementierung existieren relativ genaue Modellvorstellungen zu den unterschiedlichen Wirkmechanismen. Hier sind besonders die ausgezeichneten Pionierarbeiten von *Desbrières* aus dem Jahre 1993 zu erwähnen, die sich mit den Mechanismen der in Tiefbohrzement eingesetzten Wasserretentionsmittel beschäftigen [62, 63]. Die Entwässerung von Zementschlämmen durch einen bei einer Filtration entstehenden Filterkuchen im Tiefbohrzement erfolgt gemäß diesen Arbeiten streng nach dem Gesetz von *Darcy*, welches in Kapitel 2.3.2 genauer erläutert wird [62, 64].

Zunächst bleibt festzuhalten, dass die Wasserretentionswirkung stets auf einer Erniedrigung der Filtrationsgeschwindigkeit dV/dt beruht. Mit Hilfe des Gesetzes von *Darcy*, den gemessenen Werten der Filtratviskosität, der Filtrationsgeschwindigkeit und dem reduzierten Filterkuchenvolumen ermittelte *Desbrières* die Filterkuchenpermeabilität verschiedener Zementschlämmen. Hierbei stellte sich heraus, dass die Permeabilität in Anwesenheit üblicher Wasserretentionsmittel um den Faktor 1.000 abnimmt. Die Viskosität des Filtrats spielt hingegen nur eine untergeordnete Rolle.

Eine Reduktion der Filterkuchenpermeabilität durch Additive ist primär durch die Verengung der Filterkuchenporen möglich. Dies kann einerseits durch Adsorption von anionischen Polymeren auf die Hydratphasen des Bindemittels erfolgen, welche dann in den Porenraum ragen und diesen verringern. Alternativ ist auch die physikalische Verstopfung durch

Polymerfilme oder große Assoziate, welche ein dreidimensionales Netzwerk bilden, möglich (vgl. **Abbildung 11**).

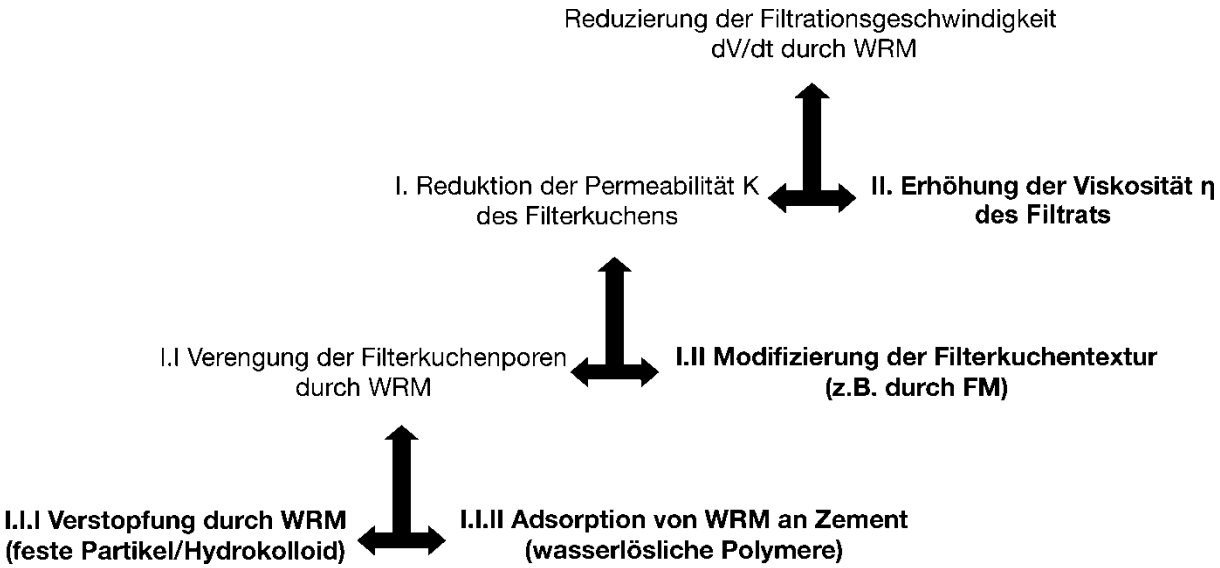

Abbildung 11 – Schema möglicher Wirkmechanismen zur Reduzierung der Filtrationsgeschwindigkeit von Wasserretentionsmittel enthaltenden Systemen.

Zusätzlich kann Anmischwasser durch Bildung von Mikrogelen oder Hydrokolloiden gebunden sein, welches dann nicht mehr durch den Porenzwischenraum ausfiltriert wird. Das außergewöhnlich hohe Wasserbindevermögen von Polysacchariden wurde in einer Studie detailliert untersucht [65]. Durch Messung an einer Sorptionswaage und einem Mikrokalorimeter wurde festgestellt, dass nicht-ionische Polysaccharide (Amylose und Amylopektin) im Sättigungsbereich bis zu vier Wassermoleküle pro Anhydroglucose-Einheit binden können.

2.3.2 Filtrationsgeschwindigkeitsgleichung nach *Darcy*

Desbrières zeigte, dass die Filtration einer Zementschlämme der Filtrationsgeschwindigkeitsgleichung nach *Darcy* folgt [62, 63]. Als Filtrationsgeschwindigkeit dV/dt bezeichnet man das Filtratvolumen V, das in der Zeiteinheit t unter einer Druckdifferenz dp durch eine elementare Schicht des Filterkuchens mit der Schichthöhe dz und der zugehörigen

Permeabilität K_z strömt. Bei einer Filterkuchenfläche A und einer Viskosität des Filtrats η gilt dann der folgende, in **Gleichung 2** dargestellte Zusammenhang.

$$\frac{dV}{dt} = \frac{K_z \cdot A}{\eta} \cdot \frac{dp}{dz}$$

Gleichung 2 – Beziehung zwischen dem zeitabhängigen Filtratvolumen und den charakteristischen Eigenschaften des Filterkuchens. K_z = Permeabilität, A = Filterkuchenfläche, η = Filtratviskosität, dp = Differenzdruck, dz = Dicke einer elementaren Schicht des Filterkuchens.

Das Filterkuchenvolumen dV_z wird erreicht wenn ein Volumen dV abfiltriert wurde. Daher kann die Beziehung $dV_z = R_z \cdot dV$ (R_z sei das Filterkuchenvolumen bei einer definierten Höhe z) angenommen werden. Wird zudem berücksichtigt, dass das Filterkuchenvolumen dV_z einer elementaren Schicht als $dV_z = A \cdot d_z$ beschrieben werden kann, ergibt sich **Gleichung 3**.

$$\frac{dV}{dt} = \frac{K_z \cdot A^2}{\eta \cdot R_z} \cdot \frac{dp}{dV}$$

Gleichung 3 – Zusammenhang zwischen zeitabhängigem Filtratvolumen und den charakteristischen Eigenschaften des Filterkuchens unter Annahme verschiedener Vereinfachungen. K_z = Permeabilität, A = Filterkuchenfläche, dp = Differenzdruck, dz = Dicke einer elementaren Schicht des Filterkuchens, η = Filtratviskosität, R_z = reduziertes Filterkuchenvolumen.

Unter den weiteren Annahmen, dass die elementaren Filterkuchenschichten inkompressibel beziehungsweise identisch sind und die Filtrationsgeschwindigkeit dV/dt zu jeder Zeit t an jeder Höhe des Filterkuchens konstant ist, so ergibt sich nach Integration **Gleichung 4**.

$$V = \sqrt{\frac{2 \cdot K_z \cdot A \cdot \Delta p}{\eta \cdot R_z}} \cdot \sqrt{t}$$

Gleichung 4 – Zusammenhang zwischen zeitabhängigem Filtratvolumen und den charakteristischen Eigenschaften des Filterkuchens. V = Volumen des Filtrats, K_z = Permeabilität, A = Filterkuchenfläche, Δp = Differenzdruck, η = Filtratviskosität, R_z = reduziertes Filterkuchenvolumen, t = Filtrationszeit.

Somit besteht zwischen dem Filtratvolumen V und der Wurzel aus der entsprechenden Filtrationszeit t ein linearer Zusammenhang. Der Gleichung ist weiterhin zu entnehmen, dass bei konstantem Druck, Fläche und relativem Filterkuchenvolumen ein niedriges Filtratvolumen V nach einer festgelegten Filtrationszeit t nur dann erreicht werden kann, wenn entweder die Permeabilität des Filterkuchens K_z erniedrigt oder die Viskosität des Filtrats η erhöht wird.

2.3.3 Weitere Studien zu Wirkmechanismen von Wasserretentionsmitteln

In Voruntersuchungen zu Fluid Loss Additiven im Bereich der Tiefbohrzementierung am Lehrstuhl für Bauchemie wurden bereits das Wasserretentionsvermögen sowie die zugehörigen Wirkmechanismen von Calcium 2-Acrylamdio-2-methylpropansulfonsäure (AMPS®)-co-N,N-Dimethylacrylamid (NNDMA), Polyvinylalkohol (PVA) sowie Polyethylenimin (PEI) untersucht. Dabei zeigte CaAMPS®-co-NNDMA einen adsorptiven Wirkmechanismus [66], wohingegen PVA die Filterkuchenporen durch Filmbildung verengte [67]. PEI wiederum bildete in Anwesenheit eines weiteren anionischen Fließmittel-Polymers einen poren-verstopfenden Polyelektrolyt-Komplex [68]. Auch zum Mechanismus der HEC im zementären System gab es bereits eine erste Studie am Lehrstuhl [4], die hier allerdings noch deutlich ausgedehnt und mit neuen Erkenntnissen erweitert wurde.

In neueren Arbeiten von *Pourchez et al*. [69] sowie *Patural et al.* [70] wurde zur Klärung des Wirkmechanismus der Einfluss von Celluloseethern (HEC, MHEC, MHPC) auf den Wassertransport in porösen, zementären Materialen untersucht. Unter anderem wurde dort Kernspinresonanz (^{1}H-NMR) eingesetzt, um die Selbstdiffusionskoeffizienten von Wasser zu bestimmen. Dort wurde zunächst festgestellt, dass die Zugabe von Celluloseethern zu einer Zementschlämme niedrigere Permeabilität im System und weniger kapillare Wasser-absorption hervorruft. In nachfolgenden Experimenten zeigte sich jedoch, dass der Selbstdiffusionskoeffizient von Wasser in Zementschlämmen durch Celluloseether nicht signifikant verändert wird. Nur im Fall des Auftretens einer Kapillarzugkraft auf einem saugenden Untergrund konnte ein messbarer Effekt des Celluloseethers ausgemacht werden. Die Autoren nehmen deshalb an, dass die rheologischen Eigenschaften der Celluloseether einen deutlichen Einfluss auf die Wasserretention ausüben müssten und schlagen deshalb weitere diesbezügliche Untersuchungen vor.

In der Vergangenheit wurden auch Versuche unternommen, den Wirkmechanismus von Methylcellulose (MC) aufzuklären. Arbeiten von *Schweizer et al.* über den Einfluss von

Celluloseethern auf die Wasserretention und Rheologie eines zementären und Gips-basierten Maschinenputzes zeigten, dass die Adsorption klar vom DS-Wert abhängt [71, 72]. Bei typischen DS-Werten > 1,6 adsorbierte jedoch nur eine sehr geringe Menge des MC-Pulvers. In einem weiteren Experiment fanden die Autoren, dass MC während des Trocknungsprozesses zusammen mit Wasser an die Oberfläche migriert und nicht durch Adsorption zurückgehalten wurde (vgl. **Abbildung 12**). Ähnliche Beobachtungen finden sich auch bei *Yammamuro et al.* [73].

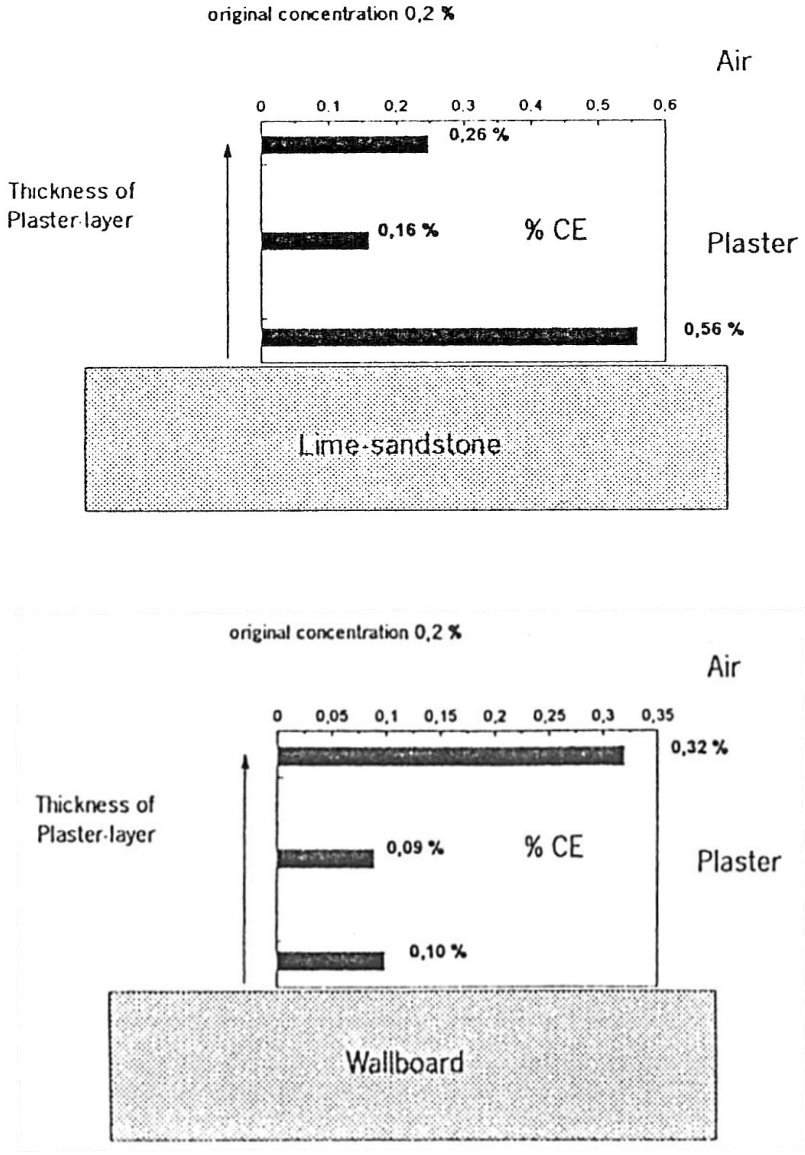

Abbildung 12 – Verteilung eines Celluloseethers im Gipsputz nach dem Austrocknen; aufgetragen auf einem Kalksandstein (oben) und einer Gipskartonplatte (unten) [71].

In einer weiteren Studie von *Jenni et al.* wurde die Migration von MHEC mit Hilfe eines fluoreszierenden Farbstoffs sichtbar gemacht (vgl. **Abbildung 13**). Der Celluloseether befand sich akkumuliert an der Grenzfläche zum Substrat und konnte durch das Porensystem wandern. Daraus folgerten die Autoren, dass keine Adsorption auf Binderpartikeln stattfindet. In einer späteren Veröffentlichung konnten die Autoren eine Migration des gelösten Celluloseethers durch die Kapillarporen zum Substrat nachweisen, wo er dann als Mikrofilter wirkt [74, 75].

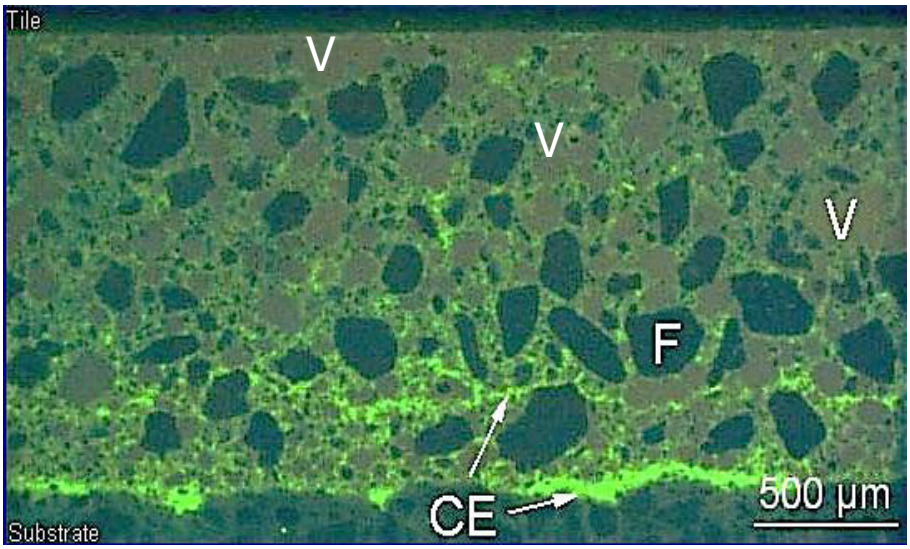

Abbildung 13 – Fluoreszenzmikroskopische Aufnahme einer Mörtelprobe, die in den hellen, grünen Bereichen Ansammlungen an Celluloseether (CE) zeigt. F = Füller, V = Luftpore [76].

Erst kürzlich (November 2012) erschien eine weitere Studie von *Marliere et al.*, in welcher gezeigt wurde, dass Celluloseether in allen porösen Feststoffen bei Filtration Wasserrückhaltung bewirken können. Durch Untersuchung verschiedener poröser Medien (Mörtel, Sand, Glaskugeln) und Flüssigkeiten wurde herausgefunden, dass eine Behinderung des Wassertransports entscheidend für den Mechanismus sein muss. Dies kann laut den Autoren durch polydisperse Aggregate oder hydrophobe Wechselwirkungen des Celluloseethers hervorgerufen werden. Des Weiteren wurde ein statistisches Modell für Filtrationen entwickelt, welches eine Vorhersage der experimentellen Ergebnisse ermöglichte [77].

In allen Studien wird beschrieben, dass MC nicht oder nur in geringem Maß adsorbiert. Keine der Arbeiten stellt jedoch ein alternatives Modell vor, welches den Mechanismus der

Wasserretention klar beschreibt und mit den chemischen Eigenschaften der Celluloseether verbindet. Daher war es überfällig, den prinzipiellen Wirkmechanismus dieser wichtigen Additivgruppe eindeutig herauszufinden.

2.3.4 Zusammenfassung

Gemäß den theoretischen Vorarbeiten existieren grundsätzlich drei Wirkmechanismen, die alleine oder in Kombination eine Reduzierung der Filtrationsgeschwindigkeit bewirken können. Neben einer Viskositätserhöhung des Filtrats kommt eine Reduzierung der Filterkuchenpermeabilität in Frage. In letzterem Fall müssten Wasserretentionsmittel den Porendurchmesser eines Filterkuchens entweder adsorptiv oder verstopfend verringern. Ebenfalls denkbar ist eine Kombination dieser Mechanismen. In **Abbildung 14** sind die drei möglichen Mechanismen der Verengung einer Filterkuchenpore durch ein Wasserretentionsmittel dargestellt.

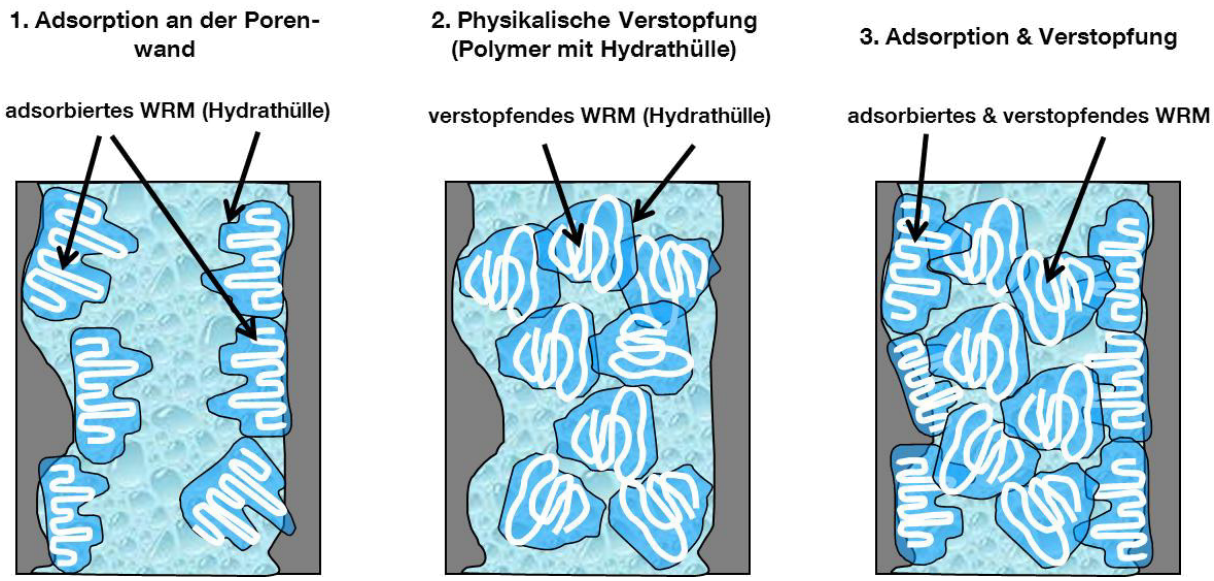

Abbildung 14 – Mögliche Mechanismen zur Reduzierung der Filterkuchenpermeabilität von Tiefbohrzement mittels Wasserretentionsmittel [78].

Da man sowohl für die Anwendung in der Tiefbohrzementierung als auch in Baustoffsystemen (z.B. Putze, Fliesenkleber) von der Ausbildung eines Filterkuchens ausgehen kann, wurde der theoretische Ansatz zu den möglichen Wirkmechanismen nach *Desbrières* für alle Untersuchungen in dieser Arbeit als Grundlage herangezogen.

2.4 Weitere bauchemische Zusatzmittel

Neben Wasserretentionsmitteln kommen sowohl in der Tiefbohrzementierung als auch in Bauanwendungen weitere Zusatzmittel zum Einsatz. Es werden daher immer optimierte Kombinationen verschiedener Additive eingesetzt. Zu Putzen beispielsweise wird häufig Hydroxypropylstärke als Stellmittel zugegeben, da diese mit Celluloseethern bezüglich des Klebeverhaltens sehr gut zusammenwirkt. Tiefbohrzementschlämmen andererseits enthalten meist Fließmittel, durch welche die Mischbarkeit der Schlämme verbessert und ihre Verpumpbarkeit erleichtert wird. Die turbulenten Strömungscharakteristika erlauben es, die im Bohrloch befindliche Spülung und den Spülungsfilterkuchen effizient von der Bohrlochwand zu verdrängen [79].

2.4.1 Fließmittel für Tiefbohrzement

Im Folgenden wird kurz auf Fließmittel im Bereich der Tiefbohrzementierung eingegangen. Polykondensate werden in diesem Gebiet sehr häufig angewandt, wobei Melamin-Formaldehyd-Sulfit (MFS) und Aceton-Formaldehyd-Sulfit (AFS) zwei typische Vertreter sind. In salzhaltigen Zementschlämmen wird AFS bevorzugt, da dieses auch dort noch eine hohe Wirksamkeit besitzt. Die chemischen Strukturen von MFS und AFS sind in **Abbildung 15** dargestellt.

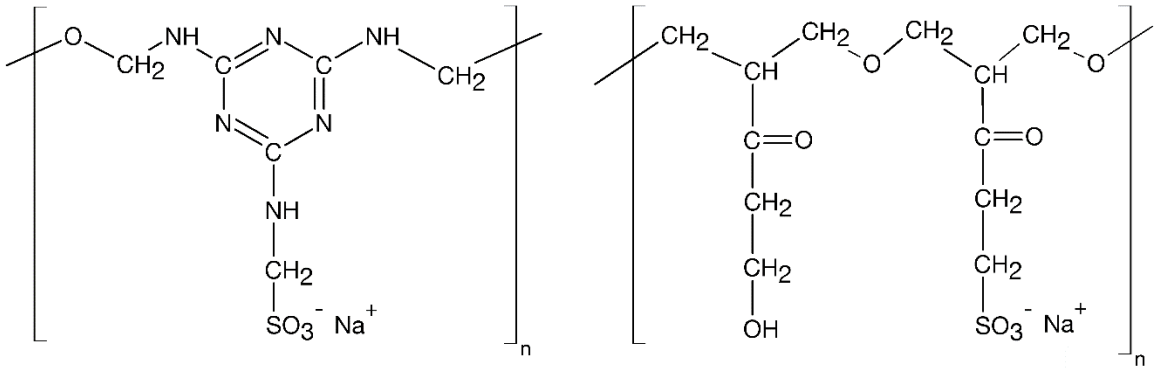

Abbildung 15 – Links: Struktur eines Melamin-Formaldehyd-Sulfit-Fließmittels, rechts: Struktur eines Aceton-Formaldehyd-Sulfit-Polykondensats.

MFS-Harze entstehen durch Umsetzung von Melamin mit Formaldehyd zu Trimethylolamin, nachfolgender Sulfitierung durch Zugabe von Natriumpyrosulfit und anschließender

Kondensation im Sauren. AFS-Harz hingegen wird über eine aldolartige Polykondensation aus Aceton, Formaldehyd und Natriumsulfit synthetisiert. Die exakte Beschreibung der Synthesen ist der Literatur zu entnehmen [80, 81].

Die Wirkung von Polykondensaten beruht auf der Adsorption der Polymere an Zementhydraten. Durch Wechselwirkung zwischen dem Polyelektrolyten und einer positiv geladenen Ionenschicht an der Oberfläche des Zements entsteht eine elektrostatische Anziehung (Physisorption). Nach dem *Gouy-Chapman* Modell führt eine sehr hohe Kationen-Konzentration bei der Hydrolyse der Klinkerphasen an der Zementoberfläche zu einer Ionenschicht, welche auch als *Stern*-Schicht bezeichnet wird [82]. Dabei sind theoretisch drei Adsorptionskonformationen (Schleppzug, Schleife oder Schwanz) möglich. Welche Konformation auftritt, hängt von der Seitenkettenlänge, der Seitenkettendichte und der anionischen Ladungsmenge des Polymers ab [83-86]. Durch die Adsorption auf den positiven Oberflächen des hydratisierenden Zements bilden sich einheitlich negativ geladene Partikel, welche sich gegenseitig elektrostatisch abstoßen. In **Abbildung 16** ist an einem vereinfachten Modell die durch Adsorption hervorgerufene elektrostatische Abstoßung von Zementpartikeln in Anwesenheit von MFS gezeigt.

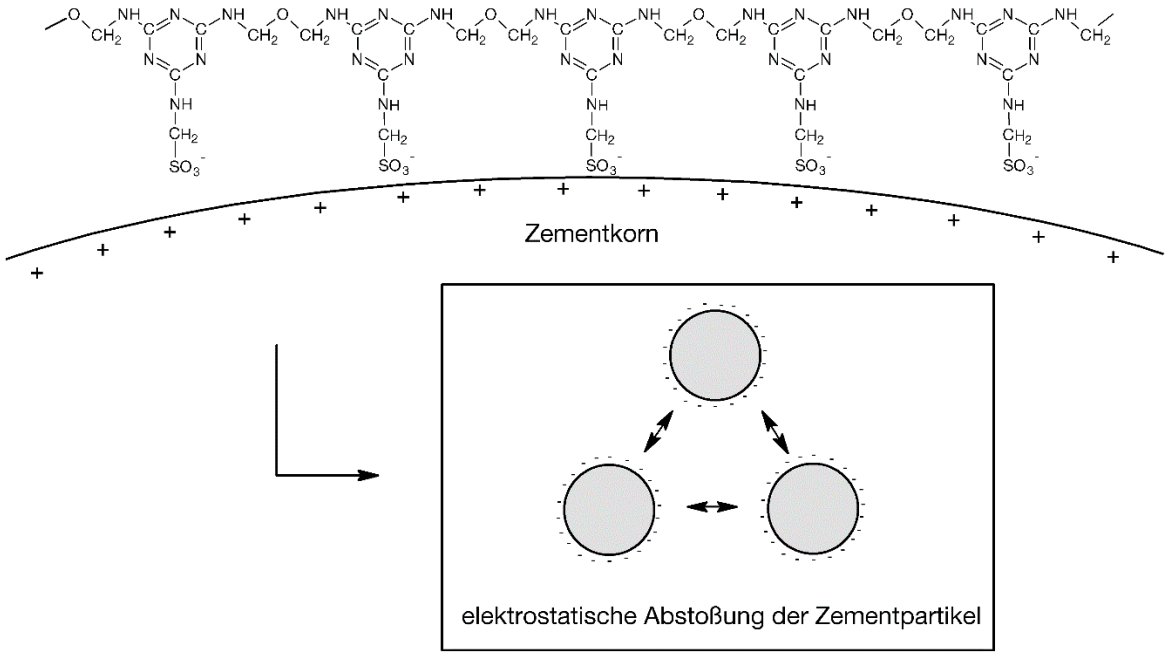

Abbildung 16 – Vereinfachtes Modell zum Wirkmechanismus eines anionischen Polykondensat-Fließmittels (hier am Beispiel MFS) durch elektrostatische Stabilisierung der Zementsuspension aufgrund von Adsorption auf der Zementkornoberfläche, nach [87].

2.4.2 Mögliche Interaktionen zwischen Zusatzmitteln

Beim gleichzeitigen Einsatz von zwei oder mehreren Additiven besteht immer die Möglichkeit, dass diese sich gegenseitig beeinflussen. Werden beispielsweise zwei anionische Polymere verwendet, so kann es zum Wettbewerb um die in begrenzter Anzahl vorliegenden positiven Ladungsplätze (Adsorptionsplätze) auf der Zementkornoberfläche kommen (sog. kompetitive Adsorption). Aber auch der umgekehrte Fall, also ein synergistischer (zusammenwirkender) Effekt, ist denkbar. In diesem Fall beeinflussen sich zwei Zusatzmittel derart, dass sich die Wirksamkeit eines oder sogar beider verbessert.

In früheren Forschungsarbeiten des Lehrstuhls wurden bereits mehrfach kompetitive Effekte untersucht [88-91]. Beispielsweise adsorbieren Zusatzmittel mit geringer anionischer Ladungsmenge in Gegenwart von Zusatzmitteln mit hoher Ladungsmenge nur dann, wenn noch Adsorptionsplätze auf der Oberfläche verfügbar sind. So kann ein Zusatzmittel von einem anderen komplett verdrängt werden und seine Wirksamkeit verlieren. Bei der Kombination aus NaAMPS®-co-Itaconsäure-Verzögerer mit CaAMPS®-co-NNDMA Fluid Loss Additiv konnte ein ähnliches Verhalten gezeigt werden, da die adsorbierte Menge an Fluid Loss Additiv in Anwesenheit des Verzögerers stark verringert wurde und die Wirksamkeit negativ beeinträchtigte.

Aber auch synergistisches Verhalten wurde bereits untersucht. So konnte festgestellt werden, dass sich CaAMPS®-co-NNDMA und Natrium-Lignosulfonat-Verzögerer gegenseitig in ihrer jeweiligen Wirkung verstärken und daher sehr gut kombinierbar sind. Durch Kopräzipitation beider Polymere bilden sich große Agglomerate, welche die Poren effektiver verstopfen (Verstärkung der Wasserretention) und eine Polymerschicht mit niedriger Permeabilität auf den Zementhydratphasen (verlängerte Verzögerungswirkung) bilden. Erstaunlicherweise handelt es sich hier um zwei anionische Polymere die synergistisch miteinander wechselwirken. Die Studie zeigte, dass diese positive Wechselwirkung über Calciumkomplexe des Lignosulfonats, welche dann positive Ladungen tragen, möglich wird [92].

Im Rahmen der hier vorliegenden Arbeit wurde ein ähnliches synergistisches Verhalten von Celluloseethern mit Fließmitteln auf Melamin-Formaldehyd-Sulfit Basis näher untersucht.

3 Materialien

Dieses Kapitel enthält eine kurze Übersicht der in dieser Arbeit verwendeten anorganischen Bindemittel (Zement, Gipsputz) sowie der untersuchten Polymere (Celluloseether und Fließmittel). Alle weiteren Details zu den Materialien können den angehängten Veröffentlichungen entnommen werden.

3.1 Zemente

In dieser Arbeit wurden der Tiefbohrzement API Class G „black label“ der Firma Dyckerhoff AG, genormt nach den Standards des American Petroleum Institute [93], sowie ein CEM I 52,5N “Milke®“ der Firma HeidelbergCement AG verwendet. Die Klinkerzusammensetzung dieser Zemente wurde mit Röntgenpulverdiffraktometrie (XRD) und *Rietveld*-Auswertung ermittelt. Die Phasenzusammensetzungen wurden an den unbehandelten Zementen (C_3S, C_2S, CaO_{frei} und Portlandit) sowie am Rückstand des Salicylsäureauszugs bestimmt [94]. Die gemessenen Phasengehalte der beiden Zemente sind **Tabelle 3** zu entnehmen.

Tabelle 3 – Phasengehalte der verwendeten Zemente, bestimmt mittels XRD-Messungen und Thermogravimetrie.

Klinkerphase	Anteil [M.-%] im Zement	
	API Class G	CEM I 52,5N
C_3S monoklin	59,6	62,9
C_2S monoklin	22,8	20,4
C_3A kubisch	1,2	3,9
C_3A orthorhombisch	0	3,3
$C_2(A,F)$	13,0	2,3
freies CaO	0,3	0,1
Gips	2,7*	3,5*
$CaSO_4 \cdot 1/2\ H_2O$	0,0*	2,0*
Anhydrit	0,7	2,1

* thermogravimetrisch bestimmt

Zur vollständigen Charakterisierung der Zemente wurden neben den Phasengehalten die Oxid-Zusammensetzungen über Röntgenfluoreszenz (RFA)-Analyse, der Freikalkgehalt nach *Franke* [95] sowie die Korngrößenverteilung der Zemente bestimmt. Eine weitere wichtige Kenngröße stellt die Mahlfeinheit eines Zements dar. Sie wurde nach dem *Blaine*-Verfahren bestimmt [96]. Hierbei ergaben sich eine spezifische Oberfläche von 3.058 cm^2/g für den API Class G Zement und von 3.316 cm^2/g für den CEM I 52,5N.

Zusammenfassend kann der Tiefbohrzement API Class G als C_3A-arm, relativ grob gemahlen und mit einem geringen Freikalkgehalt beschrieben werden. Der CEM I 52,5N „Milke®“ hingegen ist ein typischer Portlandzement, welcher als repräsentativ für hochwertige CEM I-Zemente gesehen werden kann. Die verwendeten Wasser-zu-Zement (w/z) – Werte der Studie lagen bei 0,44 für API Class G Zement sowie bei 0,35, 0,53 und 0,7 für den CEM I 52,5N.

3.2 Leichtgipsputz

Um die Wasserretention in einem Gips-basierten System zu untersuchen, wurde ein kommerzieller Leichtglättputz „Hasit 130“ der Firma Hasit Trockenmörtel GmbH verwendet. Dieses Produkt basiert auf β-Calciumsulfat-Halbhydrat als Bindemittel und enthält etwas Anhydrit. Weitere Bestandteile sind 3 % Kalkhydrat, Feinsand sowie Leichtzuschläge. Außerdem wurde das Produkt speziell für die Untersuchung des Einflusses von Celluloseethern ohne Wasserretentionsmittel und Anti-Absetzmittel (wie beispielsweise Guarether oder Xanthan gum) abgemischt. Lediglich Verzögerer in Form von L(+)-Weinsäure war im Gipsputz als Additiv enthalten, um eine Verarbeitbarkeit von > 50 Minuten zu gewährleisten.

Durch das speziell für die Forschung abgemischte Produkt war es möglich, die Wirkung und den Mechanismus von Celluloseethern in einem praxisrelevanten System zu untersuchen. Zudem konnte durch Vergleich mit der Wirkung in einem zementären System der Einfluss unterschiedlicher Bindemittel auf die Wirkung des Wasserretentionsmittels erforscht werden.

3.3 Celluloseether

Vier verschiedene Celluloseether, „HEC-59“ (HEC) der Firma Dow Chemical Co. (ehemals Union Carbide) sowie “Tylose® HC 50 NP2” (CMHEC), „Tylose® MHB 10000 P2” (MHEC) und „Tylose® MHB 60016 P4” (MHPC) von SE Tylose GmbH & Co. KG, Wiesbaden, mit charakteristischen Eigenschaften (z.B. Ladungsmenge, Viskositätsstufe, Substitutionsgrad) wurden in dieser Studie untersucht. Die Celluloseether sind kommerziell als weiße bis leicht gelbliche Pulver mit einer Korngröße unter 180 µm (Typ P2) oder unter 125 µm (Typ P4) erhältlich. **Abbildung 17** zeigt dies am Beispiel einer MHEC, wobei sich die verschiedenen Celluloseether optisch wenig unterscheiden.

Abbildung 17 – Typisches weiß-gelbes Celluloseether-Pulver; die Korngröße in dieser Probe lag bei < 180 µm.

Die spezifischen Eigenschaften unterschiedlicher Celluloseether-Typen können theoretisch andere Wirkmechanismen bedingen. Um diesen Effekt auszuschalten, wurden Typen mit unterschiedlicher molarer Masse, Substitutionsgrad oder spezifischer anionischer Ladungsmenge verwendet (vgl. **Tabelle 4**). Eine komplette Übersicht der Eigenschaften aller Celluloseether-Proben findet sich in den zugehörigen Publikationen wieder.

Tabelle 4 – Übersicht der wichtigsten Eigenschaften der in dieser Arbeit eingesetzten und untersuchten Celluloseether.

Celluloseether	molare Masse M_w [g/mol]	degree of substitution (DS)	molar degree of substitution (MS)	spezif. anionische Ladungsmenge [C/g] *
HEC	210.000	1,0 (Hydroxyethyl)	1,50 (Hydroxyethyl)	28
CMHEC	260.000	0,43 (Carboxymethyl)	1,01 (Hydroxyethyl)	236
MHEC	248.000	1,8 (Methyl)	0,15 (Hydroxyethyl)	6
MHPC	419.000	1,6 (Methyl)	0,2 (Hydroxypropyl)	8

* in Zementporenlösung gemessen

3.4 Polykondensat-Fließmittel

Bei gleichzeitigem Einsatz von Celluloseethern mit Polykondensat-Fließmitteln konnte ein synergistischer Effekt, welcher eine starke Verbesserung der Wasserretentionswirkung hervorrief, beobachtet werden. Struktur und Synthese typischer Vertreter wurden bereits in Kapitel 2.4.1 genauer beschrieben.

Hier wurde ein kommerzielles Melamin-Formaldehyd-Sulfit (MFS)-Polykondensat („Melment® F10“ der Firma BASF Construction Polymers GmbH, Trostberg) verwendet. Es handelt sich um ein typisches Fließmittel auf Melamin-Basis, allerdings ist der synergistische Effekt den Formulierern auch von anderen Polykondensaten wie β-Naphthalinsulfonsäure-Formaldehyd (NSF) oder Aceton-Formaldehyd-Sulfit (AFS) bekannt.

4 Ergebnisse und Diskussion

Die wichtigsten Erkenntnisse der angehängten Publikationen sind hier zusammengefasst dargestellt und erläutert. Zunächst wird auf die Wirkmechanismen von HEC und CMHEC in Tiefbohrzement eingegangen. Im zweiten Teil wird die Effektivität von MHEC im zementären System und anschließend der Einfluss von Sulfat-Anionen aus Gips-gebundenen Baustoffsystemen auf die Wirksamkeit von MHPC diskutiert.

4.1 Wirkmechanismus von HEC und CMHEC (Publikation 1 und 2)

In diesen Studien wurden die Wirkmechanismen von HEC und CMHEC als Fluid Loss Additive in Tiefbohrzement bei Raumtemperatur untersucht. Hierbei konnten zentrale Eigenschaften wie beispielsweise anionische Ladungsmenge, intrinsische Viskosität sowie die Wirksamkeit gemäß den API-Richtlinien mittels Hochdruckfiltrations-Test bei 70 bar und 27 °C ermittelt werden. Weitere wichtige Methoden zur Beurteilung der Wirkmechanismen beider Polymere stellten zudem die Messung des Zeta-Potentials und die Elektronenmikroskopie dar.

Die Ergebnisse der Studie zeigten, dass die Wirkung beider Polymere im hohen Dosierungsbereich auf der Bildung polymerer 3D-Netzwerkstrukturen durch Assoziation beruht und damit eine physikalische Verstopfung der Filterkuchenporen hervorgerufen wird. Dabei formen sich, wie in **Abbildung 18** schematisch dargestellt, ab einer definierten Konzentration große hydrokolloidale Partikel, welche ein Netzwerk bilden und den Wasserverlust behindern.

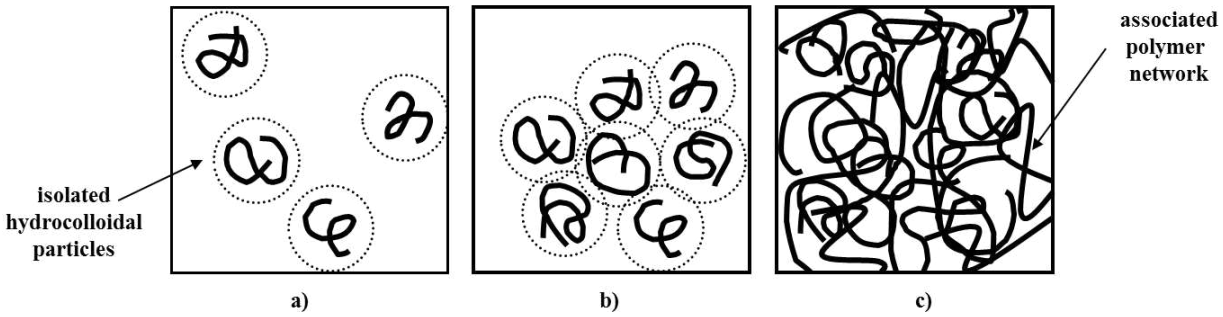

Abbildung 18 – Schematische Darstellung der Assoziation und Bildung eines 3D-Polymernetzwerks a) unterhalb, b) bei und c) oberhalb der kritischen „overlapping concentration“, nach *de Gennes* [97].

In einem System vollständig gelöster, einzeln vorliegender Moleküle beeinflussen sich die Polymerknäuel zunächst nicht (Fall a in **Abbildung 18**); bei Überschreitung der Assoziationskonzentration (sog. „overlapping concentration“) beginnen die sphärischen Polymerknäuel jedoch sich in ein Polymer-Netzwerk mit definierter Maschengröße zu überlagern (Fall b). Dieses Netzwerk verdichtet sich mit steigender Konzentration und ermöglicht somit eine zunehmende Verstopfung der Filterkuchenporen.

Eine Adsorption konnte bei der nicht-ionischen HEC sicher ausgeschlossen werden. Ein bedeutender Unterschied zwischen HEC und CMHEC wurde zudem bei niedrigen Konzentrationen herausgearbeitet. Bei HEC beruht die Wasserretentionswirkung in niedrigen Dosierungsbereichen auf Wassersorption (Wasserbindevermögen) und dem Quellverhalten. Bei CMHEC spielt hingegen ihre stark anionische Ladung eine wichtige Rolle für den Wirkmechanismus, da sie die Adsorption auf der Zementkornoberfläche ermöglicht. Aus wirtschaftlichen Gründen und zur Vermeidung von unerwünschten Verzögerungseffekten werden Anwendungsdosierungen der Celluloseether so niedrig wie möglich gehalten. Daher kann ihre Wirkung bei den verschiedenen Anwendungen und Systemen durchaus auf unterschiedlichen Mechanismen beruhen.

Rasterelektronenmikroskopische Untersuchungen mit verschieden hohen Luftfeuchtigkeiten in der Messkammer zeigten, dass HEC bereits in geringer Dosierung eine sehr große Menge Wasser aufnehmen und binden kann, wobei der Celluloseether auf ein Vielfaches seiner ursprünglichen Größe anschwillt (Quellverhalten). Mittels Zeta-Potential und einem speziellen Filtrationstest konnte herausgefunden werden, dass HEC auf Zement nicht adsorbiert. Dies war zu erwarten, da HEC nicht-ionisch ist.

CMHEC hingegen zeigte aufgrund seiner deutlich höheren anionischen Ladungsmenge von – 236 C/g bis zu einer Dosierung von 0,4 M.-%, bezogen auf Zement, eine Verstärkung des Zeta-Potentials hin zu negativeren Werten und damit deutliche Adsorption (vgl. **Abbildung 19**). Der Wert für reinen Zement beträgt – 6 mV und wird bereits durch 0,1 M.-%, bezogen auf Zement, an CMHEC auf – 10 mV abgesenkt. Abnehmende Zeta-Potential-Werte bedeuten eine verstärkte Belegung der Oberfläche mit CMHEC und stehen damit für eine zunehmende Adsorption des anionischen Polymers.

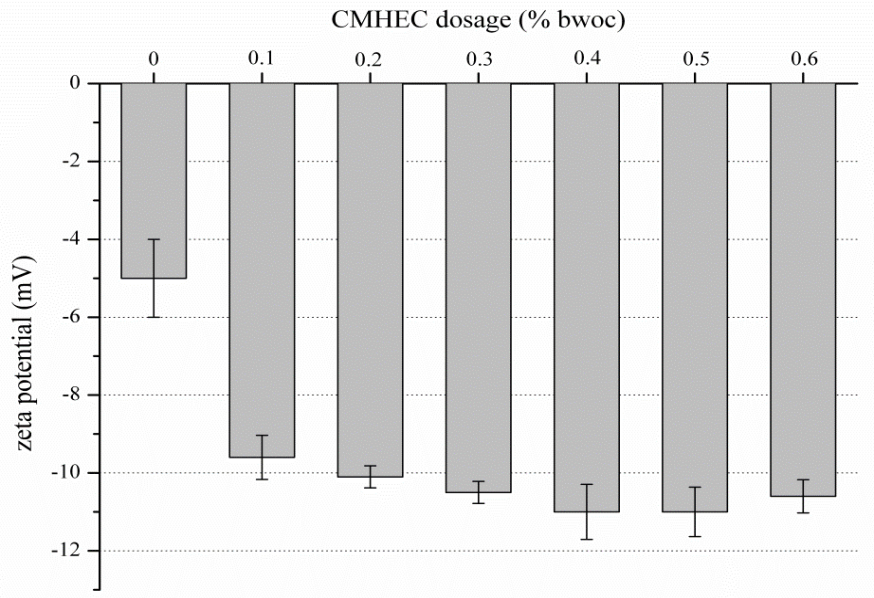

Abbildung 19 – Zeta-Potential einer Zementschlämme (w/z-Wert = 0,44) bei steigender CMHEC Dosierung.

Die beiden untersuchten Celluloseether unterscheiden sich demzufolge bei niedrigeren Konzentrationen wesentlich. Beide beruhen oberhalb ihrer spezifischen „overlapping concentration“ (HEC: ~ 15 g/L; CMHEC: ~ 10 g/L) jedoch auf der Bildung von großen, porenverstopfenden 3D-Polymer-Netzwerken, die eine sehr gute Wasserretention ermöglichen. Das Wasser kann die verengten Filterkuchenporen schlechter passieren und somit ergibt sich eine reduzierte Filtrationsgeschwindigkeit nach *Darcy*.

Des Weiteren konnte bei Anwendung mit MFS-Fließmittel für beide ein synergistischer Effekt beobachtet werden, welcher die Wirkung des Fluid Loss Additivs bei Zugabe von Fließmittel außergewöhnlich verstärkte. Dieser Effekt beruht auf dem Zusammenwirken der beiden Polymere. Messungen des Zeta-Potentials und der dynamischen Lichtstreuung konnten bestätigen, dass eine bestimmte Menge an MFS mit dem Celluloseether interagiert und die Bildung von Assoziaten bereits bei geringerer Konzentration an Fluid Loss Additiv initiiert wird. Dieser Effekt ist äußerst günstig, da bei gleichzeitiger Anwendung der Additive in einer Zementformulierung eine niedrigere Celluloseether-Dosierung notwendig ist.

4.2 Wirkmechanismus von MHEC (Publikation 3)

Zur Untersuchung von MHEC als typischem Vertreter der Celluloseether in Bauanwendungen (z.B. Trockenmörtel) wurde das Wasserrückhaltevermögen durch den Papiertuchtest (siehe Kapitel 2.2.2.4) bestimmt. In der Anwendung von Trockenmörtelprodukten findet häufig eine Filtration des Baustoffsystems an porösen Untergründen statt. Diese Situation wurde durch den einfach konzipierten Papiertuchtest nachgeahmt. Er erlaubte die Zugrundelegung der gleichen Konzepte wie bei der Filtration der Zementschlämme in der Tiefbohrzementierung.

Der Wirkmechanismus von MHEC basiert hier prinzipiell auf zwei separaten Effekten, wobei die Aufnahme von Wasser (Sorption) bei geringeren Dosierungen bis ~ 0,3 M.-%, bezogen auf Zement, (w/z-Wert = 0,53) die entscheidende Rolle spielt. Das Molekül schwillt sehr stark an und bindet den größten Teil des Wassers irreversibel, wie durch Elektronenmikroskopie (ESEM) gezeigt werden konnte. Dieses Verhalten wird bei höheren Dosierungen von der Assoziatbildung (ähnlich zu HEC und CMHEC) unterstützt. Bewiesen werden konnte dies durch konzentrationsabhängige Messung der hydrodynamischen Partikelgröße (vgl. **Abbildung 20**) von MHEC in Zementporenlösung (hohe Ionenstärke und pH ~13) mittels dynamischer Lichtstreuung.

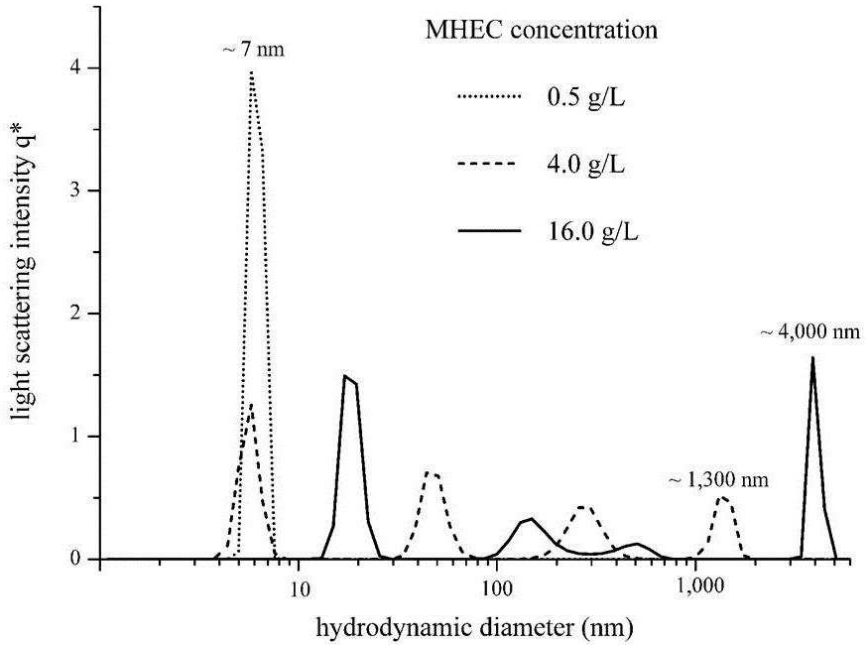

Abbildung 20 – Hydrodynamischer Durchmesser von MHEC-Molekülen bzw. Assoziaten bei verschiedener Konzentration in Zementporenlösung, bestimmt mittels dynamischer Lichtstreuung.

In verdünnter MHEC-Lösung (0,5 g/L) sind die hydrodynamischen Durchmesser mit 6,9 ± 1,1 nm relativ gering. Die Partikelgrößen steigen jedoch mit zunehmender Konzentration rasch an und erreichen bei 16 g/L eine Größe von bis zu 4 µm. Im Zwischenbereich konnte verfolgt werden, wie das Polymer zunehmend assoziiert und sich in Abhängigkeit von der Konzentration immer größere Hydrokolloide bilden.

Für eine hohe Wasserretentionswirkung von Celluloseethern sind folglich mehrere Faktoren wichtig, wobei die physikalische Verstopfung der Filterkuchenporen den stärksten Effekt erzeugt und somit den entscheidenden Parameter darstellt.

4.3 MHPC in Gips-gebundenen System und die Rolle von Sulfat (Publikation 4)

Studien zur Wasserretention von MHPC in einem Leichtgipsputz und der Wirkungsvergleich mit einem zementären System wurden in Publikation 4 durchgeführt. Eine MHPC mit hohem Polymerisationsgrad (Viskosität ~ 60.000 mPa·s) wurde gewählt, da dieser Celluloseether für Anwendungen in Putzen repräsentativ ist.

Aus der Praxis ist allgemein bekannt, dass Gipsputz höhere Dosierungen an Celluloseether erfordert, um eine vergleichbare Wasserretention wie in einem Zement-gebundenen Baustoffsystem zu erreichen. Nach experimenteller Bestätigung dieser Tatsache, wurde der Ursache für den Effekt auf den Grund gegangen. Es ist ebenso bekannt, dass Sulfat auf Polycarboxylat-Fließmittel sehr störend wirken kann. Die Sulfationen der Zement-porenlösung behindern die Adsorption des Polycarboxylatethers über den Mechanismus einer kompetitiven Adsorption [98]. Daher wurde insbesondere der Einfluss von Sulfat auf die Leistungsfähigkeit und den Wirkmechanismus von MHPC untersucht.

Als kritischer Parameter stellte sich wie bereits in Publikation 3 gezeigt die Bildung von großen, porenverstopfenden Hydrokolloiden heraus. Dies zeigte sich anhand dynamischer Lichtstreumessung, bei welcher die Partikel bei 4 und 6 g/L MHPC und steigender Sulfatkonzentration (2 - 14 g/L) untersucht wurden (vgl. **Abbildung 21**).

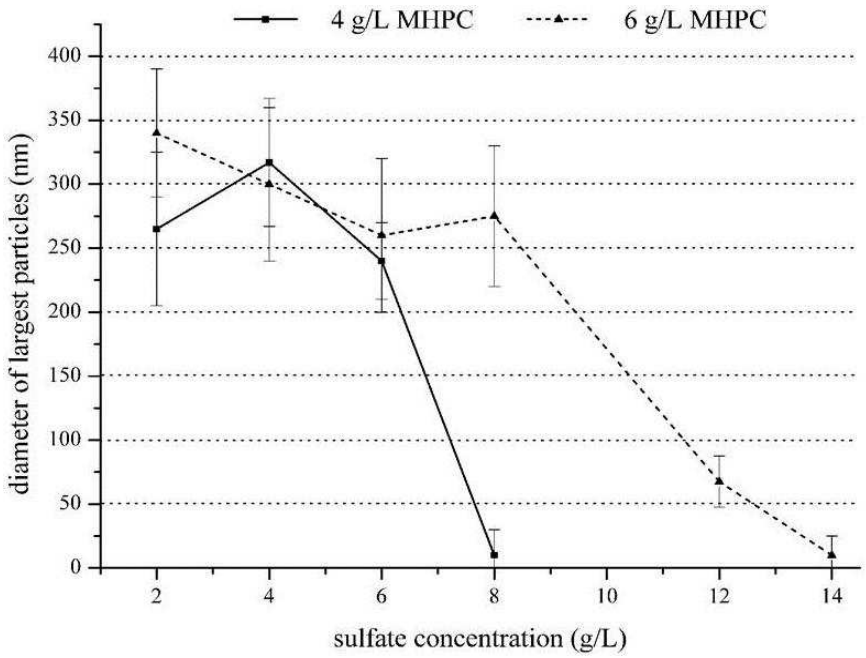

Abbildung 21 – Hydrodynamischer Durchmesser von MHPC-Partikeln in Abhängigkeit der Sulfatkonzentration, gemessen mittels dynamischer Lichtstreuung.

Die Messungen belegten, dass Sulfat-Ionen die Bildung der MHPC-Assoziate behindern und damit eine effektive Porenverstopfung der Bindemittelmatrix erschweren. Folglich waren höhere Dosierungen (Konzentrationen) an MHPC nötig, um eine ausreichende Wasserretention zu erzielen.

Eine Erklärung für diesen negativen Einfluss des Sulfats ist eine Störung der Wasserstoffbrückenbindungen zwischen einzelnen MHPC-Strängen durch den erhöhten Elektrolytgehalt der Porenlösung. Ein ähnlich schädigender, jedoch geringerer Effekt ergab sich z.B. bei Zugabe einer äquimolaren Menge an NaCl zur MHPC-Lösung. Weniger Wasserstoffbrücken führen letztlich dazu, dass höhere Mengen an MHPC nötig sind, um die gewünschte Wechselwirkung zwischen den Molekülen und damit eine ausreichende Assoziation zu erreichen. Dies konnte bereits auch für Polyethylenoxid sowie Polyvinylalkohol gezeigt werden [99, 100].

5 Zusammenfassung und Ausblick

In dieser Dissertation wurden kommerziell verfügbare und traditionell als Zusatzmittel der Tiefbohrindustrie sowie in Baustoffen verwendete Celluloseether (HEC, CMHEC, MHEC und MHPC) auf ihre Wirkmechanismen untersucht. Dies sollte zu einem besseren Verständnis für die zukünftige Weiterentwicklung von Additiven zur Wasserrückhaltung führen und helfen, bestehende Probleme zu erklären und zu lösen.

Es wurden Anwendungen in der Tiefbohrzementierung sowie in konventionellem CEM I (Portlandzement) für Baustoffe betrachtet. Außerdem sollte ein Vergleich zwischen Leichtgipsputz und Zementputz erklären, weshalb die Celluloseether-Dosierungen dieser beiden Systeme in der Anwendung unterschiedlich hoch sind.

Die Ergebnisse in zementären Systemen zeigen, dass sich Celluloseether bezüglich ihres Mechanismus gemäß ihrer charakteristischen Eigenschaften wie Molekulargewicht, Ladungsmenge oder Veretherungsgrad deutlich unterscheiden können. Außerdem muss zwischen den bis ~ 120 °C temperaturstabilen HECs oder CMHECs für die Tiefbohrzementierung sowie den nur bis ~ 60 °C löslichen Methylcellulosen für Baustoffe differenziert werden. Methylcellulosen wirken besonders durch eine enorme Wasseraufnahme (sorptives Quellen) in ihre Struktur, wobei das gebundene Wasser nur teilweise oder schwer wieder abgegeben wird.

Bei Einsatz von MHPC in Leichtgipsputz offenbarte sich ein starker Einfluss des Bindemittels auf die Wirksamkeit des Celluloseethers. Der erhöhte Sulfatgehalt in der Porenlösung von β-Calciumsulfat-Halbhydrat demonstrierte, wie empfindlich das Additiv auf kleine Veränderungen der Umgebung reagieren kann. Diese Erkenntnis muss generell bei bauchemischen Zusatzmitteln beachtet werden, wenn Probleme wie z.B. Funktionsstörungen auftreten. Relativ unscheinbare Parameter wie die Sulfatkonzentration können teure Additive in ihrer Wirkung stark beeinträchtigen. Folglich sollte auch bei der Auswahl eines geeigneten Wasserretentionsmittels bedacht werden, in welchem Bindemittel dieses später Anwendung finden soll.

Der Zentrale Befund dieser Untersuchungen war, dass alle Celluloseether ab einer bestimmten Dosierung beziehungsweise Konzentration auf einem ähnlichen Wirkmechanismus beruhen, wobei sich die Dosierungen voneinander unterscheiden. Um gute Wasserretention zu erreichen, müssen die Poren des sich bildenden Filterkuchens mit einem mittleren Durchmesser von ~ 1 µm verengt beziehungsweise physikalisch verstopft werden.

Bei der Tiefbohrzementierung entsteht der Filterkuchen durch die Druckfiltration an der Formation im Bohrloch, bei Putzen oder Mörteln durch den saugenden Untergrund, z.B. in Form einer Ziegelmauer oder einer Gipskartonplatte. Alle Celluloseether erreichen diese physikalische Verstopfung ab einer definierten Konzentration, welche als „overlapping concentration“ bezeichnet wird. Diese Konzentration ist je nach Celluloseether-Typ individuell unterschiedlich. Bei Überschreiten der „overlapping concentration“ assoziieren die Polymerknäuel zu großen, raumfüllenden 3D-Polymernetzwerken.

Unterhalb der Schwellenkonzentration jedoch unterscheiden sich anionische von nicht-ionischen Produkten. So zeigt die anionische CMHEC klar adsorptives Verhalten und kann bereits in sehr kleinen Dosierungen effektiv den Porendurchmesser verringern. HEC und Methylcellulosen (MHEC, MHPC) als nicht-ionische Polymere hingegen nehmen zunächst viel Wasser in ihre Hydrathülle auf und binden dieses teilweise irreversibel. Allgemein aber liefern alle Produkte bei ausreichend hoher Dosierung ausgezeichnete Wasserretentionswerte. Je nach Celluloseether-Typ müssen auch negative Nebeneffekte wie eine sehr hohe Viskosität des Baustoffs oder starke Verzögerung der Zementhydratation berücksichtigt werden.

Basierend auf der Klärung der Wirkmechanismen von Celluloseethern gemäß dieser Arbeit ergeben sich neue Ansätze für zukünftige Untersuchungen zur Wechselwirkung von Celluloseethern mit anderen, in einer Formulierung enthaltenen Additiven. Da dort stets Kombinationen von Zusatzmitteln zur Anwendung kommen, sind Additiv-Additiv-Interaktionen von besonderem Interesse. Für die Industrie ist das Optimierungspotential durch geschickt gewählte Kombinationen wichtig. So wird typischerweise Hydroxypropylstärke als Stellmittel in Maschinenputz eingesetzt. Der bekannte positive Einfluss dieses Additivs auf die Verdickungswirkung des Celluloseethers wurde bisher nicht genauer ermittelt. Auch eine detaillierte Untersuchung mit anderen Polykondensaten als dem hier untersuchten MFS, z.B. modernen Polycarboxylat-Fließmitteln oder Verdickern wie Welan gum, Xanthan gum oder Diutan gum wäre denkbar. Ergeben sich auch hier Synergismen oder können spezielle Polykondensate oder Polycarboxylate synthetisiert werden, welche besonders effektiv mit Celluloseether-basierten Wasserretentionsmitteln zusammenwirken?

Weiterhin wäre auch eine chemische Modifizierung von Celluloseethern für die Tiefbohrzementierung denkbar, um z.B. die Temperaturbeständigkeit weiter zu erhöhen und den Einsatz bei ultratiefen Bohrungen zu ermöglichen. Da ab ~ 100 °C ausschließlich synthetische Polymere aus relativ teuren Monomeren eingesetzt werden, wäre ein Ersatz durch kostengünstigere Celluloseether vorteilhaft. Es besteht die Frage, ob die Möglichkeit

besteht Substituenten einzuführen, welche das Polymer temperaturstabiler machen. Außerdem müsste ein solches Polymer deutliche Vorteile gegenüber etablierten Hochtemperatur-Additiven wie beispielsweise eine gute Bioabbaubarkeit für offshore-Bohrungen aufweisen.

Bezüglich der Wirksamkeit von Methylcellulosen in Gips-basierten Bindemitteln könnte zukünftig noch ein breiteres Spektrum an Celluloseethern sowie Gipsputzformulierungen untersucht werden, um die Sulfat-Empfindlichkeit mit der chemischen Zusammensetzung des Celluloseethers genauer korrelieren zu können. Außerdem könnte gezeigt werden, ob eine spezielle Formulierung des Gipsputzes den schädlichen Effekt des Sulfats lindern kann. Auch geht der Trend dazu, in Putzen vermehrt Methylhydroxyethylcellulosen anzuwenden, da diese aufgrund der höheren Reaktivität des Ethylenoxids – im Vergleich zum Propylenoxid – schneller und leichter herzustellen sind. Daher sollte auch für MHEC der Einfluss von Sulfat erforscht werden. MHEC ist allerdings deutlich weniger oberflächenaktiv als MHPC und führt deshalb weniger Luftporen in den Putz ein. Bei Verwendung von MHEC in Putzen muss daher zusätzlich ein Tensid zugesetzt werden, um ausreichend Luftporen einzuführen und damit die Ergiebigkeit des Putzes zu erhöhen.

6 Literaturliste

[1] Dönges, R.: *Non-Ionic Cellulose Ethers*, British Polymer Journal 23, **1990**, 315-326.

[2] Klemm, D.; Heublein, B.; Fink, H.-P.; Bohn, A.: *Cellulose: faszinierendes Biopolymer und nachhaltiger Rohstoff*, Angewandte Chemie 117, **2005**, 3422-3458.

[3] Brandt, L.: *Cellulose ethers,* In: *Industrial Polymers Handbook (Band 3)*, Ed.: Wilks, E. S., Wiley-VCH: Weinheim, **2001**, 1569-1613.

[4] Sagmeister, C.: *Untersuchungen zum Wirkmechanismus von Wasserretentionsmitteln im zementären Bindemittelsystem*, Diplomarbeit, Technische Universität München, Lehrstuhl für Bauchemie, **2003**.

[5] Bülichen, D.: *Die Bildung von Molekülassoziaten der Hydroxyethylcellulose und ihre Bedeutung für die Wasserretentionswirkung in Zement*, Master's Thesis, Technische Universität München, Lehrstuhl für Bauchemie, **2009**.

[6] Thielking, H.; Schmidt, M.: *Cellulose Ethers,* In: *Ullmann's Encyclopedia of Industrial Chemistry*, Wiley-VCH: Weinheim, **2006**, 1-18.

[7] Suida, W.: *Über den Einfluss der aktiven Atomgruppen in den Textilfasern auf das Zustandekommen von Färbungen*, Monatshefte Chemie 26, **1905**, 413-427.

[8] Lilienfeld, L.: *Alkyl ethers of cellulose and process of making the same*, US 1,188,376, **1916**.

[9] Leuchs, O.: *Verfahren zur Darstellung von Cellulosederivaten*, DE 322,586, **1912**.

[10] Dreyfus, H.: *Procédé pour la fabrication d'éthers cellulosiques et de leurs produits de transformation*, FR 462,274, **1912**.

[11] Jansen, E.: *Verfahren zur Herstellung von Celluloseverbindungen*, DE 332,203, **1918**.

[12] Hubert, E.: *Verfahren zur Darstellung von Cellulosederivaten*, DE 363,192, **1920**.

[13] Plank, J.: *Applications of Biopolymers in Construction Engineering,* In: *Biopolymers*, Ed.: Steinbüchel, A., Wiley-VCH: Weinheim, **2003**, 29-95.

[14] Klemm, D.; Schmauder, H.-P.; Heinze, T.: *Cellulose,* In: *Biopolymers, Vol 6: Polysaccharides II*, Eds.: Steinbüchel, A., De Baets, S., Vandamme, E., Wiley-VCH: Weinheim, **2002**, 275-319.

[15] Nelson, E. B.; Guillot, D.: *Well Cementing (2nd Edition),* Schlumberger: Sugar Land, **2006**.

[16] Müller, I.; Schweizer, D.; Hohn, W.; Bosbach, D.; Putnis, A.; Weyer, H.; Schmitt, B.: *Influence of Cellulose Ethers on the Kinetics of Early Portland Cement Hydration*, GDCh-Monographie Band 36, **2006**, 3-10.

[17] Müller, I.: *Influence of cellulose ethers on the kinetics of early Portland cement hydration,* Dissertation, Westfälische Wilhelms-Universität Münster: **2006**.

[18] Fink, J. K.: *Oil Field Chemicals,* Gulf Professional Publishing:: Burlington, MA, **2003**.

[19] The Dow Chemical Company, *CELLOSIZE™ Hydroxyethyl cellulose (HEC) polymers for use in oilfield cementing applications*, dow.com/webapps/lit/litorder.asp?filepath=cello/pdfs/noreg/325-00039.pdf&pdf=true (Abruf am: 28.09.11).

[20] Lutz, H.; Bayer, R.: *Dry Mortars,* In: *Ullmann's Encyclopedia of Industrial Chemistry*, Wiley-VCH: Weinheim, **2010**, 1-41.

[21] Jenni, A.; Holzer, L.; Zurbriggen, R.; Herwegh, M.: *Influence of polymers on microstructure and adhesive strength of cementitious tile adhesive mortars*, Cement and Concrete Research 35, **2005**, 35-50.

[22] Grover, J. A.: *Methylcellulose and its derivatives,* In: *Industrial Gums*, Eds.: Whistler, R. L., BeMiller, J. N., Academic Press: San Diego, **1993**, 475-504.

[23] Statistisches Bundesamt Deutschland, destatis.de (Abruf am: 17.07.12).

[24] Koslowski, T.; Ludwig, U.: *Zum Einfluß von Zusätzen bei der Herstellung und Anwendung von Baugipsen*, ZKG International 52, **1999**, 274-286.

[25] Dönges, R.: *Entwicklung in der Herstellung und Anwendung von Celluloseethern*, Das Papier 51, **1997**, 653-660.

[26] SE Tylose GmbH & Co. KG, *Herstellung Celluloseether*, setylose.de/wDeutsch/grundlagen/Herstellung_Tylose/3_2_Herstellung_Chemie.pdf (Abruf am: 26.11.2012).

[27] Williamson, A.: *Über die Theorie der Aetherbildung*, Liebigs Annalen der Chemie 77, **1851**, 37-49.

[28] Rosell, K.-G.: *Distribution of Substituents in Methylcellulose*, Journal of Carbohydrate Chemistry 7, **1988**, 525-536.

[29] Wirick, M. G.: *Study of the substitution pattern of hydroxyethylcellulose and its relationship to enzymic degradation*, Journal of Polymer Science Part A-1: Polymer Chemistry 6, **1968**, 1705-1718.

[30] Engelskirchen, K.: *Umwandlung von Cellulose* In: *Methoden der organischen Chemie, Vierte Ausgabe*, Ed.: Bartel, H., Falbe, J., Thieme: Stuttgart-New York, **1987**, 2051-2058.

[31] Savage, A. B.; Young, A. E.; Maasberg, A. T.: *Cellulose and Cellulose Derivates,* In: *High Polymers, Vol V, Part II*, Eds.: Ott, E., Spurlin, H. M., Grafflin, M. W., Interscience: New York, **1954**, 882.

[32] Chang, S. A.; Gray, D. G.: *The surface tension of aqueous hydroxypropyl cellulose solutions*, Journal of Colloid and Interface Science 67, **1978**, 255-265.

[33] SE Tylose GmbH & Co. KG, *Grenzflächenaktivität*, setylose.de/wDeutsch/grundlagen/Eigenschaften_Tylose/Grenzflaechenaktivitaet/index.php (Abruf am: 26.11.2012).

[34] Sarkar, N.: *Thermal gelation properties of methyl and hydroxypropyl methylcellulose*, Journal of Applied Polymer Science 24, **1979**, 1073-1087.

[35] Takahashi, S.-I.; Fujimoto, T.; Miyamoto, T.; Inagaki, H.: *Relationship between distribution of substituents and water solubility of O-methyl cellulose*, Journal of Polymer Science Part A: Polymer Chemistry 25, **1987**, 987-994.

[36] *Technische Grundlagen zu Celluloseethern,* In: *Produktinformation SE Tylose® GmbH & Co KG*, SE Tylose GmbH & Co. KG: Wiesbaden, **2005**, 17.

[37] Mondt, J. L.: *The use of cellulose derivatives in the paint and building industries,* In: *Cellulose sources and exploitation*, Eds.: Kennedy, J. F., Phillips, G. O., Williams, P. A., Ellis Horwood: New York, **1990**, 269-278.

[38] Schulz, L.; Seger, B.; Burchard, W.: *Structures of cellulose in solution*, Macromolecular Chemistry and Physics 201, **2000**, 2008-2022.

[39] Burchard, W.; Schulz, L.: *Lösungsstruktur verschiedener Cellulose-Derivate*, Das Papier 47, **1993**, 1-10.

[40] Burchard, W.: *Solubility and Solution Structure of Cellulose Derivatives*, Cellulose 10, **2003**, 213-225.

[41] Sagmeister, C.; Winter, C.; Sun, L.; Seebauer, M.; Plank, J.: *Wirkmechanismus von Celluloseether-basierten Wasserretentionsmitteln*, GDCh-Monographie Band 27, **2003**, 195-201.

[42] Burchard, W.; Schulz, L.; Seger, B.: *Lichtstreuuntersuchungen an Polysaccharidlösungen*, Das Papier 48, **1994**, 755-764.

[43] Knapen, E.; Van Gemert, D.: *Cement hydration and microstructure formation in the presence of water-soluble polymers*, Cement and Concrete Research 39, **2009**, 6-13.

[44] Pourchez, J.; Grosseau, P.; Ruot, B.: *Current understanding of cellulose ethers impact on the hydration of C_3A and C_3A-sulphate systems*, Cement and Concrete Research 39, **2009**, 664-669.

[45] Pourchez, J.; Grosseau, P.; Ruot, B.: *Changes in C_3S hydration in the presence of cellulose ethers*, Cement and Concrete Research 40, **2010**, 179-188.

[46] Pourchez, J.; Peschard, A.; Grosseau, P.; Guyonnet, R.; Guilhot, B.; Vallée, F.: *HPMC and HEMC influence on cement hydration*, Cement and Concrete Research 36, **2006**, 288-294.

[47] Hohn, W.: *New Cellulose Ethers with Minimized Cement Set Retardation Effect,* In: *Drymix Mortar Yearbook 2007 (First International Drymix Mortar Conference idmmc one, Nürnberg, Germany, 09 May 2007)*, Ed.: Leopolder, F.: **2007**, 80-85.

[48] Plank, J.: Kunststoffforschung Bauchemie: *Anwendung synthetischer Wasserretentionsmittel in der Bauchemie*, Chemanager Spezial 1, **2000**.

[49] Rao, P. S.; Burkhalter, J. F.: *Hydrolytically stable polymers for use in oil field cementing methods and compositions*, **1985**, US 4,555,269.

[50] Tiemeyer, C.; Plank, J.: *Synthesis, characterization, and working mechanism of a synthetic high temperature (200°C) fluid loss polymer for oil well cementing containing allyloxy-2-hydroxy propane sulfonic (AHPS) acid monomer*, Journal of Applied Polymer Science, **2012**, DOI: 10.1002/app.38262.

[51] Smith, D. K.: *Cementing (2nd Ed.),* Society of Petroleum Engineers Inc.; SPE Monograph: New York, **1990**.

[52] Dugonjić-Bilić, F.: *Chemical Admixtures for Oil Well and CO_2-Tolerant Cements: Synthesis, Characterization, Effectiveness and Working Mechanism*, Dissertation, Technische Universität München, Lehrstuhl für Bauchemie, **2010**.

[53] Smith, R. C.: *Successful Primary Cementing Can Be a Reality*, Journal of Petroleum Technology, **1984**, 1851.

[54] *API Recommended Practice 10B-2, 1st ed.*, American Petroleum Institute, Washington, USA, **2005**.

[55] *Instruction manual, HPHT Filter Press 500ML*, Ofite Testing Equipment, Houston, Texas, USA, **2003**.

[56] Recalde Lummer, N.: *Adsorption behavior and effectiveness of AMPS®-based cement fluid loss additives at high temperature and in combination with lignosulfonate and biogums*, Dissertation, Technische Universität München, Lehrstuhl für Bauchemie, **2010**.

[57] Guldner, M.: *Production and Processing of Dry, Factory-Mixed Mortars*, ZKG (Zement, Kalk, Gips) International 52, **1999**, 628-631.

[58] Konietzko, A.: *The Application of Modern Dry, Factory Mixed Mortar Products*, ZKG (Zement, Kalk, Gips) International 48, **1985**, 625-659.

[59] Plank, J.: *Knauf PFT G5 Verputzmaschine, Informationsmaterial,* Vorlesung Bauchemie III, Technische Universität München, Lehrstuhl für Bauchemie: **2012**.

[60] *Testing of Mortars Containing Mineral Binders; Part 7: Determination of Water Retentivity of Freshly Mixed Mortar by the Filter Plate Method*, Standard DIN 18555-7, Deutsches Institut für Normung, **2000**.

[61] *Building lime - Part 2: Test methods*, European Commitee for Standardization, EN 459-2, **2010**.

[62] Desbrières, J.: *Cement Cake Properties In Static Filtration - Influence Of Polymeric Additives On Cement Filter Cake Permeability*, Cement and Concrete Research 23, **1993**, 347-358.

[63] Desbrières, J.: *Cement cake properties in static filtration. On the role of fluid loss control additives on the cake porosity*, Cement and Concrete Research 23, **1993**, 1431-1442.

[64] Dhir, R. K.; Hewlett, P. C.; Dyer, T. D.: *Mechanism of water retention in cement pastes containing a self-curing agent*, Magazine of Concrete Research 50, **1998**, 85-90.

[65] Fringant, C.; Desbrières, J.; Milas, M.; Rinaudo, M.; Joly, C.; Escoubes, M.: *Characterisation of sorbed water molecules on neutral and ionic polysaccharides*, International Journal of Biological Macromolecules 18, **1996**, 281-286.

[66] Plank, J.; Brandl, A.; Zhai, Y. N.; Franke, A.: *Adsorption behavior and effectiveness of poly(N,N-dimethylacrylamide-co-Ca 2-acrylamido-2-methylpropanesulfonate) as cement fluid loss additive in the presence of acetone-formaldehyde-sulfite dispersant*, Journal of Applied Polymer Science 102, **2006**, 4341-4347.

[67] Plank, J.; Dugonjić-Bilić, F.; Recalde Lummer, N.; Taye, S.: *Working mechanism of poly(vinyl alcohol) cement fluid loss additive*, Journal of Applied Polymer Science 117, **2010**, 2290-2298.

[68] Dugonjić-Bilić, F.; Plank, J.: *Polyelectrolyte Complexes from Polyethylene Imine/Acetone Formaldehyde Sulfite Polycondensates: A Novel Reagent for Effective Fluid Loss Control of Oil Well Cement Slurries*, Journal of Applied Polymer Science 121, **2011**, 1262-1275.

[69] Pourchez, J.; Ruot, B.; Debayle, J.; Pourchez, E.; Grosseau, P.: *Some aspects of cellulose ethers influence on water transport and porous structure of cement-based materials*, Cement and Concrete Research 40, **2010**, 242-252.

[70] Patural, L.; Porion, P.; Van Damme, H.; Govin, A.; Grosseau, P.; Ruot, B.; Devès, O.: *A pulsed field gradient and NMR imaging investigations of the water retention mechanism by cellulose ethers in mortars*, Cement and Concrete Research 40, **2010**, 1378-1385.

[71] Schweizer, D.: *The Role Of Cellulose Ethers in Gypsum Machine Plaster,* In: *ConChem - International Exhibition & Conference - Conference Proceedings*, Verlag für chemische Industrie, H. Ziolkowsky GmbH: Düsseldorf, **1997**, 277-284.

[72] Schweizer, D.; Dewald, G.: *Rheological Evaluation of Mortars Containing Cellulose Ethers,* In: *Industrial Water Soluble Polymers*, Ed.: Finch, C. A., Royal Society of Chemistry: Manchester, **1996**, 42-51.

[73] Yammamuro, H.; Izumi, T.; Mizunuma, T.: *Study of non-adsorptive viscosity agents applied to self-compacting concrete*, 5th CANMET/ACI International Conference on Superplasticizers and Other Chemical Admixtures in Concrete, ACI SP-173, Detroit, **1997**, 427-444.

[74] Jenni, A.; Herwegh, M.; Zurbriggen, R.; Aberle, T.; Holzer, L.: *Quantitative microstructure analysis of polymer-modified mortars*, Journal of Microscopy 212, **2003**, 186-196.

[75] Jenni, A.; Zurbriggen, R.; Herwegh, M.; Holzer, L.: *Changes in microstructures and physical properties of polymer-modified mortars during wet storage*, Cement and Concrete Research 36, **2006**, 79-90.

[76] Elotex AG, elotex.de/Elotex/Western+Europe/German/Innovation/Applied+Research.htm (Abruf am: 26.11.2012).

[77] Marliere, C.; Mabrouk, E.; Lamblet, M.; Coussot, P.: *How water retention in porous media with cellulose ethers works*, Cement and Concrete Research 42, **2012**, 1501-1512.

[78] Brandl, A.: *Die Interaktion zwischen CaAMPS®-co-NNDMA und Aceton-Formaldehyd-Sulfit-Polykondensat bei der Adsorption an Zement: Ein Beispiel für Zusatzmittelunverträglichkeiten und Wege zu deren Lösung*, Dissertation, Technische Universität München, Lehrstuhl für Bauchemie, **2007**.

[79] Weaver, J.; Ravi, K. M.; Eoff, L. S.; Gdanski, R.; Wilson, M. J.: *Drilling fluid and filter cake removal methods and compositions*, Halliburton Company, US 5,501,276, **1996**.

[80] Plank, J.; Dugonjić-Bilić, F.; Lummer, N. R.: *Modification of the molar anionic charge density of acetone-formaldehyde-sulfite dispersant to improve adsorption behavior and effectiveness in the presence of CaAMPS®-co-NNDMA cement fluid loss polymer*, Journal of Applied Polymer Science 111, **2009**, 2018-2024.

[81] Yunchao, H.; Fansen, Z.; Hu, Y.; Chunying, L.; Zhaoqiang, W.; Weining, L.; Shukai, Y.: *Synthesis and properties of high-sulfonated melamine-formaldehyde resin*, Journal of Applied Polymer Science 56, **1995**, 1523-1526.

[82] Nachbaur, L.; Nkinamubanzi, P.-C.; Nonat, A.; Mutin, J.-C.: *Electrokinetic Properties which Control the Coagulation of Silicate Cement Suspensions during Early Age Hydration*, Journal of Colloid and Interface Science 202, **1998**, 261-268.

[83] Bajpai, A. K.: *Interface Behaviour of Ionic Polymers*, Progress in Polymer Science 22, **1997**, 523-564.

[84] Hirsch, C.: *Untersuchungen zur Wechselwirkung zwischen polymeren Fließmitteln und Zementen bzw. Mineralphasen der frühen Zementhydratation*: Dissertation, Technische Universität München, Lehrstuhl für Bauchemie, **2005**.

[85] Mollah, M. Y. A.; Adams, W. J.; Schennach, R.; Cocke, D. L.: *A review of cement-superplasticizer interactions and their models*, Advances in Cement Research 12, **2000**, 153-161.

[86] Elias, H.-G.: *Makromoleküle, Band 2,* 6. Auflage, Wiley-VHC Verlag: Weinheim, **1999**.

[87] Plank, J.: *40 Jahre Fließmittel - von Polykondensaten zu Polycarboxylaten*, GDCh-Monographie Band 24, **2002**, 13-17.

[88] Plank, J.; Brandl, A.; Lummer, N. R.: *Effect of different anchor groups on adsorption behavior and effectiveness of poly(N,N-dimethylacrylamide-co-Ca 2-acrylamido-2-methylpropanesulfonate) as cement fluid loss additive in presence of acetone–formaldehyde–sulfite dispersant*, Journal of Applied Polymer Science 106, **2007**, 3889-3894.

[89] Plank, J.; Brandl, A.; Vlad, D.; Chatziagorastou, P.: *Kompetitive Adsorption von anionischen Zusatzmitteln am Beispiel Fließmittel - Verzögerer - Wasserretentionsmittel*, GDCh-Monographie Band 31, **2004**, 189-193.

[90] Recalde Lummer, N.: *Kompetitive Adsorption zwischen N,N-Dimethylacrylamid-Co- und Terpolymeren und Aceton-Formaldehyd-Sulfit-Polykondensat an Tiefbohrzement*, Master's Thesis, Technische Universität München, Lehrstuhl für Bauchemie, **2006**.

[91] Tiemeyer, C.; Plank, J.: *Working mechanism of a high temperature (200°C) synthetic cement retarder and its interaction with an AMPS®-based fluid loss polymer in oil well cement*, Journal of Applied Polymer Science 124, **2012**, 4772-4781.

[92] Recalde Lummer, N.; Plank, J.: *Combination of lignosulfonate and AMPS®-co-NNDMA water retention agent - An example for dual synergistic interaction between admixtures in cement*, Cement and Concrete Research 42, **2012**, 728-735.

[93] *API Specification 10A, 23rd ed.*, American Petroleum Institute, Washington, USA, **2002**.

[94] Le Saoût, G.; Kocaba, V.; Scrivener, K.: *Application of the Rietveld method to the analysis of anhydrous cement*, Cement and Concrete Research 41, **2011**, 133-148.

[95] Franke, B.: *Bestimmung von Calciumoxyd und Calciumhydroxyd neben wasserfreiem und wasserhaltigem Calciumsilikat*, Zeitschrift für anorganische und allgemeine Chemie 247, **1941**, 180-184.

[96] Gille, F.: *Die Prüfung der Mahlfeinheit mit dem Gerät von Blaine*, Zement-Kalk-Gips IV 4, **1951**, 85-89.

[97] de Gennes, P. G.: *Scaling Concepts in Polymer Physics,* Cornell University Press: Ithaca, New York, **1979**.

[98] Habbaba, A.; Zouaoui, N.; Plank, J.: *Synergistic and Antagonistic Effect of SO_4^{2-} Ions on the Dispersing Power of PC*, ACI Materials Journal, accepted on 14th of December 2012, **2012**.

[99] Briscoe, B.; Luckham, P.; Zhu, S.: *Rheological Study of Poly(ethylene oxide) in Aqueous Salt Solutions at High Temperature and Pressure*, Macromolecules 29, **1996**, 6208-6211.

[100] Briscoe, B.; Luckham, P.; Zhu, S.: *The effects of hydrogen bonding upon the viscosity of aqueous poly(vinyl alcohol) solutions*, Polymer 41, **2000**, 3851-3860.

Publikation 1

Role of Colloidal Polymer Associates for the Effectiveness of Hydroxyethyl Cellulose as a Fluid Loss Control Additive in Oil Well Cement

Bülichen, D., Plank, J.

Journal of Applied Polymer Science 126, Special Issue:
Polysaccharides (2012), E25-E34

Role of Colloidal Polymer Associates for the Effectiveness of Hydroxyethyl Cellulose as a Fluid Loss Control Additive in Oil Well Cement

Daniel Bülichen, Johann Plank

Institute for Inorganic Chemistry, Technische Universität München, Lichtenbergstrasse 4, 85747 Garching, Germany

Received 5 April 2011; accepted 23 November 2011
DOI 10.1002/app.36529
Published online 7 February 2012 in Wiley Online Library (wileyonlinelibrary.com).

ABSTRACT: The working mechanism of hydroxyethyl cellulose (HEC) as a fluid loss additive in oil well cement was investigated. The specific anionic charge amount, intrinsic viscosity, and associative behavior in a cement pore solution were determined. The fluid loss performance was probed through the static filtration of cement slurries. HEC achieves fluid loss control by reducing cement filtercake permeability. No influence on the filtercake microstructure was observed. ζ Potential measurements and a special filtration test indicated that no adsorption on cement occurred. Environmental scanning electron microscopy images revealed that in a wet environment, HEC swelled to a multiple of its size and possessed an enormous water-sorption capacity. Concentration-dependent measurements of the hydrodynamic diameter of HEC dissolved in a cement pore solution showed that large associates were formed. These colloidal associates physically obstructed the filtercake pores. Finally, the addition of sulfonated melamine formaldehyde dispersant to the cement slurries containing HEC greatly improved the fluid loss control. A specific interaction was responsible for this synergistic effect. © 2012 Wiley Periodicals, Inc. J Appl Polym Sci 126: E25–E34, 2012

Key words: hydroxyethyl cellulose; fluid loss additive; working mechanism; dispersant; oil well cement

INTRODUCTION

Oil well cementing is considered one of the most important operations performed in the construction of a well bore.[1,2] The placement of the cement slurry under pressure across a permeable formation, however, may lead to rapid dehydration and result in poor pumpability and incomplete cement hydration. To control the properties of oil well cement slurries, admixtures are included in the formulation.[3] Fluid loss additives (FLAs) are applied to reduce uncontrolled water loss from the slurry while it is pumped along porous formations in the bore hole.[4,5] Because of their environmental compatibility and good performance at temperatures up to 150°C, cellulose ethers are popular FLAs. Hydroxyethyl cellulose (HEC) is among the most widely used cellulosic fluid loss control agents, whereas carboxymethyl hydroxyethyl cellulose is less common.[6,7] Here, the working mechanism of HEC as an FLA in oil well cement was investigated.

According to previous studies by Desbrières,[8,9] three fundamental working mechanisms for polymeric FLAs are known: First, an increased dynamic viscosity (η_{dyn}) of the cement filtrate stemming from polymer addition can decelerate the filtration rate. Second, anionic FLAs may adsorb onto hydrating cement particles and obstruct the cement filtercake pores by polymer segments, which either freely protrude into the pore space or even bridge cement particles. Through this adsorptive mechanism, filtercake permeability is reduced, and a low fluid loss is achieved. Third, once a certain polymer dosage is exceeded, FLAs may plug cement filtercake pores through the formation of a polymer film or through associates, which can bind an enormous amount of water molecules in their inner sphere and hydrate shells. This way, a large portion of the mixing water is physically bound and will not be released during the filtration process.

In recent studies, we investigated the fluid loss behaviors of 2-acrylamido-2-methylpropanesulfonic acid-*co*-*N*,*N*-dimethylacrylamide (CaAMPS®-*co*-NNDMA)[10] and poly(vinyl alcohol).[11] We found that these FLAs worked either by adsorption onto the surface of the hydrating cement (CaAMPS®-*co*-NNDMA) or by physical plugging as a result of polymer film formation [poly(vinyl alcohol)]. Recent publications have discussed the influence of cellulose ethers on water transport in the porous structure of cement-based materials and investigated their effect on cement hydration.[12,13] However, the fundamental processes underlying the mechanism for water retention have yet not been investigated

Correspondence to: J. Plank (johann.plank@bauchemie.ch.tum.de).

TABLE I
Phase Composition (quantitative X-ray diffraction, Rietveld), Specific Density, Specific Surface Area (Blaine), and d_{50} Value of API Class G Oil Well Cement Sample

C_3S (wt %)	C_2S (wt %)	C_3A_c (wt %)	C_4AF (wt %)	CaO (wt %)	$CaSO_4 \cdot 2H_2O$ (wt %)	$CaSO_4 \cdot 0.5\ H_2O$ (wt %)	$CaSO_4$ (wt %)	Specific density (kg/L)	Specific surface area (cm^2/g)	d_{50} value (μm)
59.6	22.8	1.2	13.0	<0.3	2.7[a]	0.0[a]	0.7	3.18	3,058	11

C_3S, tricalcium silicate [$Ca_3(SiO_4)O$]; C_2S, dicalcium silicate (Ca_2SiO_4); C_3A_c, cubic modification of tricalcium aluminate ($Ca_9Al_6O_{18}$); C_4AF, tetra calcium aluminate ferrite ($Ca_4Al_2Fe_2O_{10}$).
[a] Measured by thermogravimetry.

thoroughly. For that reason, the filtercake permeability and dynamic filtrate viscosity of high-pressure (HP)/high-temperature (HT) filtrates from American Petroleum Institute (API) class G oil well cement slurries incorporating HEC were measured here. Furthermore, HEC adsorption on cement was probed via ζ potential and adsorption measurements. Finally, the concentration-dependent hydrodynamic diameters of the HEC particles present in the cement pore solution were determined.

In addition to FLAs, oil well cement slurries often contain dispersants. It has been shown before that different additives can interact with each other. This can lead to either severe incompatibility or a positive synergistic effect.[11,14] Surprisingly, it was found that sulfonated melamine formaldehyde (SMF) addition to cement slurries containing HEC greatly improved the fluid loss control. This effect was unexpected because when used individually, dispersants such as SMF typically increase fluid loss. To understand the mechanism of interaction between HEC and SMF, the η_{dyn} value of the cement filtrates and the ζ potential of the cement slurries containing both admixtures were measured. Moreover, the synergistic effect of the combination was investigated by quantification of the hydrodynamic diameters of the polymers present in the cement pore solution.

EXPERIMENTAL

Materials

Oil well cement

An API class G oil well cement (black label from Dyckerhoff AG, Wiesbaden, Germany) corresponding to API specification 10A was used.[15] Its clinker composition was determined through powder quantitative X-ray diffraction (QXRD) technique with Rietveld refinement. The amounts of gypsum ($CaSO_4 \cdot 2H_2O$) and hemihydrate ($CaSO_4 \cdot 0.5H_2O$) present in the cement sample were measured by thermogravimetry. Free lime (CaO) was quantified by the extraction method established by Franke.[16] Using a Blaine instrument, we determined the specific surface area to be 3,058 cm^2/g. The specific density of this sample was 3.18 kg/L, as measured by helium pycnometry. The particle size distribution of the cement sample was determined by a laser-based particle size analyzer. Its average particle size distribution (d_{50}) value was 11 μm (see Table I).

HEC

A commercial sample of HEC (HEC-59, Cellosize®, Dow Chemical Co., Midland, MI) was used. The Brookfield viscosity of an aqueous solution containing 2 wt % of this FLA was 185 mPa·s, as measured at 27°C. The chemical structure of the HEC sample is presented in Figure 1. Its characteristic properties are shown in Table II. Size exclusion chromatography (SEC) analysis (HEC concentration = 0.2 wt % in 0.2*M* $NaNO_3$ at pH 9 adjusted with NaOH) produced molar masses for the FLA of about 2.1×10^5 g/mol [weight-average molecular weight (M_w)] and 1.2×10^5 g/mol [number-average molecular weight (M_n)]. With SEC analysis, a hydrodynamic radius [$R_{h(z)}$] of 20.5 nm and a gyration radius [$R_{g(z)}$] of 27.1 nm were found for this polymer. In an alkaline cement pore solution, HEC exhibited a specific anionic charge amount of −28 C/g, as measured by charge titration with poly(diallyl dimethylammonium chloride (polyDADMAC) as a cationic polymer.[17] This negative charge was due to partial deprotonation of the hydroxyl groups present in the anhydroglucose rings of HEC.

SMF polycondensate

A commercial sample of SMF (Melment® F10, BASF Construction Polymers GmbH, Trostberg, Germany) was used. The chemical structure of the SMF polycondensate is presented in Figure 1. SEC analysis (eluent = 0.1M $NaNO_3$ at pH 10 adjusted with NaOH) produced molecular weights for the FLA of about 2.0×10^5 g/mol (M_w) and $1.4 \cdot \times 10^5$ g/mol (M_n). $R_{h(z)}$ of this polymer was found to be 1.6 ± 0.08 nm. In a cement pore solution, SMF provided a specific anionic charge amount of −269 C/g.

Instruments

Cement characterization

The phase composition of the cement sample was obtained by X-ray powder diffraction with a Bruker

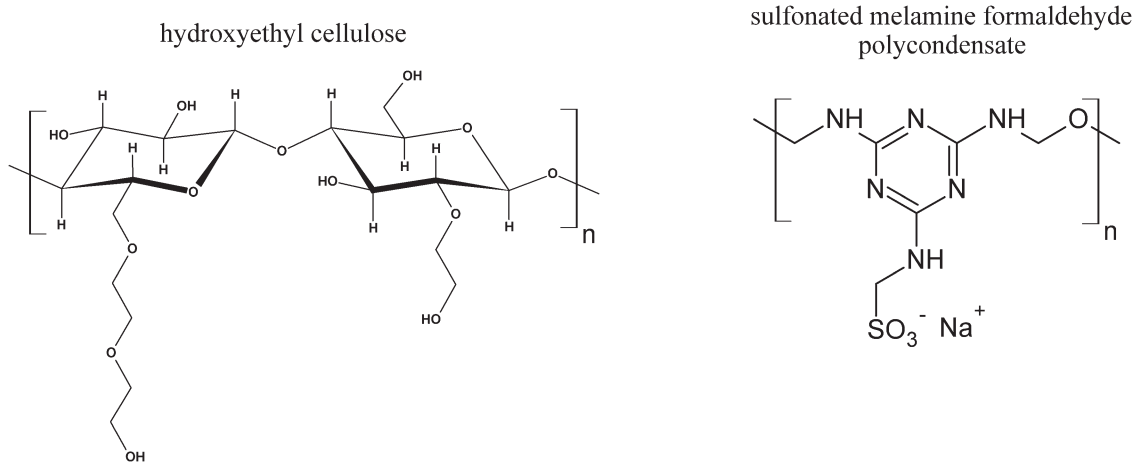

Figure 1 Chemical structures of the HEC fluid loss polymer possessing a degree of substitution of 1.0 and a molar degree of substitution of 1.5 and the SMF polycondensate dispersant.

AXS D8 Advance instrument from Bruker (Karlsruhe, Germany) with Bragg–Bretano geometry. Topas 3.0 software from Bruker (Karlsruhe, Germany) was used to quantify the amounts of individual phases present in the sample according to Rietveld's method of refinement.[18] The instrument was equipped with a scintillation detector with Cu Kα radiation (λ = 1.5406 Å) with a scanning range between 2θ values of 5 and 80°. $CaSO_4 \cdot 2H_2O$ and $CaSO_4 \cdot 0.5H_2O$ present in the cement sample were quantified by thermogravimetry with an STA 409 CD instrument (Netzsch Gerätebau GmbH, Selb, Germany). Measurement was conducted under a nitrogen atmosphere at a heating rate of 10°C/min. The specific density of the cement sample was measured on an Ultrapycnometer 1000 (Quantachrome Instruments, Boynton Beach, FL). The specific surface area of the sample was determined with a Blaine instrument (Toni Technik, Berlin, Germany). The d_{50} value was obtained from a laser-based particle size analyzer (1064 instrument from Cilas, Marseille, France).

Polymer characterization

The viscosity of the polymer solution was quantified with a Brookfield viscometer (model HAT from Brookfield Engineering Labs., Inc., Middleboro, MA) equipped with a #H2 spindle. The measurement was carried out at 50 rpm and at room temperature. By multiplying the dimensionless reading with the correspondent factor, we obtained the viscosity in millipascal seconds.

The kinematic viscosities of the cement pore solutions containing HEC and the solutions containing HEC and SMF, respectively, were determined on an Ubbelohde viscometer with 501 10/I, 501 20/II, and 501 30/III capillaries supplied by Schott Instruments (Mainz, Germany). The kinematic viscosities of the cement slurry filtrates containing dosages between 0 and 1% (by weight of cement, bwoc) of HEC (incremental steps of 0.22% bwoc) and of aqueous HEC/SMF solutions were determined at 27°C with the Ubbelohde viscometer. The filtrate (15 mL) was filled into the reservoir of the viscometer, and the flow time (t) was measured. From this, the kinematic viscosity of the filtrate (υ) was calculated according to eq. (1):

$$\upsilon = K(t - \zeta) \tag{1}$$

where K is the viscometer constant (0.1004 mm^2/s^2) and ζ is the flow-time-dependent Hagenbach–Couette correction term, which was provided in the instrument instruction sheet. Multiplying the value for the kinematic viscosity with the specific density of the filtrate produced the value for η_{dyn}, as expressed by eq. (2):

$$\eta_{dyn} = \upsilon \cdot \rho \tag{2}$$

TABLE II
Characteristic Properties of the HEC Sample

Molar mass (g/mol)							
M_w	M_n	Polydispersity index (M_w/M_n)	$R_{h(z)}$ (nm)	Specific anionic charge (C/g)[a]	Intrinsic viscosity at 27°C (L/g)[a]	Degree of substitution	Molar degree of substitution
210,000	120,000	1.7	20.5	28	0.28	~ 1.0	~ 1.5

[a] In cement pore solution.

where ρ is the specific density of the filtrate at 27°C (0.9965 g/mL). From this, the reduced viscosity of the filtrate (η_{red}) was calculated according to eq. (3). η_0 is the dynamic viscosity of the cement filtrate containing the polymer, and c represents the respective concentration of HEC in the filtrate:

$$\eta_{red} = \frac{\eta_{dyn} - \eta_0}{\eta_0 \cdot c} \quad (3)$$

An SEC instrument (Waters Alliance 2695, Waters, Eschborn, Germany) equipped with a refractive-index detector (Waters 2414) and an 18-angle dynamic light-scattering detector (Dawn EOS, Wyatt Technologies, Clinton, SC) was used. HEC was separated on a precolumn and two Aquagel-OH 60 columns (Polymer Laboratories, distributed by Varian, Darmstadt, Germany). The molecular weights (M_w and M_n) and radii [$R_{h(z)}$ and $R_{g(z)}$] of the FLA were determined with a 0.2*M* aqueous $NaNO_3$ solution (adjusted to pH 9.0 with NaOH) as an eluent at a flow rate of 1.0 mL/min. The value of dn/dc (differential index of refraction) used to calculate M_w, and the M_n values for HEC were 0.159 mL/g (HEC)[19] and 0.135 mL/g [poly(ethylene oxide)][20] for SMF, respectively.

The specific anionic charge amounts of the polymers used in this study were determined in a cement pore solution at room temperature with a PCD 03 pH apparatus (BTG Mütek GmbH, Herrsching, Germany). Charge titration was carried out according to a literature description with a 0.001*N* solution of laboratory-grade poly(diallyl dimethylammonium chloride) from BTG Mütek GmbH as a cationic polyelectrolyte.[17] The values presented in this study are the averages obtained from three different measurements. The standard deviation of this method was found to be ±5 C/g.

The d_{50} values of the associates were measured in a cement pore solution with a dynamic light-scattering particle size analyzer (LB-550, Horiba, Irvine, CA).

The surface tension was quantified on a drop shape analyzer (DSA 100, Krüss GmbH, Hamburg, Germany) with the pendant drop method. Before the measurement of the HEC solution, the surface tension of the deionized water was measured to calibrate the system. In accordance with the literature, this water exhibited a surface tension of 71.7 mN/m at 27°C.[21] The surface tension was recorded continuously as a function of the HEC concentration (from 1 to 20 g/L).

Cement slurry preparation

Cement slurries were prepared in accordance with the procedures set forth in the Recommended Practice for Testing Well Cements, API Recommended Practice 10B-2, issued by API.[22] The slurries were mixed at a water-to-cement (w/c) ratio of 0.44 with a blade-type laboratory blender manufactured by Waring Products, Inc. (Torrington, CT). The admixture dosages are stated in percentages by weight of cement (bwoc). Before cement addition, the powdered HEC was dry-blended with the cement. The homogenized mixture was added within 15 s to the water placed in a Waring blender cup and mixed for 35 s at 12,000 rpm. To ensure a homogeneous consistency, all slurries were stirred in an atmospheric consistometer (model 1250, Chandler Engineering, Tulsa, OK) for 20 min at 27°C. The pore solution of the cement slurry prepared without polymer addition was produced by vacuum filtration (12 mbar) with a diaphragm vacuum pump (Vacuubrand GmbH, Wertheim, Germany).

Fluid loss test

The static fluid loss was measured at 27°C with a 500-mL HP/HT stainless steel filter press cell manufactured by OFI Testing Equipment, Inc. (Houston, TX). The design of this HP/HT filter cell and its operation were described in detail in a norm issued by API.[22] After pouring the homogenized slurry obtained from the atmospheric consistometer into the HT/HP cell, we used a heating jacket (OFI Testing Equipment) to adjust the test temperature. Then, a differential pressure of 70 bar of N_2 was applied at the top of the cell. Filtration proceeded through a 22.6-cm^2 (3.5-$in.^2$) mesh metal sieve placed at the bottom of the cell. The fluid volume collected within 30 min was doubled, as described by API RP 10B-2, and regarded as the API fluid loss of the corresponding slurry. The value reported for the respective API fluid loss test represents the average obtained from three separate measurements. The maximum deviation of the fluid loss value was ±10 mL/30 min.

Retention of HEC in the cement filtercake

The retained amount of the HEC FLA was determined from the filtrate collected in the respective fluid loss test. Generally, the depletion method was applied; that is, it was assumed that the decrease in the polymer concentration before and after contact with cement solely resulted from interaction with cement and not from insolubility of the polymer. This assumption was confirmed through a solubility test. For this purpose, 11.36 g/L HEC (this concentration correlated to a polymer dosage of 0.5% bwoc) was dissolved in a cement pore solution and stored for 1 day. No precipitation of HEC was observed. The retained amount was calculated from the difference in the equilibrium concentration of the polymer present in the liquid phase before and after contact

with cement (depletion method). A High total organic carbon (TOC) II apparatus (Elementar, Hanau, Germany) equipped with a CO_2 detector was used to quantify polymer retention. Before conducting the TOC analysis, we adjusted the alkaline cement filtrate containing the nonretained, dissolved HEC polymer to pH 1.0 by adding 0.1*M* HCl. Here, the maximum deviation of the measurement was found to be ±0.1 mg of polymer/g of cement.

ζ Potential measurement

The ζ potential values of the cement slurries were measured at room temperature on an electro-acoustic spectrometer (DT-1200, Dispersion Technology, Inc., Bedford Hills, NY).[17] Because the ζ potential was determined as a function of time (here, 30 min), the cement slurries were poured immediately after they were mixed into the cup of the spectrometer and measured without homogenization in the atmospheric consistometer. The accuracy of this method was ±1 mV.

Environmental scanning electron microscopy (ESEM) and mercury intrusion porosimetry

The surface of the cement filtercake was analyzed with an environmental scanning electron microscope (XL 30 ESEM FEG from FEI Co., Eindhoven, The Netherlands) at 1.0 mbar pressure in the sample chamber. The water sorption (swelling) of the HEC powder in a wet environment was investigated by exposure of the cellulose ether to relative humidities between 47.5 and 100%. These humidities corresponded to water vapor pressures of 3.5 and 7.1 mbar, respectively, in the ESEM chamber.

The hardened cement filtercake (curing time = 2 days) was analyzed by mercury intrusion porosimetry (Poremaster 60 from Quantachrome, Odelzhausen, Germany). A small piece of the cement filtercake (~ 0.5 g) was exposed to HP mercury intrusion.

RESULTS AND DISCUSSION

Fluid loss performance of HEC

The filtrate volumes of the cement slurries containing increased dosages of HEC were measured at 27°C. As shown in Figure 2, higher concentrations of HEC produced lower API fluid loss values. For example, the API fluid loss decreased from 318 mL at 0.4% bwoc of HEC to 36 mL at 1.0% bwoc of HEC. The concentration of HEC needed to achieve an API fluid loss of below 100 mL/30 min at 27°C was found to lie at 0.7% bwoc. HEC dosages higher than 1.0% bwoc produced enormously viscous cement slurries and, thus, were not investigated.

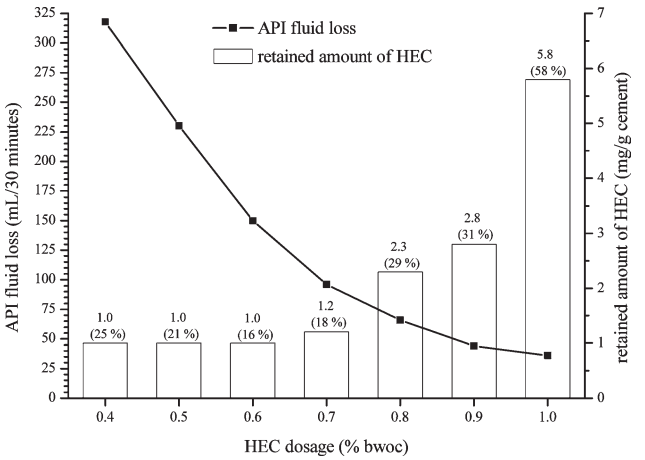

Figure 2 API fluid loss (line) of the API class G oil well cement slurries (w/c = 0.44) and retained amount of HEC (white bars) as a function of dosage.

Mechanistic study

To uncover the working mechanism of HEC and to understand its fluid loss performance, a series of experiments was devised. Following the procedure described by Desbrières,[8,9] we found that HEC significantly reduced the filtercake permeability (see Table III). A low filtercake permeability was always observed when an effective fluid loss control was achieved. For example, at 27°C, the filtercake permeability dropped from 1,711 μD for 0.4% bwoc of HEC to 36 μD at 1.0% bwoc of HEC. At the same time, the API fluid loss decreased from 318 mL/30 min to 24 mL/30 min.

Next, at different HEC dosages, the influence of the dynamic filtrate viscosity on the API fluid loss performance was probed (Table III). Up to a dosage of 0.7% bwoc of HEC, the dynamic filtrate viscosity increased, and a correlation, albeit a poor correlation, with the API fluid loss control was found. However, when this threshold concentration was exceeded, a decrease in the dynamic filtrate viscosity values was observed. Accordingly, between 0.7 and 1.0% bwoc of HEC, a drop in viscosity from 11 to 7.9 mPa·s was measured. Opposite to this trend in the viscosity development, the filtercake permeability decreased steadily with increasing HEC dosage (from 6,366 μD for the neat cement slurry to 36 μD for the cement slurry containing 1.0% bwoc of HEC). Thus, a direct relationship between the filtercake permeability and the cement fluid loss control became obvious. The results confirmed that the reduction in filtercake permeability and not the increased filtrate viscosity was the predominant reason for the low fluid loss achieved by HEC.

To determine the mechanism behind this reduction in filtercake permeability, the effects as follows were considered: (1) modification of the filtercake

TABLE III
API Fluid Loss, Reduced Filter Cake Volume, Dynamic Filtrate Viscosity, and Filter Cake Permeability of the Cement Slurries as a Function of FLA Dosage

FLA dosage (% bwoc)	API fluid loss at 27°C (mL/30 min)	Filter cake permeability (K; μD)	Dynamic filtrate viscosity (η; mPa·s)	Reduced filter cake volume
0	1,270 (calculated)	6,366	1.0	2.0
0.4	318 (calculated)	1,711	4.8	2.7
0.5	230 (calculated)	1,566	6.9	2.6
0.6	150	1,016	9.8	2.4
0.7	96	587	11.9	2.7
0.8	60	207	10.5	2.8
0.9	44	80	8.9	2.4
1.0	34	36	7.9	2.0

structure, (2) adsorption of HEC on the cement particles, and (3) physical plugging and obstruction of the filtercake pores by retained polymer particles. First, fresh filtercakes of cement slurries without and holding 0.8% bwoc of HEC were comparable with ESEM imaging (Fig. 3). After the addition of HEC, no modification of the filtercake structure was observed. The packing and size of the hydrating cement particles and the pore sizes in the filtercake were comparable. Fresh filtercakes prepared from cement slurries without and holding 0.8% bwoc of HEC exhibited similar pore sizes of about 1 μm, as measured by mercury intrusion porosimetry.

Because HEC did not modify the microstructure of the filtercake with respect to the packing and size of hydrating cement particles, the constriction of filtercake pores through adsorption or physical plugging was studied next.

For this purpose, the amounts of HEC adsorbed on cement or otherwise retained were measured. If the working mechanism of HEC was based on physical adsorption, the retained amount should have increased with dosage until a plateau was reached. At this saturation point, the cement surface was covered with the maximum possible amount of polymer. This behavior was represented by a Langmuir adsorption isotherm. As shown in Figure 2, at dosages up to 0.7% bwoc, the depleted amount of HEC did not change much, whereas the API fluid loss values decreased significantly. However, starting at a dosage of 0.8% bwoc HEC, the retained amount increased significantly from 2.3 mg of polymer/g of cement (at 0.8% bwoc HEC) to 5.8 mg of polymer/g of cement (at 1.0% bwoc). The occurrence of polymer adsorption could be confirmed experimentally by the increased negative ζ potential values of the cement slurries when polymer was added to the cement slurry.[10] Thus, to clarify whether the adsorption of HEC took place, the ζ potentials of the cement pastes without and with increased dosages of HEC were measured. After the addition of HEC, no change in the charge of the cement particles was observed (−6 mV for the neat cement slurry vs −5 mV for the cement slurry containing 0.8% bwoc of HEC). Thus, it was confirmed that no adsorption of HEC took place and that the adsorption played no role in its working mechanism.

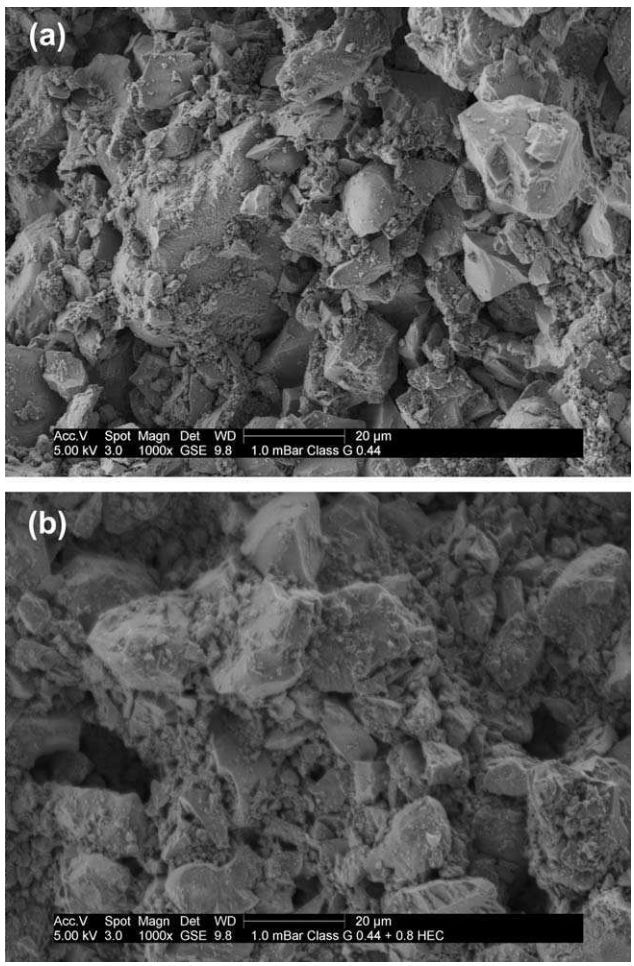

Figure 3 ESEM images of the microstructures of the cement filtercakes prepared without FLA (a) magnification, 1,000× and in the presence of 0.8% bwoc HEC (b) magnification, 1,000×

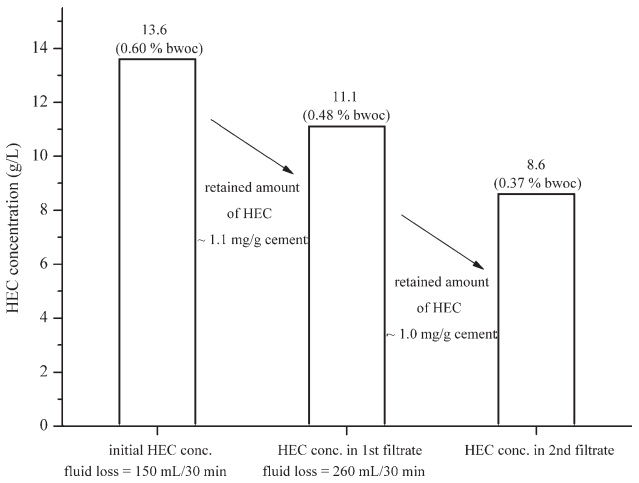

Figure 4 Initial HEC concentration present in the cement pore solution before static filtration and HEC concentrations present after two static filtration tests.

To probe further into the working mechanism, the following experiment was conducted: the filtrate obtained from an HT/HP filtration test was used for the preparation of the cement slurry, which was subjected to a subsequent second static filtration test. The results presented in Figure 4 clearly exclude an adsorptive working mechanism. There, the concentration of HEC in the filtrate as added (13.6 g/L, corresponding to 0.6% bwoc) decreased to 11.1 g/L (corresponding to 0.45% bwoc) after the first filtration test. This indicated that about 25% of the total HEC dosage added was retained. Repeating the static filtration test by using this filtrate containing about 0.45% bwoc of HEC as mixing water, we observed that the same amount (and not percentage) of HEC was lost during filtration (the HEC concentration dropped from 11.1 to 8.6 g/L in the second filtrate). Thus, it became obvious that in every filtration test, a certain constant amount of HEC ($\sim$ 2.5 g/L) was retained in the filtercake through a mechanism that was independent of adsorption.

Role of hydrocolloidal polymeric associates for HEC performance

Because the fluid loss control achieved by HEC was not caused by filtercake modification or adsorption on cement, a physical plugging effect was considered next for the working mechanism. Generally, HEC is a hydrocolloid that in a moist atmosphere sorbs significant amounts of water, as was revealed by ESEM imaging (Fig. 5). At relative humidities ranging from 47.5 to 100%, the polymer increased its volume considerably as a result of the uptake of water. Massive swelling of the polymer to a multiple of its particle size was observed. When the humidity was reduced back to 47.5%, the polymer did not release much of the water sorbed. Thus, a strong binding capacity of water by HEC was confirmed. The existence of large hydrated hydrocolloidal particles also became evident from dynamic light-scattering measurements performed in the cement pore solution at 27°C. At 1 g/L of HEC dissolved in the cement pore solution, a d_{50} value of 5.2 nm for the HEC particles was found, with no particles less than 3 nm or greater than 8 nm being present. The particle size remained constant up to a concentration of 3.5 g/L HEC. There, sharply increased particle sizes ($\sim$ 100 nm) were measured; this indicated that from this concentration onward, the association of the HEC molecules occurred. Unfortunately, higher HEC concentrations could not be measured because of the rapid increase of viscosity of the solution containing greater than 4 g/L HEC.

Another important observation was the exponential increase in the viscosity of cement pore solutions containing HEC at concentrations above 15 g/L (this corresponded to 0.66% bwoc HEC). At concentrations below 15 g/L, the viscosities of the solutions were nearly constant (Fig. 6). The exponential

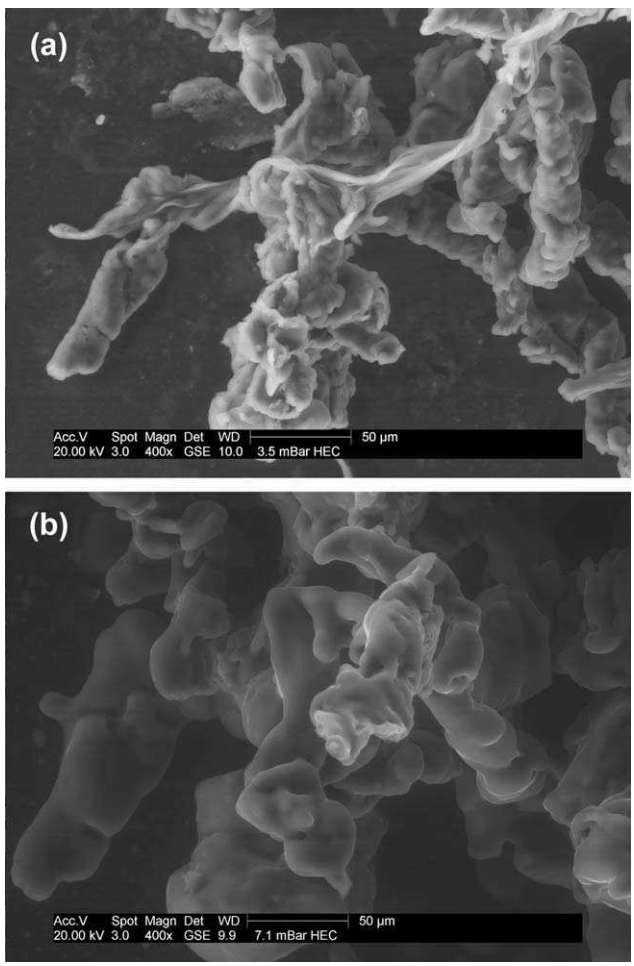

Figure 5 ESEM images of HEC at relative humidities of 47.5% (a) and 100% (b).

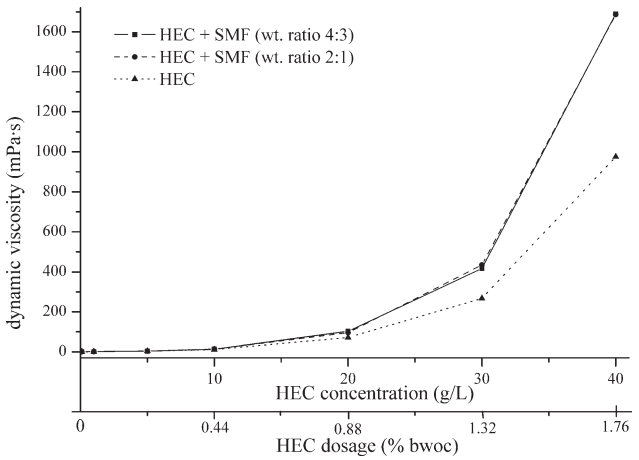

Figure 6 η_{dyn} values of the cement pore solutions containing individual HEC and HEC/SMF combinations.

increase in viscosity that occurred when this threshold concentration of 15 g/L HEC was transgressed indicated that above this concentration, HEC might have formed associated polymer networks, as has been described for hydrocolloids in general.[23] A schematic illustration of the concentration-dependent HEC polymer association is shown in Figure 7. According to the viscosity measurements, at low dosages of hydrocolloid (here, <15 g/L HEC), no interaction took place between individual hydrated polymer molecules, which remained separated. However, beginning at about 15 g/L HEC, individual polymer particles entangled and associated to form larger hydrocolloids with defined hydrodynamic diameters. The specific concentration at which such association commences is generally called the *overlapping concentration*. Here, it was about 15 g/L HEC. At further increased HEC dosages, the polymer associates formed a dense network. As a result, increasing amounts of water were retained, and consequently, the cement fluid loss was improved further.

To evidence the association of HEC further, surface tension measurements were conducted at 27°C for cement pore solutions holding different concentrations of HEC. Normally, cellulose ethers exhibit surface activity, depending on their anionic charge amount. The higher the anionic charge is, the lower the surface activity will be. Thus, the occurrence of association will clearly result in an altered surface tension. As is shown in Figure 8, upon HEC addition, the surface tension rapidly decreased to about 65 mN/m and remained constant at HEC dosages of up to 10 g/L. Beyond this concentration, however, the surface tension decreased further to about 61 mN/m. This effect could be ascribed to the beginning association of HEC molecules. Thus, the results indicate that the working mechanism of HEC was based on the obstruction of filtercake pores by large hydrocolloidal polymeric associates, which formed a three-dimensional network.

Synergistic interaction between HEC and SMF

The second part of this study dealt with the interaction between HEC and the SMF dispersant. When 0.4% bwoc of HEC was used in combination with increasing amounts (0–0.4% bwoc) of SMF, at up to 0.2% bwoc of SMF, no effect on the cement fluid loss was observed (Fig. 9). However, at further increased SMF dosages, a synergistic effect between HEC and SMF occurred. The improvement generally began at a specific ratio between the two polymers of 2 : 1 (w/w) and reached its maximum when the HEC/SMF ratio attained a value of 1.3 or lower. For example, in a combined system containing 0.4% bwoc of HEC and 0.4% bwoc of SMF, the API fluid loss decreased from 318 mL/30 min (at 0.4% bwoc of individual HEC) to 36 mL/30 min for the combination. To understand the reason behind this effect, first, η_{dyn} of the cement pore solution containing both polymers was investigated (Fig. 6). It revealed that in the presence of SMF, the increase in the viscosity of the HEC solution was much more pronounced than in the absence of SMF.

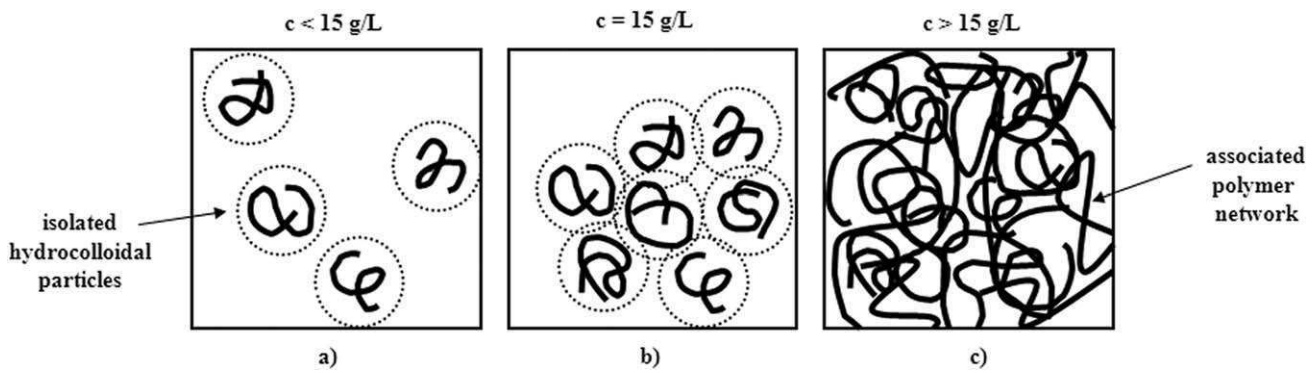

Figure 7 Schematic illustration of the formation of associated polymer networks by HEC in solution: (a) below, (b) at, and (c) above the overlapping concentration (after de Gennes[23]).

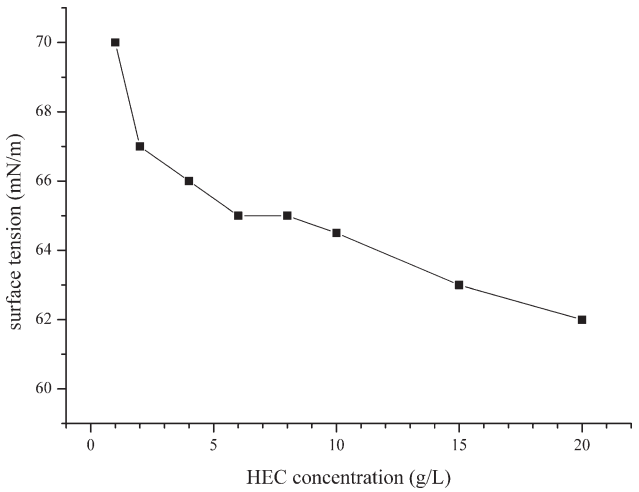

Figure 8 Surface tension of the cement pore solutions and its dependence on HEC concentration at 27°C.

Obviously, SMF instigates the formation of large polymer networks from HEC to occur at lower HEC dosages. Furthermore, a comparison of the ζ potentials of the cement slurries containing 0.3% bwoc of individual SMF (−27 mV) with that of a cement slurry containing 0.3% bwoc of SMF and 0.4% bwoc of HEC (−18 mV) showed that both molecules interacted. Obviously, the anionic charge amount of SMF was partially shielded. Because competitive adsorption between the two polymers was excluded, on the basis of HEC's low anionic charge amount, apparently, an intermolecular interaction between HEC and SMF took place. Finally, dynamic light-scattering measurements with cement pore solution confirmed that in the presence of SMF, the increased formation of large associated polymer particles incorporating both HEC and SMF occurred. Already, at a dosage of 0.1 wt % of HEC and SMF each (HEC/SMF weight ratio = 1), an average particle size (R_h) of 80 nm was found. This was significantly higher than that for individual HEC. In the cement pore solution, an R_h of about 5 nm was found for HEC. Hence, it became obvious that SMF significantly reduced the threshold dosage at which HEC formed associated networks. Moreover, a threshold amount of SMF had to be exceeded to produce the strong synergistic effect with HEC with regard to fluid loss control.

CONCLUSIONS

The working mechanism of HEC as a cement FLA relied on a dual effect, which stemmed from its enormous water-binding capacity and a concentration-dependent formation of hydrocolloidal associated polymer networks. At concentrations below 15 g/L of HEC (this corresponded to 0.66% bwoc), fluid loss control was mainly achieved through the water-binding capacity of hydrocolloidal HEC. Above 15 g/L HEC, this working mechanism was supplemented by the formation of highly associated polymer networks.

From a previous work, it was already known that nonionic cellulose ethers work by reducing the filtercake permeability of oil well cement.[9] Here, we investigated the reason behind this effect. First, a direct correlation between the HP/HT filtrate viscosity and the API fluid loss could not be established. Second, ESEM images revealed that HEC did not change the filtercake structure. Additionally, adsorption was excluded by ζ potential measurement and consecutive static filtration tests. The only potential mechanism left was physical plugging of the filtercake pores. It was found that at low HEC concentrations, the obstruction of filtercake pores was due to water sorption and swelling of the HEC molecules, whereas at higher concentrations, the formation of large hydrocolloidal particles consisting of associated HEC molecules further contributed to reduced cement fluid loss.

Additionally, it was found that HEC and SMF could act synergistically with respect to fluid loss control. The effect occurred only at specific HEC/SMF ratios. Dynamic light-scattering measurements revealed that in the presence of SMF, the association of HEC molecules was greatly enhanced. Those larger hydrocolloidal polymer associates plugged the filtercake pores more effectively.

Further studies are underway to determine HEC compatibility with other common oil well cement additives. The goal was to obtain a fundamental understanding of the parameters impacting admixture compatibility and to establish guidelines for the avoidance of undesired interactions. This should allow a more economical use of those expensive admixtures and result in safer applications.

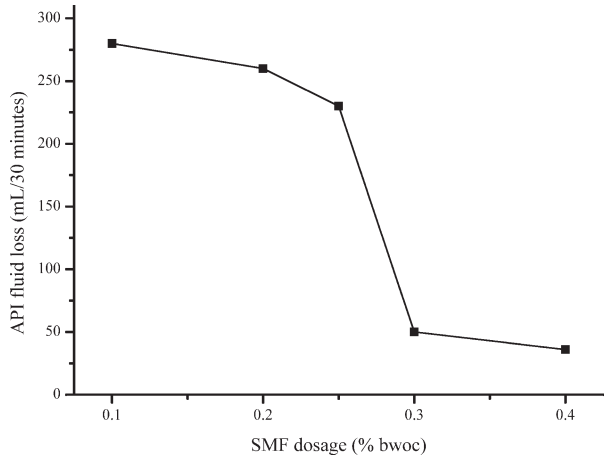

Figure 9 API fluid loss of API class G oil well cement slurries (w/c = 0.44) containing 0.4% bwoc HEC as a function of increasing SMF dosage (0.1–0.4% bwoc).

References

1. Garnier, A.; Frauoulet, B.; Saint-Marc, J. Offshore Tech Conf Texas SPE 2007, 18, 754.
2. Lootens, D.; Hébraud, P.; Lécolier, E.; van Damme, H. Oil Gas Sci Technol Rev IFP 2004, 59, 31.
3. Smith, D. K. Cementing; SPE Monographs Vo. 4; Society of Petroleum Engineers: New York, 1990.
4. Fink, J. K. Oil Field Chemicals; Gulf Professional: Burlington, MA, 2003.
5. Nelson, E. B.; Guillot, D. Well Cementing; Schlumberger Dowell: Sugar Land, TX, 2006.
6. Raines, R. H. U.S. Pat. 4,629,573 (1986).
7. Hook, F. E. U.S. Pat. 3,483,007 (1969).
8. Desbrières, J. Cem Concr Res 1993, 23, 347.
9. Desbrières, J. Cem Concr Res 1993, 23, 1431.
10. Plank, J.; Brandl, A.; Zhai, Y. N.; Franke, A. J Appl Polym Sci 2006, 102, 4341.
11. Plank, J.; Dugonjić-Bilić, F.; Recalde Lummer, N.; Taye, S. J Appl Polym Sci 2011, 117, 2290.
12. Pourchez, J.; Grosseau, P.; Ruot, B. Cem Concr Res 2010, 40, 179.
13. Pourchez, J.; Ruot, B.; Debayle, J.; Pourchez, E.; Grosseau, P., Cem Concr Res 2010, 40, 242.
14. Plank, J.; Brandl, A.; Recalde Lummer, N. J Appl Polym Sci 2007, 106, 3889.
15. American Petroleum Institute. API Specification 10A, 23rd ed.; American Petroleum Institute: Washington, DC, 2002.
16. Franke, B., Z Anorg Allgem Chem 1941, 247, 180.
17. Plank, J.; Sachsenhauser, B. Cem Concr Res 2009, 39, 1.
18. McCusker, L. B.; Von Dreele, R. B.; Cox, D. E.; Louër, D.; Scardi, P. J Appl Crystallogr 1999, 32, 36.
19. Picton, L.; Merle, L.; Muller, G. Int J Polym Anal Ch 1996, 2, 103.
20. Kawaguchi, S.; Aikaike, K.; Zhang, Z.-M.; Matsumoto, K.; Ito, K. Polym J 1998, 30, 1004.
21. Cini, R.; Loglio, G.; Ficalbi, A. J Colloid Interface Sci 1972, 41, 287.
22. American Petroleum Institute. API Recommended Practice 10B-2; American Petroleum Institute: Washington, DC, 2005.
23. de Gennes, P. G. Scaling Concepts in Polymer Physics; Cornell University Press: Ithaca, NY, 1979.

Publikation 2

Mechanistic Study on Carboxymethyl Hydroxyethyl Cellulose as Fluid Loss Control Additive in Oil Well Cement

Bülichen, D., Plank, J.

Journal of Applied Polymer Science 124, (2012), 2340-2347

Mechanistic Study on Carboxymethyl Hydroxyethyl Cellulose as Fluid Loss Control Additive in Oil Well Cement

Daniel Bülichen, Johann Plank

Chair for Construction Chemicals, Institute for Inorganic Chemistry, Technische Universität München, Garching, Germany

Received 19 May 2011; accepted 18 July 2011
DOI 10.1002/app.35278
Published online 26 October 2011 in Wiley Online Library (wileyonlinelibrary.com).

ABSTRACT: The working mechanism of carboxymethyl hydroxyethyl cellulose (CMHEC, M_w 2.6 × 10^5 g/mol) as fluid loss control additive (FLA) for oil well cement was investigated. First, characteristic properties of CMHEC such as anionic charge amount, intrinsic viscosity in cement pore solution, and static filtration properties of cement slurries containing CMHEC were determined at 27°C and 70 bar. Effectiveness of the FLA was found to rely on reduction of cement filter cake permeability. Consequently, the working mechanism is ascribed to constriction of cement filter cake pores. Zeta potential measurements confirm that at low CMHEC dosages (0–0.3% by weight of cement, bwoc), adsorption of the polymer onto the surface of hydrating cement occurs. However, at dosages of 0.4% bwoc and higher, an associated polymer network is formed. This was evidenced by a strong increase in hydrodynamic diameter of solved CMHEC molecules, an exponential increase in viscosity and a noticeable reduction of surface tension. Thus, the working mechanism of CMHEC changes with dosage. At low dosages, adsorption presents the predominant mode of action, whereas above a threshold concentration of ~ 10 g/L (the "overlapping concentration"), formation of associated polymer networks is responsible for effectiveness of CMHEC. Addition of anionic polyelectrolytes (e.g., sulfonated melamine formaldehyde polycondensate, M_w 2.0 × 10^5 g/mol) to cement slurries containing CMHEC greatly improves fluid loss control. Apparently, the presence of such polyelectrolytes causes the formation of colloidal associates from CMHEC to occur at lower dosages. Through this mechanism, effectiveness of CMHEC as cement fluid loss additive is enhanced. © 2011 Wiley Periodicals, Inc. J Appl Polym Sci 124: 2340–2347, 2012

Key words: carboxymethyl hydroxyethyl cellulose; fluid loss additive; hydrocolloid; polymer associates; oil well cement

INTRODUCTION

Oil well cementing is often considered as one of the most important operations performed in the construction of a well bore. Placement of the cement slurry under pressure across a permeable formation, however, may lead to rapid dehydration, resulting in poor pumpability and incomplete cement hydration.[1,2] To control the properties of oil well cement slurries, additives are included into the formulation.[3] Fluid loss additives (FLAs) are added to oil well cement to reduce uncontrolled water loss from the slurry while being pumped along porous formations in the bore hole.[4,5] Because of their environmental compatibility, cellulose ethers are popular FLAs. In the late 1950s, carboxymethyl hydroxyethyl cellulose (CMHEC) was introduced for fluid loss control first in water-based drilling fluids and later also in oil well cement slurries.[6] In spite of this long history of successful application, the working mechanism of CMHEC as cement fluid loss polymer has never been investigated before.

According to Desbrières,[7,8] three fundamental working mechanisms for polymeric FLAs are known. First, increased dynamic viscosity of the cement filtrate can decelerate the rate of filtration. Second, anionic FLAs may adsorb onto hydrating cement particles and obstruct filter cake pores either by polymer segments which freely protrude into the pore space or even bridge adjacent cement particles. Through this adsorptive mechanism, filter cake permeability is reduced and low fluid loss can be achieved. And third, some FLAs may plug the pores of the cement filter cake either through formation of polymer films, of polyelectrolyte complexes or through polymer associates, which can bind an enormous amount of water molecules in their inner sphere and hydrate shells. In the latter case, performance of the fluid loss polymer is further enhanced because a significant portion of the mixing water is physically bound and will not be released during the filtration process.

In recent studies, we have investigated the fluid loss behavior of poly(Ca 2-acrylamido-2-methylpropanesulfonate-*co*-*N*,*N*-dimethylacryamide) (CaAMPS®-*co*-

Correspondence to: J. Plank (johann.plank@bauchemie.ch.tum.de).

TABLE I
Phase Composition (QXRD, Rietveld), Specific Density, Specific Surface Area (Blaine), and d_{50} Value of API Class G Oil Well Cement Sample

C_3S (wt %)	C_2S (wt %)	C_3A_c (wt %)	C_4AF (wt %)	Free CaO (wt %)	$CaSO_4 \cdot 2H_2O$ (wt %)	$CaSO_4 \cdot 0.5$ H_2O (wt %)	$CaSO_4$ (wt %)	Specific density (kg/L)	Specific surface area Blaine (cm^2/g)	d_{50} value (μm)
59.6	22.8	1.2	13.0	<0.3	2.7[a]	0.0[a]	0.7	3.18	3058	11 ± 1.1

C_3S, tricalcium silicate ($Ca_3(SiO_4)O$); C_2S, dicalcium silicate (Ca_2SiO_4); $C_3A_{c,}$ cubic modification of tricalcium aluminate ($Ca_9Al_6O_{18}$); C_4AF, tetra calcium aluminate ferrite ($Ca_4Al_2Fe_2O_{10}$).
[a] Measured by thermogravimetry.

NNDMA),[9] polyvinyl alcohol (PVA),[10] polyethylene imine (PEI),[11] and hydroxyethyl cellulose (HEC).[12] We found that these FLAs work either by adsorption onto the surface of hydrating cement (CaAMPS®-*co*-NNDMA) or through a plugging mechanism instigated by the formation of a polymer film (PVA), of polyelectrolyte complexes (PEI in combination with anionic dispersants), and of associated polymer networks (HEC), respectively.

Here, it was attempted to establish the working mechanism of CMHEC. For CMHEC which is an anionic, high molecular weight hydrocolloid, adsorption on cement, high filtrate viscosity, and/or polymer association appear to be likely candidates for the mechanism. To probe, cement filter cake permeability and dynamic viscosity of filtrates collected from static filtration tests of cement slurries containing CMHEC were determined. Furthermore, adsorption of CMHEC on cement was probed via measurement of zeta potential and dissolved total organic carbon content of cement filtrates. Finally, the concentration-dependant hydrodynamic diameter of dissolved CMHEC molecules in cement pore solution and the surface tension of aqueous CMHEC solutions were investigated. From this data, a model for the working mechanism of CMHEC cement FLA was developed.

EXPERIMENTAL

Materials

Oil well cement

An API Class G oil well cement ("black label" from Dyckerhoff AG, Wiesbaden, Germany) corresponding to American Petroleum Institute (API) Specification 10A was used.[13] Its clinker composition was determined through powder QXRD technique using Rietveld refinement. The amounts of gypsum ($CaSO_4 \cdot 2\ H_2O$) and hemi-hydrate ($CaSO_4 \cdot 0.5\ H_2O$) present in the cement sample were measured by thermogravimetry. Free lime (CaO) was quantified following the extraction method established by Franke.[14] Using a Blaine instrument, the specific surface area was found at 3058 cm^2/g. The specific density of this sample was 3.18 kg/L, as measured by Helium pycnometry. The particle size distribution of the cement sample was determined using a laser-based particle size analyzer. Its d_{50} value was 11 μm (see Table I).

Carboxymethyl hydroxyethyl cellulose

A commercial sample of CMHEC (®Tylose HC 50 NP2, a white powder supplied by SE Tylose GmbH and Co. KG, Wiesbaden, Germany) exhibiting a degree of substitution (DS carboxymethyl) of 0.43 and a molar degree of substitution (MS hydroxyethyl) of 1.01 was used (DS and MS terminology and values are supplier information); according to this, DS carboxymethyl represents the average number of carboxyl groups substituting hydroxyl groups per anhydro glucose unit, whereas MS hydroxyethyl expresses the average number of hydroxyethyl groups per anhydro glucose ring. The statistical chemical structure of the CMHEC sample is presented in Figure 1. GPC analysis (CMHEC concentration: 0.2 wt % in 0.2*M* $NaNO_3$ at pH of 9 adjusted with 50 wt % NaOH) produced molar masses for the FLA of 2.6×10^5 g/mol (M_w, ± 0.6%) and of 1.5×10^5 g/mol (M_n, ± 0.5%), respectively. Additional characteristic properties of the CMHEC sample are shown in Table II. In alkaline cement pore solution, CMHEC exhibited a specific anionic charge amount of −236 C/g, as measured by charge

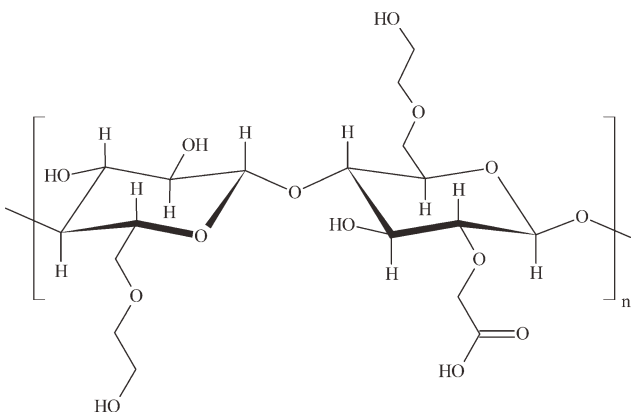

Figure 1 Chemical structure of carboxymethyl hydroxyethyl cellulose exhibiting a DS (carboxymethyl) of 0.5 and an MS (hydroxyethyl) of 1.0.

TABLE II
Characteristic Properties of CMHEC and SMF Samples Used in the Study

Polymer	Molar masses (g/mol) M_w	M_n	Polydispersity index (M_w/M_n)	Hydrodynamic radius $R_{h(z)}$ (nm)	Specific anionic charge amount ε (C/g)[a]	Intrinsic viscosity η at 27°C (L/g)
CMHEC	260,000	150,000	1.8	4.6 ± 0.14	236 ± 18	0.24 ± 0.065
SMF	200,000	140,000	1.5	1.6 ± 0.08	269 ± 10	–

[a] Measured in cement pore solution.

titration using polyDADMAC as a cationic polymer.[15] The negative charge is primarily owed to deprotonation of the carboxymethyl groups. It is comparable to that of other common oil well cement additives such as lignosulfonate retarder (−210 C/g) but lower than CaAMPS®-*co*-NNDMA fluid loss polymer (−370 C/g) or NaAMPS®-*co*-itaconic acid retarder (−528 C/g).

Sulfonated melamine formaldehyde polycondensate

A commercial sample of sulfonated melamine formaldehyde (SMF) resin (Melment® F10, BASF Construction Polymers GmbH, Trostberg, Germany) was used. Its chemical structure is shown in Figure 2. This product is manufactured from melamine, formaldehyde, and sodium pyrosulfite at molar ratios of 1 : 3 : 0.5 through a polycondensation reaction carried out at pH 5–6. The resulting 40% liquid is spray-dried to yield a white powder. GPC analysis (eluent: 0.1*M* $NaNO_3$ at pH 10 adjusted with 50 wt % NaOH) produced molecular weights for SMF of 2.0×10^5 g/mol (M_w, ± 1.0%) and 1.4×10^5 g/mol (M_n, ± 1.2%), respectively. Further characteristic properties of the polymer are shown in Table II.

Instruments and procedures

Cement characterization

Phase composition of the cement sample was obtained by X-ray powder diffraction using a Bruker axs D8 Advance instrument from Bruker, Karlsruhe, Germany with Bragg-Bretano geometry. Topas 3.0 software was used to quantify the amounts of individual phases present in the sample by following Rietveld's method of refinement.[16] The instrument was equipped with a scintillation detector using Cu K_α (λ = 1.5406 E) radiation with a scanning range between 5° and 80° 2θ. Specific density of the cement sample was measured on an Ultrapycnometer® 1000 (Quantachrome Instruments, Boynton Beach, FL/USA). The specific surface area of the sample was determined using a Blaine instrument (Toni Technik, Berlin, Germany). The average particle size (d_{50} value) was obtained from a laser-based particle size analyzer (Cilas 1064 instrument, Marseille, France).

Polymer characterization

Size exclusion chromatography (Waters Alliance 2695 from Waters, Eschborn, Germany) equipped with RI detector 2414 (Waters, Eschborn, Germany) and an 18 angle dynamic light scattering detector (Dawn EOS from Wyatt Technologies, Santa Barbara, CA/USA) was used. Before application on the columns, the solution was filtered through a 5 μm filter. CMHEC was separated on a precolumn and two Aquagel-OH 60 columns (Polymer Laboratories, distributed by Varian, Darmstadt, Germany). Molecular weights (M_w and M_n) and hydrodynamic radius ($R_{h(z)}$) of the FLA were determined using a 0.2*M* aqueous $NaNO_3$ solution (adjusted to pH 9.0 with NaOH) as an eluant at a flow rate of 1.0 mL/min. The value of dn/dc used to calculate M_w and M_n for CMHEC was 0.159 mL/g (value for hydroxyethyl cellulose)[17] and 0.135 mL/g (value for polyethylene oxide)[18] for SMF, respectively.

Kinematic viscosities of cement pore solutions containing CMHEC were measured at 27°C, 50°C, and 80°C on an Ubbelohde viscometer using 501 10/I, 501 20/II, and 501 30/III capillaries supplied by Schott Instruments, Mainz, Germany. The kinematic viscosities of cement slurry filtrates containing dosages between 0 and 0.5% by weight of cement (bwoc) of CMHEC (incremental steps of 0.1% bwoc) were determined at 27°C using the Ubbelohde viscometer. A total of 15 mL of solution were filled into the reservoir of the viscometer and the flow time

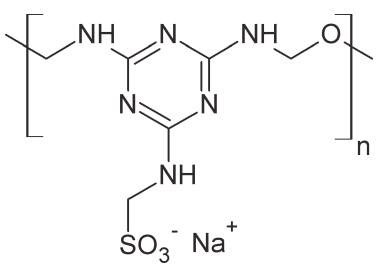

Figure 2 Chemical structure of sulfonated melamine formaldehyde (SMF) polycondensate sample used in the study.

was measured. From this, the kinematic viscosity of the solution was calculated according to eq. (1).

$$\upsilon = K(t - \zeta) \quad (1)$$

where K is the viscometer constant (0.1004 mm^2/s^2), t is the flow time, and ζ is the flow time dependant Hagenbach-Couette correction term, which is provided in the instrument instruction sheet. Multiplying the value for the kinematic viscosity with the specific density ρ of the filtrate produced the value for the dynamic viscosity η_{dyn}, as is expressed by eq. (2).

$$\eta_{dyn} = \upsilon \cdot \rho \quad (2)$$

The specific anionic charge amounts of the polymers used in this study were determined in cement pore solution at room temperature using a PCD 03 pH apparatus (BTG Mütek GmbH, Herrsching, Germany). Charge titration was carried out according to a literature description using a 0.001*N* solution of laboratory grade poly(diallyl dimethylammonium chloride) from BTG Mütek GmbH, Herrsching, Germany as cationic polyelectrolyte.[15] The values presented in this study are the average obtained from three different measurements.

Hydrodynamic particle size (d_{50} value) of the associates was measured in cement pore solution using a dynamic light scattering particle size analyzer (LB-550 from Horiba, Irvine, CA/USA). This property of CMHEC was determined by dissolving, e.g., 1 g of the polymer in 1 L cement pore solution. The CMHEC solution was then filtered through 1.2 μm filter to eliminate undesired dust particles. For our instrumentation, a viscosity below 3 mPa.s was required.

Surface tension at room temperature was quantified on a Processor Tensiometer K100 (Krüss GmbH, Hamburg, Germany) applying the Wilhelmy plate method using a platinum plate. Before the measurement of the CMHEC solutions, the surface tension of deionized water was measured. In accordance with literature, this water exhibited a surface tension of 71.7 mN/m at 27°C. Surface tension was recorded continuously as a function of concentration (10 steps from 20 to 1 g/L, with decreasing intervals from 5 to 0.3 g/L). Further concentrations were determined on a Drop Shape Analyzer DSA 100 (Krüss GmbH, Hamburg, Germany) using the pendant drop method.

Cement slurry preparation

Cement slurries were prepared in accordance with the procedures set forth in Recommended Practice for Testing Well Cements, API Recommended Practice 10B-2, issued by the American Petroleum Institute.[19] The slurries were mixed at a water-to-cement (w/c) ratio of 0.44 using a blade-type laboratory blender manufactured by Waring Products Inc. (Torrington, CT/USA). Admixture dosages are stated in % by weight of cement (bwoc). Before cement addition, the powdered CMHEC was dry blended with the cement. The homogenized mixture was added within 15 s to the deionized water placed in a Waring blender cup and mixed for 35 s at 12,000 rpm. To ensure homogeneous consistency, all slurries were stirred in an atmospheric consistometer (model 1250 from Chandler Engineering, Tulsa, OK/USA) for 20 min at 27°C. The pore solution of the cement slurry prepared without polymer addition was produced by vacuum filtration (12 mbar) using a diaphragm vacuum pump (Vacuubrand GmbH, Wertheim, Germany).

Fluid loss test

Static fluid loss was measured at 27°C using a 500 mL high pressure, high temperature (HP/HT) stainless steel filter press cell manufactured by OFI Testing Equipment Inc. (Houston, Texas/USA). Design of this HP/HT filter cell and its operation are described in detail in a norm issued by the American Petroleum Institute (API).[19] After pouring the homogenized slurry obtained from the atmospheric consistometer into the HT/HP cell, a heating jacket (OFI Testing Equipment Inc., Houston, Texas/USA) was used to adjust the test temperature. Then, a differential pressure of 70 bar N_2 was applied at the top of the cell. Filtration proceeded through a 22.6 cm^2 (3.5 in^2) mesh metal sieve placed at the bottom of the cell. The fluid volume collected within 30 min was doubled as described by API RP 10B-2 and regarded as API fluid loss of the corresponding slurry. The value reported for the respective API fluid loss test represents the average obtained from three separate measurements.

Adsorption/retention of CMHEC in cement filter cake

Adsorbed/retained amount of the CMHEC FLA was determined from the filtrate collected in the respective fluid loss test. Generally, the depletion method was applied, i.e., it was assumed that the decrease in the polymer concentration before and after contact with cement solely resulted from interaction with cement or pore plugging, and not from insolubility of the polymer. This assumption was confirmed through a solubility test. For this purpose, 20 g/L of CMHEC (this concentration correlates to a polymer dosage of 0.88% bwoc) was dissolved in cement pore solution and stored for one day. No precipitation of CMHEC was observed. The retained amount was calculated from the difference in the equilibrium concentration of the polymer present in the

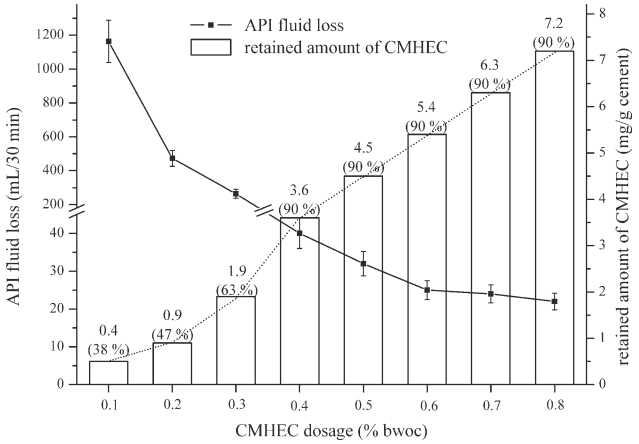

Figure 3 API fluid loss and retained amount of CMHEC as a function of polymer dosage.

liquid phase before and after contact with cement (depletion method). A High TOC II apparatus (Elementar, Hanau, Germany) equipped with a CO_2 detector was used to quantify polymer retention. Before conducting the TOC analysis, the alkaline cement filtrate containing the nonretained, dissolved CMHEC polymer was adjusted to pH 1.0 by adding 0.1*M* HCl. Here, the maximum deviation of the measurement was found to be ± 0.1 mg polymer/g cement.

Zeta potential measurement

Zeta potential of cement slurries was measured at room temperature on an electro acoustic spectrometer (DT-1200 from Dispersion Technology Inc., Bedford Hills, NY/USA).[15] As zeta potential was determined as a function of time (here 30 min), cement slurries were poured immediately after mixing into the cup of the spectrometer and measured without homogenization in the atmospheric consistometer. The accuracy of this method is $\sim \pm 1$ mV.

RESULTS AND DISCUSSION

Fluid loss performance of CMHEC

Filtrate volumes of cement slurries containing increased dosages of CMHEC were measured at 27°C. As is shown in Figure 3, higher amounts of CMHEC produce lower API fluid loss. For example, API fluid loss decreases from 1163 mL at 0.1% bwoc of CMHEC to 32 mL at a dosage of 0.5% bwoc. At 27°C, the minimum CMHEC concentration needed to achieve an API fluid loss below 100 mL/30 min was $\sim$ 0.4% bwoc. This API fluid loss value is generally considered to provide adequate filtration control for successful placement of the cement slurry behind the casing. Small increases of CMHEC dosage result in an enormous improvement of fluid loss control. Compared to HEC,[12] which is another cellulose ether commonly applied for fluid loss control in oil well cement, CMHEC requires lower dosage for comparable fluid loss control.

Dynamic viscosity of CMHEC in cement pore solution

Most cellulose ethers exhibit high viscosity in aqueous and cement pore solution, respectively. The results obtained at 27°C, 50°C, and 80°C for the dynamic viscosity of CMHEC in cement pore solution are presented in Figure 4. At 27°C and for CMHEC concentrations below 10 g/L (this corresponds to a dosage of 0.44% bwoc), only a minor and almost linear increase in viscosity appears. Above this concentration, an exponential increase of viscosity was found. This effect has been described before for other hydrocolloids, and the threshold concentration, which presents the on-set point for the steep viscosity increase, is generally designated as "overlapping concentration."[20] Beyond this concentration, the molecules of the hydrocolloid can entangle with each other and thus form a 3D network which is responsible for the drastic increase in viscosity. For the CMHEC sample tested here, the "overlapping concentration" was found to lie between 10 to 15 g/L. At temperatures of 50°C and 80°C, respectively, the on-set of the exponential viscosity increase (and thus the "overlapping concentration") shifts to higher concentrations. This effect explains the decreased fluid loss control performance of CMHEC at higher temperatures.

Mechanistic study

To probe into the working mechanism of CMHEC, a series of experiments were devised. First, following the procedure of Desbrières, it was found that

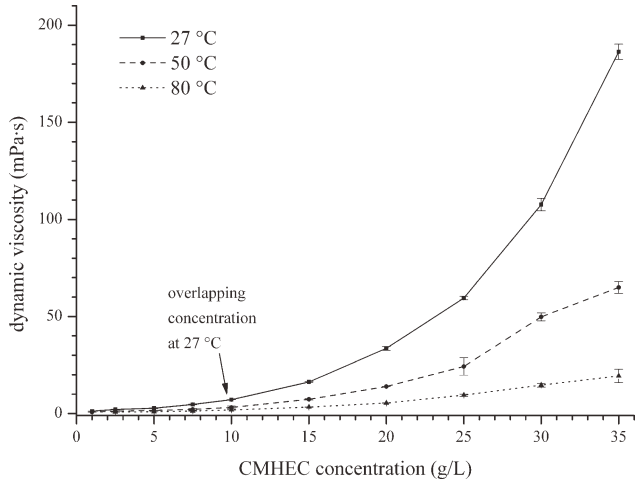

Figure 4 Dynamic viscosity of cement pore solutions containing CMHEC as a function of polymer concentration and temperature.

TABLE III
API Fluid Loss, Filter Cake Permeability, and Dynamic Filtrate Viscosity of Cement Slurries as a Function of CMHEC Dosage

CMHEC dosage (% bwoc)	API fluid loss at 27°C (mL/30 min)	Filter cake permeability K (μD)	Dynamic filtrate viscosity η (mPa.s)
0	1270 (calculated)[a]	6366	1.0
0.1	1163 (calculated)[a]	2645	1.0
0.2	473 (calculated)[a]	1556	1.1
0.3	264	824	1.4
0.4	40	33	0.9
0.5	32	18	0.8

[a] Dehydration of slurry occurred in less than 30 min.

CMHEC strongly reduces filter cake permeability (see Table III).[8] Low filter cake permeability was always observed when effective fluid loss control was achieved. For example, filter cake permeability dropped from 2645 μD (at 0.1% bwoc of CMHEC) to 33 μD (at 0.4% bwoc dosage). At the same time, the API fluid loss decreased from 1163 mL/30 min to 40 mL/30 min.

Next, the influence of dynamic filtrate viscosity on API fluid loss performance at different CMHEC dosages was studied (Table III). There, no correlation with API fluid loss control was found. At first, a slight increase in dynamic filtrate viscosity (from 1 to 1.4 mPa.s) up to a dosage of 0.3% bwoc was observed, but at higher CMHEC concentrations, this effect was reversed. This result indicates that the filtrate viscosity virtually has no influence on the fluid loss performance of CMHEC. Contrary to this, filter cake permeability was reduced dramatically by increased dosages. Accordingly, the results instigate that the reduction in filter cake permeability is the predominant reason for low fluid loss achieved by CMHEC.

To clarify the reason behind this reduction in filter cake permeability, the points as follows were considered and probed: (a) modification of the filter cake microstructure, (b) adsorption of CMHEC on cement particles, and (c) physical plugging of the pores. Here, in presence of CMHEC, no modification of the filter cake microstructure was observed on SEM images (not shown here). Packing and size of the hydrating cement particles as well as the pore sizes present in the filter cake were comparable for all investigated samples, whether or not they contained CMHEC. Consequently, constriction of the filter cake pores through adsorption or physical plugging was studied next as a potential mechanism for fluid loss control achieved by CMHEC.

Adsorption of CMHEC

Thus, the adsorbed amount of CMHEC on cement was measured. If the working mechanism of CMHEC was in fact owed to adsorption, then the adsorbed amount should linearly increase with dosage up to a plateau (the saturation point) at which the cement surface has been covered with the maximum possible amount of polymer. This behavior is presented by a Langmuir isotherm. CMHEC adsorption onto positively charged cement hydrates seemed to present a plausible mechanism because of the significant anionic charge of the polymer, which in cement pore solution was found to lie at 236 C/g (see Table II). As is shown in Figure 3, no adsorption maximum was attained. Instead, the amount of CMHEC retained at first increases gradually (dosage range 0–0.3% bwoc CMHEC) until a stable retention of 90% of dosage added is obtained. This behavior clearly indicates that at low dosages (0–0.3%), increased amounts of CMHEC are retained by cement, possibly through a combination of physical adsorption and obstruction by associated polymer molecules. Beyond a dosage of 0.4% bwoc of CMHEC, the retained amount always presents 90% of polymer dosage added. Consequently, practically the entire quantity of CMHEC polymer added is retained. The remaining nonretained 10% are water-soluble impurities such as glycolates and salts present in the industrial CMHEC sample.

The fact that no saturated adsorption is achieved although cement fluid loss levels off at CMHEC dosages of $\geq$ 0.6% bwoc contradicts polymer adsorption. Instead, depletion of CMHEC might be attributable to retention of polymer associates within the pores of the cement filter cake. An adsorptive mechanism generally can be confirmed by zeta potential measurement which increases with polymer dosage to more negative values if adsorption occurs. Thus, zeta potentials of cement pastes in absence and presence of increased amounts of this anionic FLA were measured (Fig. 5). They indicate that adsorption takes place at low (0–0.4% bwoc) CMHEC dosages (zeta potential −5.0 mV for the neat cement slurry versus −10.5 mV for the slurry containing 0.4% bwoc of CMHEC). At a dosage of 0.4% bwoc, the

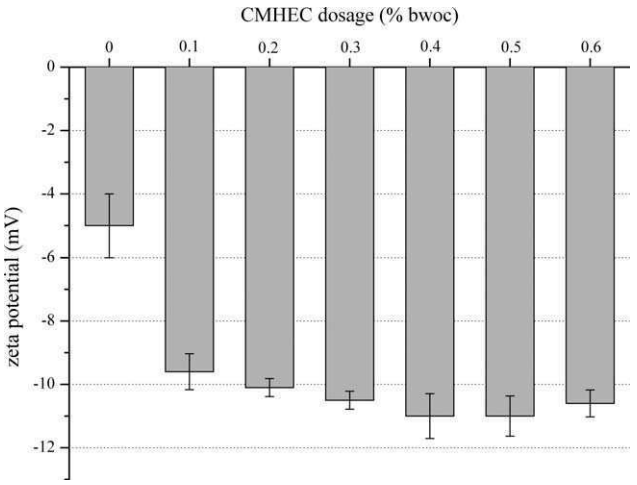

Figure 5 Zeta potential of cement slurries (w/c = 0.44) containing increased dosages of CMHEC, measured at 27°C.

most negative zeta potential (supposedly representing saturation adsorption) is reached. However, at this dosage, cement fluid loss is still high. The results allow to conclude that while some adsorption of anionic CMHEC on cement seems to occur at low dosages, it cannot explain the excellent fluid loss control achieved at higher CMHEC dosages. There, another mechanism seems to come into place.

Formation of associated polymer network

To probe into this, physical plugging of the cement filter cake owed to polymer associates was investigated. Occurrence of large hydrocolloidal particles at higher CMHEC concentrations was confirmed by dynamic light scattering measurement in cement pore solution. At CMHEC concentrations of 1–2 g/L only, a constant d_{50} value of $\sim 6 \pm 1$ nm was found for the hydrodynamic diameter, with no particles < 5 nm and > 10 nm present, whereas at 5 g/L of CMHEC, a significantly higher diameter was obtained for the solved molecules (d_{50} value = 380 $\pm$ 20 nm), thus indicating beginning association of CMHEC molecules. Unfortunately, concentrations > 5 g/L could not be measured, due to the rapid increase of viscosity of such CMHEC solutions. This exponential increase in solution viscosity observed at higher CMHEC concentrations (see Fig. 4) also supports the concept of a plugging mechanism for CMHEC originating from the formation of associated polymer networks. To conclude, at first no interaction takes place in a system of soluted and separated polymer molecules. At higher concentrations, however, associated polymer networks with increasing particle size are formed. This association occurs at a specific concentration which is called the "overlapping concentration."[20]

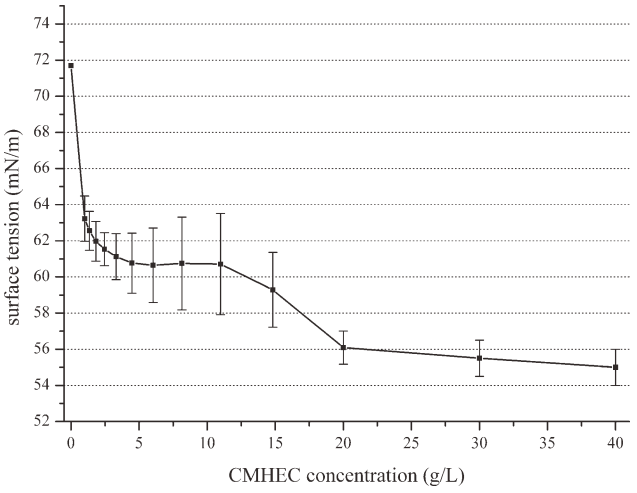

Figure 6 Surface tension of aqueous solutions in dependence of CMHEC concentration, measured at 27°C.

To finally prove the association of CMHEC, surface tension measurements were conducted in aqueous solution at 27°C and at different concentrations. Because of instrumental limitations, surface tension had to be measured in aqueous solution. Nevertheless, the general behavior of CMHEC here can be expected to be similar to that in cement pore solution. Polymer association would clearly reduce surface tension. The surface activity of cellulose ethers is influenced by their anionic charge amount. The higher the anionic charge, the lower the surface activity. As is shown in Figure 6, surface tension decreases rapidly with dosage to 61 mN/m and remains constant till a CMHEC concentration of $\sim$ 10 g/L is attained. This behavior can be explained by the simultaneous presence of hydrophobic and hydrophilic charged functional groups which render the CMHEC molecule an anionic surfactant. Beginning at the "overlapping concentration" of $\sim$ 10 g/L CMHEC, surface tension is reduced further to 56 mN/m. Even at concentrations as high as 40 g/L, no further reduction was obtained. This behavior can be ascribed to association of polymer molecules.

To conclude, the results instigate that at low dosages, the working mechanism of CMHEC mainly

TABLE IV
API Fluid Loss of Class G Cement Slurries as a Function of CMHEC and SMF Dosages

CMHEC dosage (% bwoc)	SMF dosage (% bwoc)	API fluid loss at 27°C (mL/30 min)
0.2	0	473 (calculated)[a]
0.2	0.1	295 (calculated)[a]
0.2	0.2	160
0.2	0.3	90
0.2	0.4	50
0.2	0.5	52

[a] Dehydration of slurry occurred in less than 30 min.

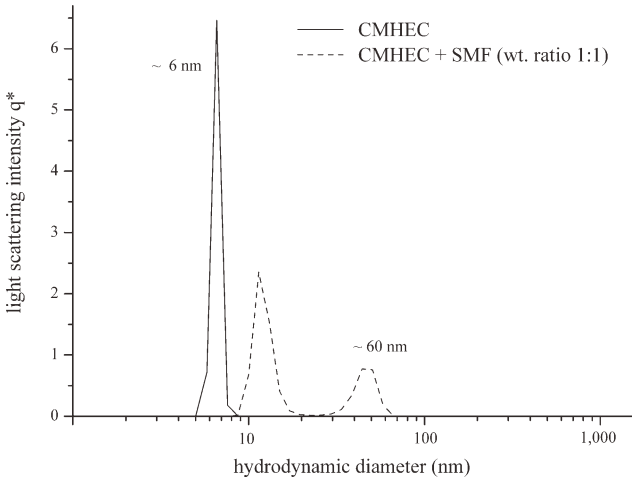

Figure 7 Hydrodynamic diameter of CMHEC molecule (2 g/L) and a mixture of CMHEC (2 g/L) and SMF (2 g/L) in cement pore solution.

results from physical adsorption onto cement, whereas at higher dosages (0.4–0.8% bwoc), large associated polymer networks of CMHEC plug the pores of the cement filter cake.

Interaction between CMHEC and SMF

To further prove this concept, combinations of CMHEC with SMF dispersant were probed for API fluid loss and hydrodynamic diameter of solved molecules in cement pore solution. Such combination is frequently used in actual field application. First, it was found that SMF significantly improves fluid loss performance of CMHEC (Table IV). Furthermore, the hydrodynamic diameter of CMHEC (2 g/L) solved in combination with SMF (2 g/L) was obtained (Fig. 7). Individual CMHEC and SMF molecules possess hydrodynamic sizes of 6 nm and of less than 1 nm, respectively. For the combination, a bimodal particle size distribution exhibiting significantly higher polymer diameters were observed. Two species possessing hydrodynamic diameters of $\sim$ 12 nm and $\sim$ 60 nm (d_{50} values) were detected. Apparently, anionic SMF molecules promote the formation of larger colloidal associates from CMHEC which exhibit an increased plugging effect in the cement filter cake.

CONCLUSIONS

The working mechanism of CMHEC as cement FLA is concentration dependant. Below 10 g/L of CMHEC (this corresponds to a dosage of $\sim$ 0.4% bwoc), adsorption on cement presents the predominant reason for fluid loss control. Above 10 to 15 g/L, the working mechanism changes completely and is henceforth governed by the formation of highly associated polymer networks, which physically plug cement filter cake pores. Formation of polymer associates from CMHEC is much enhanced by the presence of anionic polyelectrolytes such as SMF. This effect explains the synergistic action of SMF and other common cement dispersants on CMHEC relative to fluid loss, an observation which is frequently made by applicators in the field.

Further studies are underway to investigate the associative behavior of CMHEC with other hydrocolloids used in oil well cementing. Among them are welan and diutan gum, two microbially produced biopolymers that are used in cement slurries as free water agents and viscosifiers.

The authors thank Dyckerhoff AG for supplying Class G oil well cement and SE Tylose GmbH for providing the cellulose ether sample.

References

1. Smith, R. C. J Pet Technol 1984, 36, 1851.
2. Plank, J. In 13th ICCC International Congress on the Cement Chemistry; Abstracts and Proceedings, Madrid, Spain, July 03–08.
3. Smith, D. K. Cementing; Society of Petroleum Engineers, SPE Monograph: New York, 1990.
4. Fink, J. K. Oil Field Chemicals; Gulf Professional Publishing: Burlington, MA, 2003.
5. Nelson, E. B.; Guillot, D. Well Cementing; Schlumberger Dowell: Sugar Land, TX, 2006.
6. Greminger, G. K. US Pat. 2, 844, 480, 1958.
7. Desbrières, J. Cem Concr Res 1993, 23, 347.
8. Desbrières, J. Cem Concr Res 1993, 23, 1431.
9. Plank, J.; Brandl, A.; Zhai, Y. N.; Franke, A. J Appl Polym Sci 2006, 102, 4341.
10. Plank, J.; Dugonjić-Bilić, F.; Recalde Lummer, N.; Taye, S. J Appl Polym Sci 2010, 117, 2290.
11. Dugonjić-Bilić, F.; Plank, J. J Appl Polym Sci 2011, 121, 1262.
12. Bülichen, D.; Plank, J. J Appl Polym Sci, to appear.
13. American Petroleum Institute. API Specification 10A, 24th ed.; American Petroleum Institute: Washington, 2010.
14. Franke, B. Z Anorg Allgem Chem 1941, 247, 180.
15. Plank, J.; Sachsenhauser, B. Cem Concr Res 2009, 39, 1.
16. McCusker, L. B.; Von Dreele, R. B.; Cox, D. E.; Louër, D.; Scardi, P. J Appl Crystallogr 1999, 32, 36.
17. Picton, L.; Merle, L.; Muller, G. Int J Polym Anal Ch 1996, 2, 103.
18. Kawaguchi, S.; Aikaike, K.; Zhang, Z.-M.; Matsumoto, K.; Ito, K. Polym J 1998, 30, 1004.
19. American Petroleum Institute. API Recommended Practice 10B-2, 1st ed.; American Petroleum Institute: Washington, 2005.
20. de Gennes, P. G. Scaling Concepts in Polymer Physics; Cornell University Press: Ithaca, New York, 1979.

Publikation 3

Working mechanism of methyl hydroxyethyl cellulose (MHEC) as water retention agent

Bülichen, D., Kainz, J., Plank, J.

Cement and Concrete Research 42, (2012), 953-959

Cement and Concrete Research 42 (2012) 953–959

Contents lists available at SciVerse ScienceDirect

Cement and Concrete Research

journal homepage: http://ees.elsevier.com/CEMCON/default.asp

Working mechanism of methyl hydroxyethyl cellulose (MHEC) as water retention agent

D. Bülichen, J. Kainz, J. Plank *

Technische Universität München, Chair for Construction Chemicals, 85747 Garching, Lichtenbergstraße 4, Germany

ARTICLE INFO

Article history:
Received 19 December 2011
Accepted 23 March 2012

Keywords:
Cellulose ether (A)
Water retention (C)
Cement (D)
Admixture (C)
Working mechanism

ABSTRACT

The working mechanism of methyl hydroxyethyl cellulose, MHEC ($M_w = 2.5 \cdot 10^5$ g/mol, $DS_{methyl} = 1.81$, $MS_{hydroxyethyl} = 0.15$) as water retention agent in cement was investigated. First, the hydrocolloid was characterized and its performance as non-ionic water retention agent was determined employing the filter paper test. Also, water sorption and swelling of individual MHEC fibers under conditions of different humidities were monitored by ESEM imaging. Second, its working mechanism was established. It was found that at low dosages, MHEC achieves water retention by intramolecular sorption of water and concomitant swelling while at higher dosages, MHEC molecules agglomerate into large hydrocolloidal microgel particles ($d > 1\,\mu m$) which effectively plug the pores in the mortar matrix. MHEC association was evidenced by an exponential increase in solution viscosity as concentration rises, a strong increase in the hydrodynamic diameter of solved MHEC molecules, and a noticeable reduction of surface tension.

1. Introduction

Water retention additives play an important role in modern building products, particularly in dry-mix mortars [1]. Their function is to prevent uncontrolled water loss into porous substrates such as brick, lime stone, and aerated concrete. In industrial products, cellulose ethers dominate this market because of their favorable cost effectiveness and their good environmental compatibility [2]. The first reports on the preparation of methyl cellulose and its derivates originate from Lilienfeld [3], Leuchs [4] and Dreyfus [5]. Based on their pioneering work in cellulose ether synthesis, production started in Germany in the 1920s and in the United States in 1938. Major current applications of cellulose ethers include wall renders and plasters, joint compounds for gypsum board paneling, cementitious tile adhesives (CTAs), floor screeds, self-leveling underlayments (SLUs) and water-proofing membranes [6]. In dry mortars, cellulose ethers serve to provide water retention and viscosity. Some types retard Portland cement hydration severely [7,8]. The effect depends on the specific composition (e.g. degree and type of substitution) of the cellulose ether. Application dosages may range between 0.1 and 1.5% by weight of binder, depending on the desired properties. Among the most frequently used cellulose ethers are methyl hydroxyethyl cellulose (MHEC, also referred to as HEMC) and methyl hydroxypropyl cellulose (MHPC) [9–11]. MHEC is predominantly applied in self-leveling flooring compounds and cementitious tile adhesives (CTAs) while MHPC, because of its air-entraining effect stemming from the hydrophobic hydroxypropyl groups, is the product of choice for wall renders and plasters.

In previous publications, the impact of molecular weight of cellulose ethers on both water retention and rheological properties of mortars has been investigated. The authors conclude that consistency was increased and water retention was improved by higher molecular weight ethers. The mortar rheology is highlighted as one of the key properties relative to water retention [12]. Other studies discussed the influence of cellulose ethers on water transport in the porous structure of cement-based materials and investigated their effect on cement hydration [13,14]. They found that the type of substituents attached to the anhydro glucose ring of the cellulose ether is critical for water transport and development of the microstructure of fresh and hardened cement. Furthermore, the degree of substitution represents the key parameter relative to cement hydration, as was evidenced by different time periods at which portlandite precipitation occurs.

In the past, attempts have been made to clarify the working mechanism of methyl cellulose (MC). Early works from Schweizer et al. present the effect of cellulose ethers on water retention and rheology of cementitious mortars and gypsum-based machinery plasters [15,16]. They demonstrate that adsorption of methyl cellulose is clearly dependent on the degree of substitution (DS). At DS values of >1.6 which are typical for MC products used in the

* Corresponding author. Tel.: +49 89 289 13151; fax: +49 89 289 13152.
E-mail address: sekretariat@bauchemie.ch.tum.de (J. Plank).

0008-8846/$ – see front matter © 2012 Elsevier Ltd. All rights reserved.
doi:10.1016/j.cemconres.2012.03.016

building industry, only a minor amount (~20%) of the MC powder adsorbs. In a very skillful experiment the authors show that during the drying process of a gypsum-based render, MC migrates with the water to the surface of the render and is not retained by adsorption. Thus, they conclude that MC does not adsorb on the binder or its hydrates. Similar observations have been made by Yammamuro et al. [17].

In another study, Jenni et al. stained MHEC with a fluorescent dye and visualized and quantified the migration of MHEC through the capillaries of mortars. They found that MHEC accumulates at system interfaces exhibiting a reduced porosity. From this, they conclude that the cellulose ethers can migrate through the pore system and are therefore not or only partly adsorbed on cement particles under wet conditions [18]. In a later publication from this group they state that the dissolved CE is transported downwards through the capillary pores, but accumulates at the contact layer and substrate surface, which act as micro-filters [19].

Thus, there seems to be agreement that methyl cellulose does not adsorb. None of these works, however, offers an alternative model which clearly can describe the mechanism behind water retention capability of MC. Accordingly, there is still a need for clarification.

Generally, three principle working mechanisms for water retention can come into place whenever a cement paste is subject to filtration on a substrate. These potential mechanisms have been proposed in earlier works by Desbrières and are as follows [20,21]: (a) Water retention as a result of increased viscosity: increased dynamic filtrate viscosity can decelerate the filtration rate. (b) Water retention as a result of adsorption: anionic polymers may adsorb onto hydrating cement particles and obstruct filter cake pores either by polymer segments which freely protrude into the pore space or even bridge cement particles. Through this mechanism, filter cake permeability is reduced. (c) Water retention as a result of physical pore plugging: polymers may plug pores in the cementitious matrix through formation of polymer films (e.g. latexes), or through large polymer associates which form a 3D network, or through simple swelling and expansion caused by the uptake of an enormous amount of water into the inner sphere and hydrate shells of polymers. This process leads to the formation of large microgel particles. Through this mechanism, a large portion of the mixing water is physically bound and cannot leak-off into a porous substrate. The enormous water-binding capacity of polysaccharides has been described in an earlier study. By using a sorption balance and a microcalorimeter it was found that at the saturation level, neutral polysaccharides (amylose and amylopectin) can bind up to four water molecules per anhydroglucose unit [22].

In recent studies we have investigated the water retention behavior of hydroxyethyl cellulose (HEC) and carboxymethyl hydroxyethyl cellulose (CMHEC) in oil well cement, respectively. We found that the working mechanism of HEC relies on a dual effect, namely its enormous intramolecular water sorption (binding) capacity and a concentration dependent formation of hydrocolloidal associated polymer networks [23]. Contrary to this, the working mechanism of CMHEC changes with dosage. At low dosages (up to ~0.3% by weight of cement), adsorption presents the predominant mode of action, whereas above a certain threshold concentration (the "overlapping" concentration), formation of associated polymer networks is responsible for its effectiveness [24].

Here, an attempt was made to establish the working mechanism of MHEC. For this purpose, its water retention effectiveness in cement paste and its dynamic viscosity in cement pore solution were measured. Furthermore, its potential adsorption on cement was probed via a specifically designed static filtration test. Finally, concentration-dependent hydrodynamic diameters of solved MHEC molecules, and their surface tension in cement pore solution were measured to establish the mechanism underlying the effectiveness of MHEC as water retention agent.

2. Materials and methods

2.1. Cement

This study was conducted using a CEM I 52.5N sample ("*Milke*®" from HeidelbergCement AG, Heidelberg, Germany). Its properties are presented in Table 1. Composition of the cement was obtained by Q-XRD using a Bruker axs D8 Advance instrument (Bruker, Karlsruhe, Germany) with Bragg–Brentano geometry. Topas 4.0 software was employed to quantify the amounts of individual phases present in the sample by following *Rietveld's* method of refinement. The amounts of gypsum ($CaSO_4 \cdot 2H_2O$) and hemi-hydrate ($CaSO_4 \cdot 0.5H_2O$) were measured by thermogravimetry. Free lime (CaO) was 3.0 wt.% as quantified following the extraction method established by Franke [25]. Using a *Blaine* instrument (Toni Technik, Berlin, Germany), the specific surface area was found at 3316 cm^2/g. The specific density of this sample was 3.16 kg/L, as measured by Helium pycnometry (Ultrapycnometer® 1000 from Quantachrome Instruments, Boynton Beach, FL, USA). Particle size distribution of this cement was determined employing a laser-based particle size analyzer (CILAS 1064 instrument from Cilas, Marseille, France). Average particle size (d_{50} value) was 10 μm (see Table 1).

2.2. MHEC

A commercial sample of methyl hydroxyethyl cellulose (Tylose® MHB 10000 P2, supplied by SE Tylose GmbH & Co KG, Wiesbaden, Germany) exhibiting a degree of substitution (DS methyl) of 1.81 and a molar degree of substitution (MS hydroxyethyl) of 0.15 was used (DS and MS terminology and values are supplier information). Its characteristic properties are shown in Table 2. Particle size measurement produced a d_{50} value of 116 μm for the dry MHEC powder.

For determination of molar masses (M_w and M_n), polydispersity index and molecular size in solution ($R_{h(z)}$), size exclusion chromatography (Waters Alliance 2695 instrument) equipped with RI detector 2414 from Waters, Eschborn, Germany and an 18 angle dynamic light scattering detector (Dawn EOS from Wyatt Technology, Santa Barbara, CA/USA) was utilized. Prior to application on the columns, the 2 g/L MHEC solution was filtered through a 5 μm filter and separated on a precolumn and two Aquagel-OH 60 columns (Polymer Laboratories, distributed by Varian, Darmstadt, Germany). Eluent was 0.2 M aqueous $NaNO_3$ solution (adjusted to pH 9.0 with NaOH) pumped at a flow rate of 1.0 mL/min. The value of dn/dc used to calculate M_w and M_n was 0.159 mL/g (value for hydroxyethyl cellulose) [26].

The specific anionic charge amount of the polymer in cement pore solution was determined at room temperature using a PCD 03 pH apparatus (BTG Mütek GmbH, Herrsching, Germany). Charge titration was carried out according to a literature description employing a 0.001 N solution of laboratory grade poly(diallyl dimethylammonium chloride) from BTG Mütek GmbH, Herrsching, Germany as cationic polyelectrolyte [27]. The value presented is the average obtained from three different measurements. Deviation of this method was found to be ±3 C/g.

Dynamic viscosities of cement pore solutions containing dissolved MHEC polymer and of filtrates obtained from static filtration tests were determined on an *Ubbelohde* viscometer using 501 10/I, 501 20/II, 501 30/III, and 501 40/IV capillaries supplied by Schott Instruments, Mainz, Germany. 15 mL of individual solutions was filled into the reservoir of the viscometer and the flow time was measured. From this, the kinematic viscosity of the filtrate was calculated according to Eq. (1).

$$\upsilon = K(t - \zeta) \quad (1)$$

where K is the viscometer constant (0.1004 mm^2/s^2), t is the flow time and ζ is the flow time dependent *Hagenbach–Couette* correction

Table 1
Phase composition (Q-XRD, *Rietveld*), specific density, specific surface area (*Blaine*) and d_{50} value of cement sample CEM I 52.5N.

C_3S (wt.%)	C_2S (wt.%)	C_3A_c (wt.%)	C_3A_o (wt.%)	C_4AF (wt.%)	free CaO (wt.%)	$CaSO_4 \cdot 2H_2O$ (wt.%)	$CaSO_4 \cdot 0.5H_2O$ (wt.%)	$CaSO_4$ (wt.%)	Specific density (kg/L)	Specific surface area Blaine (cm^2/g)	d_{50} value (μm)
62.9	20.4	3.9	3.3	2.3	0.1	3.5 [a]	2.0 [a]	2.1	3.16	3316	10 ± 1.0

[a] Measured by thermogravimetry.

term which is provided in the instrument instruction sheet. Multiplying the value for the kinematic viscosity with the specific density of the filtrate produced the value for the dynamic viscosity η_{dyn}, as is expressed by Eq. (2).

$$\eta_{dyn} = \upsilon \cdot \rho. \tag{2}$$

Water sorption (swelling) of MHEC powder in moist atmosphere was investigated by exposing the cellulose ether to relative humidities of 10%, 50% and 60%, respectively, under an environmental scanning electron microscope (XL 30 ESEM FEG from FEI Company, Eindhoven, The Netherlands). These humidities correspond to water vapor pressures of 0.6, 2.0 and 3.3 mbar, respectively, in the ESEM chamber.

Hydrodynamic diameter (d_{50} value) of the MHEC polymer associates were measured in cement pore solution using a dynamic light scattering particle size analyzer (LB-550 from Horiba, Irvine, CA, USA).

Surface tension of cement pore solution containing dissolved MHEC was quantified on a Processor Tensiometer K100 (Krüss GmbH, Hamburg, Germany) employing the *Wilhelmy* plate method using a platinum plate. First, the surface tension of deionized water was established using a Drop Shape Analyzer DSA 100 (Krüss GmbH, Hamburg, Germany) whereby a value of 71.7 mN/m was attained. Next, the surface tension of MHEC solutions was recorded as a function of concentration (10 steps from 10 to 1 g/L, with decreasing intervals of 2 to 0.4 g/L). Furthermore, the surface tension of solutions holding 15 and 20 g/L MHEC was determined using the pendant drop method. All experiments were performed at room temperature.

2.3. Preparation of cement paste

For water retention and static filtration tests, cement pastes were prepared using *Milke*® cement CEM I 52.5 N and deionized water. The cement paste was mixed at a water-to-cement ratio of 0.53 using a blade type laboratory Waring blender (Torrington/CT, USA). 700 g of cement and the respective amount of MHEC powder (0.1–0.8% bwoc) were dry-blended and homogenized. Within 15 s, the cement/polymer blend was added to 371 g of DI water placed in the cup of the Waring blender and was mixed for 35 s at "low" speed (4000 rpm). To ensure homogeneous consistency, all pastes were stirred for 20 min and homogenized in an atmospheric consistometer (Model 1250, Chandler Engineering, Broken Arrow/OK, USA) at 25 °C.

2.4. Water retention test

Water retention effectiveness was determined using a modified version of the filter paper method which is specified in EN 495-2 (former DIN-18555-7) [28,29]. Here, in a typical experiment 15 half-folded filter papers (size 240 mm × 105 mm from Einzinger, Munich, Germany) were covered with a tissue (Delicarta S.p.A., Porcari, Italy) and a Vicat cone (70 × 80 × 40 mm) was placed on top of the stack, with the smaller diameter facing the bottom (see Fig. 1). To establish the value for water retention, a cement paste was prepared at a water-to-cement ratio of 0.53 using the procedure from Section 2.3, filled into the Vicat cone exactly to the brim and leveled with a spatula. After a test period of 7.5 min during which water is sucked from the paste by the filter papers, both the Vicat cone holding the cement paste and the tissue were removed carefully from the stack of filter papers. The amount of water absorbed (w_{abs}) was determined from the difference in weight between the stack of paper after and before exposure to the cement paste. From this, the value for water retention in % was calculated relative to the amount of mixing water contained in the paste placed in the Vicat cone (w_0; here: 113.6 g), as presented in Eq. (3).

$$water\,retention(\%) = \left(1 - \frac{w_{abs}}{w_0}\right) \cdot 100 \tag{3}$$

Static filtration tests of cement pastes were conducted using a 500 mL HTHP filter press (Part No. 171-00-C, OFI Testing Equipment Inc., Houston/TX, USA). The test procedure followed the recommended practice for testing oil well cements established by the American Petroleum Institute (API RP 10B-2) [30]. After pouring the homogenized cement paste into the filter cell, a differential pressure of 7 bar (N_2) was applied at the top of the cell. Filtration proceeded through a 3.5 in.^{2} mesh metal sieve placed at the bottom of the cell. The filtrate produced by the differential pressure was collected for 15 min.

2.5. Retention on cement

The amount of MHEC retained by cement was determined from the filtrate collected in the static filtration experiment described above. Generally, the depletion method was applied, i.e. it was assumed that the decrease in polymer concentration before and after contact with cement solely resulted from interaction with cement, and not from insolubility of the polymer. This assumption was confirmed through a solubility test. For this purpose, 20 g/L of MHEC (this concentration correlates to a polymer dosage of 1.06% bwoc) was dissolved in cement pore solution and stored for one day. No precipitation of MHEC was observed. Note that the calculated amounts of MHEC retained include all polymers present. Thus, all further statements on retained amount of MHEC refer to MHEC plus any minor constituent or by-product. The retained amount was calculated from the difference in the equilibrium concentrations of the polymer present in the liquid phase before and after contact with cement. A High TOC II apparatus (Elementar, Hanau, Germany) equipped with a CO_2 detector was used to quantify polymer concentration. Before conducting the TOC analysis, the alkaline

Table 2
Characteristic properties of the MHEC sample.

Molar masses (g/mol)		Polydispersity index (M_w/M_n)	Hydrodynamic radius $R_{h(z)}$ (nm)	Radius of gyration $R_{g(z)}$ (nm)	Specific anionic charge amount ε (C/g)*	Intrinsic viscosity η at 25 °C (L/g)*
M_w	M_n					
248,000	174,000	1.4	31.0	39.7	6 ± 3	0.32 ± 0.058

* Measured in cement pore solution.

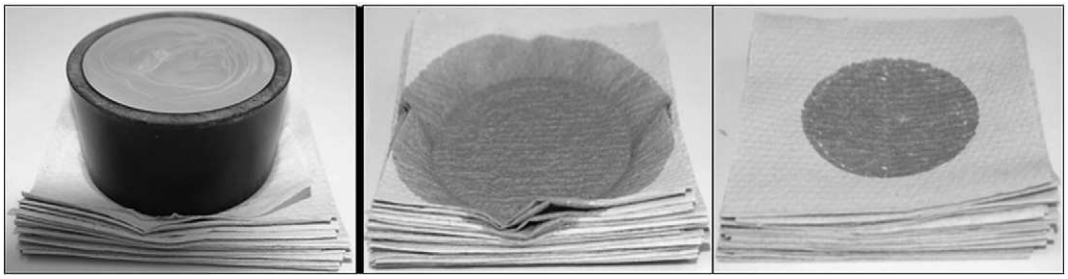

Fig. 1. "Filter paper test" to determine water retention by cement paste; left: placement of Vicat cone on the paper stack at beginning of test; middle: paper stack showing large quantity of sorbed water at end of test from a cement paste without and (right) after addition of 0.8% bwoc of MHEC.

cement filtrate containing the non-retained polymer was diluted with 0.1 M HCl at a ratio of 1:10 (v./v.). Final pH of the solution was 1.0. Maximum deviation of the measurement was found to be ±0.1 mg polymer/g cement.

3. Results and discussion

3.1. Characteristics properties of MHEC sample

The general chemical structure of MHEC is presented in Fig. 2. According to supplier information, the sample employed in the study exhibited a degree of substitution relative to methylation (DS value) of 1.81, and a molar degree of substitution relative to hydroxyethylation (MS) of 0.15. Gel permeation chromatography (GPC) analysis produced molar masses of $2.48 \cdot 10^5$ g/mol (M_w) and of $1.74 \cdot 10^5$ g/mol (M_n), respectively (Table 2). Using the GPC method, a hydrodynamic radius $R_{h(z)}$ of 31.0 nm and a radius of gyration $R_{g(z)}$ of 39.7 nm were found for this polymer. From this data, the *Burchard* parameter $\rho = R_{g(z)}/R_{h(z)}$ which describes the solved conformation of macromolecules can be calculated [31,32]. According to this model, a value of 1.3 which corresponds to a polymer architecture close to that of a linear statistic coil was established [33].

In alkaline cement pore solution (pH ~ 12.8), the MHEC sample exhibited an almost negligible specific anionic charge amount of −6 ± 3 C/g, as measured by charge titration employing polyDADMAC as cationic counter polymer [27]. According to this result, MHEC is practically non-ionic in cement pore solution.

3.2. Water retention capability of MHEC

Water retention of cement pastes containing increasing dosages of MHEC was measured at 25 °C. As is shown in Fig. 3, increased amounts of MHEC produce improved water retention. For example, water retention increases from 84% at 0% bwoc dosage to 97% at 0.3% bwoc MHEC. At 25 °C, the minimum concentration needed to achieve a water retention capability of >98% which is common in high performance dry-mortar products was found to lie at 0.4% bwoc. Obviously, effectiveness of MHEC first increases rapidly with dosage and then asymptotically approaches a value of 100%. MHEC dosages higher than 1% bwoc produce extremely viscous cement pastes and thus were not investigated.

3.3. Viscosifying property

Generally, most cellulose ethers viscosify aqueous or cement pore solutions. Apart from concentration, this effect is dependent on the molecular weight (chain length) of the sample. The MHEC sample selected for this study was a type which develops medium viscosity. Here, the dynamic viscosities of cement pore solutions holding 0–0.8% bwoc of MHEC were measured at 25, 40, and 60 °C, respectively. The results are presented in Fig. 4. At 25 °C and for concentrations below 6 g/L (0.32% bwoc) only a minor increase of viscosity appears. Above this threshold ("overlapping") concentration [34], an exponential rise in viscosity was found, indicating that beginning at this concentration, MHEC molecules start to associate and form a 3D network which is the reason behind the steep increase in viscosity.

At 40 °C, "overlapping" of MHEC molecules occurs at a higher concentration (~8 g/L), and viscosity increases less than at 25 °C. This explains the reduced water retention performance of MHEC at elevated temperatures. When temperature was further increased to 60 °C, the sample did not viscosify anymore due to its insolubility at higher temperatures. The effect of a steep viscosity increase as well as the "overlapping" at higher concentrations was no longer observed at high temperatures.

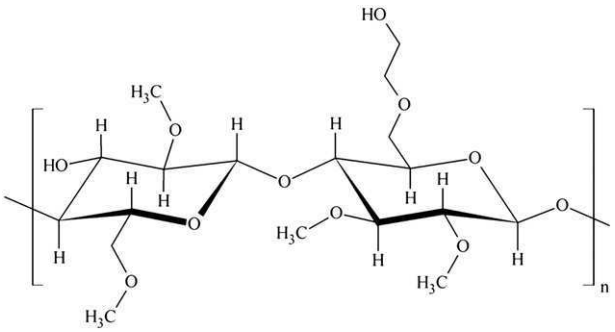

Fig. 2. Chemical structure of methyl hydroxyethyl cellulose exhibiting a DS (methyl) of 2.0 and an MS (hydroxyethyl) of 0.5.

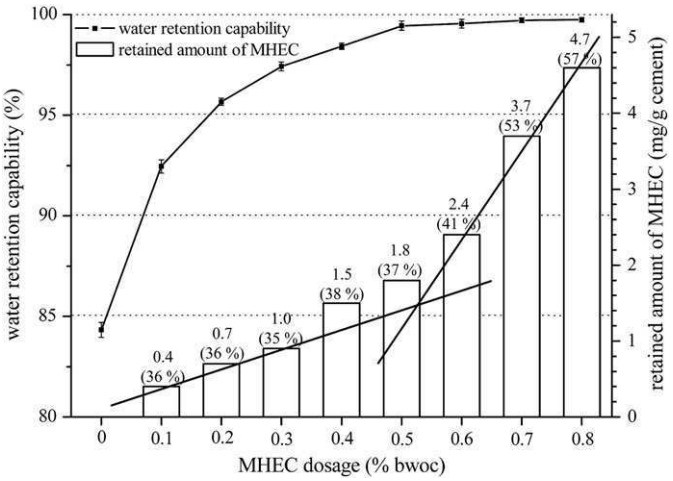

Fig. 3. Water retention capability and retained amount of MHEC as a function of polymer dosage.

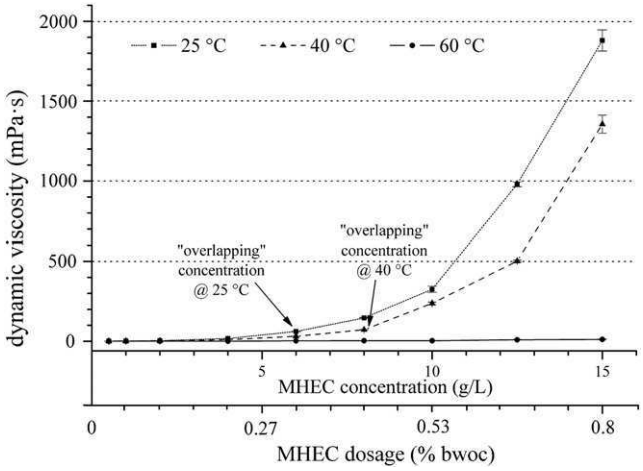

Fig. 4. Dynamic viscosity of cement pore solutions containing MHEC as a function of polymer concentration/dosage and temperature.

3.4. Water sorption by MHEC

Uptake of water by an individual MHEC fiber at different relative humidities (10, 50, and 60%) was monitored using an ESEM instrument (see Fig. 5). It was observed that as a result of water sorption, the polymer swells and its volume increases considerably. For example, at 60% relative humidity, the diameter of the MHEC fiber was increased by a factor of ~3, thus confirming huge uptake of water. It is interesting to note that when the humidity in the ESEM chamber was reduced to 10%, the swollen polymer did not release all of the sorbed water. Instead, formation of polymer films and of cross-linked network structures was observed. This confirms the strong water-binding capacity of the hydrated hydrocolloidal molecule. Additionally, it instigates that films of MHEC polymer are present in the cementitious matrix. This way, MHEC provides a dual effect for mortar: In the fresh, wet paste (within the first ~60 min), MHEC solely acts as a water retention agent while later, when the water has been consumed by hydration and desiccation, MHEC modifies the mechanical properties of mortar through polymer film formation in the cementitious matrix. It should be noted here that Jenni et al. reported instantaneous film formation in the fresh matrix [19]. According to them, particle coalescence occurs at specific locations in the microstructure, namely in the water films present between air voids. Such immediate film formation was not observed here.

3.5. Mechanistic study

To uncover the working mechanism of MHEC and to understand its water retention performance, a series of experiments was devised. Theoretically, the filtration rate of mortar can be reduced either by a lower filter cake permeability or a higher filtrate viscosity. The dynamic viscosity values of cement pore solutions presented before in Section 3.3. imply that increased filtrate viscosity may play a role in the working mechanism of MHEC. And indeed, the dynamic filtrate viscosities measured in cement pore solution (see Table 3) rise from 2.1 mPa·s for 0.1% bwoc of MHEC to 64.8 mPa·s for a dosage of 0.8% bwoc. Nevertheless, a value of ~65 mPa·s is by far not high enough to explain the enormous water retention capability of MHEC.

In his earlier study Desbrières found that in most cases, a reduction in filter cake permeability is the predominant mechanism for effective water retention achieved by polymers. This concept was adopted and the following possibilities were considered: (a) adsorption of MHEC on cement and (b) physical plugging of pore spaces existing in the cement paste by associated 3D polymer networks. Both mechanisms would lead to a reduced permeability of the mortar matrix. Model (b) coincides well with the findings of Jenni et al. [11,18,19]. In their study, utilizing laser-scanning microscopy, MHEC was found to be trapped in micro cracks of the concrete substrate. The hydrated, swollen MHEC aggregates could possibly plug pores, micro cracks or an entire interface to a porous substrate.

3.5.1. Retention of MHEC on cement

The amount of MHEC retained in the cement paste was determined from filtrates collected from a static filtration test

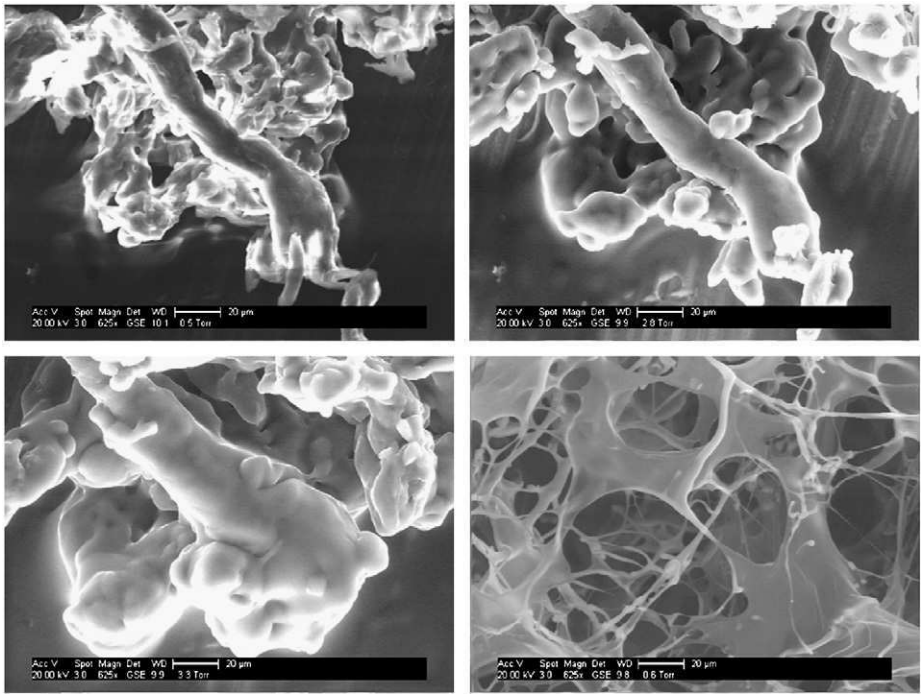

Fig. 5. ESEM images of dry MHEC sample before water sorption (top left); after exposure for 5 min to rel. humidities of 50 and 60% (top right and bottom left); and of MHEC polymer films after reduction of rel. humidity to 10% (bottom right).

Table 3
Dynamic filtrate viscosity of the MHEC sample in cement pore solution as a function of dosage.

MHEC dosage (% bwoc)	Dynamic filtrate viscosity η (mPa·s)
0	1.0
0.1	2.1
0.2	5.1
0.3	10.8
0.4	22.3
0.5	49.9
0.6	59.8
0.7	61.8
0.8	64.8

conducted on a filter press at 7 bar differential pressure. If the working mechanism was indeed relying on adsorption, then the depleted amount of MHEC should increase linearly with dosage until it reaches a plateau which indicates that the cement surface has been covered with the maximum possible amount of polymer (= saturation equilibrium). This behavior is presented by a *Langmuir* isotherm. As is shown in Fig. 3, below a dosage of up to 0.3% bwoc, the amount of MHEC retained increases nearly linear. Due to its very low charge amount, adsorption of MHEC seems highly unlikely. This indicates that another effect may come into play here. Industrial MHEC samples normally contain certain amounts of auxiliaries or by-products which can adsorb on cement. For example, cellulose ethers often contain impurities such as glycolates, thickeners (~15%) such as e.g. anionic polyacrylamides, or rheology modifiers (e.g.: hydroxypropyl starch). Some of these by-products are highly anionic and therefore can lead to this adsorbed amount. Beyond an MHEC dosage of 0.5% bwoc, the retained amount again increases linearly, but steeper than at the lower dosages, thus indicating that a second regime comes into play here. These results perfectly agree with the concentration-dependent values for dynamic viscosities of MHEC solutions (see Fig. 4). There, also two linear regimes were observed, one at a MHEC dosage ≤0.3% bwoc ($R^2 = 0.98$) and one at >0.5% dosage ($R^2 = 0.99$). The combined findings can be interpreted as such that at low MHEC dosages, minor parts (presumably impurities and auxiliary admixtures) adsorb on cement while at higher dosages, MHEC agglomerates formed by the "overlapping" mechanism are retained within the pores of the cementitious matrix because of their large size. In this second regime, adsorption on cement can be excluded because no direct correlation between the retained amount of MHEC and its water-retention capability exists and no equilibrium state (point of saturated adsorption) is reached (see Fig. 3).

To confirm the existence of two different regimes for the working mechanism of MHEC, the experiments as follows were devised: First, two different concentrations of MHEC were selected, one representing the adsorptive regime (5.0 g/L, corr. to a dosage of 0.27% bwoc) and the second the associative/agglomerated regime (13.0 g/L or 0.69% bwoc). For both cement pastes, water-retention as well as the retained amount of MHEC was measured using a static filtration test. In both cases, the filtrate collected from this first static filtration test was used as mixing water for the preparation of a second cement paste which was then subjected to another static filtration test. The results are shown in Table 4. In the cement paste containing the lower dosage of the cellulose ether, MHEC concentration drops by 12% only from initially 5.0 g/L to 4.4 g/L in the first filtration test and nearly stabilizes at 4.2 g/L after the second filtration. This result indicates that the MHEC sample contains some constituents (by-products etc.) which are screened off by cement through adsorption, but are irrelevant for achieving water-retention. Whereas, a completely different behavior is observed for the paste containing a high concentration of MHEC. Therefore, after the first filtration the MHEC

Table 4
Dosage-dependent development of MHEC concentration in cement filtrate and after two subsequent static filtration steps.

Initial concentration added to cement paste		MHEC concentration in 1st filtrate		MHEC concentration in 2nd filtrate	
(g/L)	(% bwoc)	(g/L)	(% bwoc)	(g/L)	(% bwoc)
5.0	0.27	4.4	0.23	4.2	0.22
13.0	0.69	6.2	0.33	3.3	0.17

concentration is halved (from 13.0 g/L to 6.2 g/L) and drops by another 50% after the second filtration (to 3.3 g/L only). Such behavior is well explained by the mechanism of overlapping cellulose ether molecules. They are so voluminous that in every filtration step, a large amount is retained in the pores of the filter-cake. As a result of this considerable MHEC depletion, water-retention is significantly reduced.

These results further support our mechanistic model whereby at low additions (<0.3% bwoc), MHEC attains its water-retention capability from uptake of water through hydration and swelling while at higher dosages (≥0.6% bwoc), water-retention mainly results from physical plugging of the cement pores achieved by large agglomerates of MHEC molecules.

3.5.2. Formation of polymer associates

To confirm occurrence of MHEC agglomerates at concentrations beyond the "overlapping" point, dosage dependent diameters of MHEC molecules solved in cement pore solution were determined at 25 °C using dynamic light scattering technique.

Therefore, when 0.5 g/L of MHEC were dissolved, a d_{50} value for the hydrodynamic diameter of 6.9 ± 1.1 nm was found; with no particles being <4 nm and >10 nm (see Fig. 6). At higher MHEC concentrations (4.0 g/L and 16.0 g/L, respectively), however, increased formation of large associates possessing diameters up to 1.3 μm and 4 μm was observed. For example, at a dosage of 4.0 g/L additional particle diameters at ~60 nm, ~450 nm and ~1.3 μm were recorded while at 16 g/L, even associates as large as ~4 μm were found. Consequently, this experiment allows to conclude that in cement pore solution already at remarkably low dosages (~0.2% bwoc), MHEC molecules begin to form large associates. They are responsible for the viscosity increase and water retention effectiveness. Thus, at low MHEC concentrations no intermolecular interaction takes place in a system of soluted and separated polymer molecules. As concentration increases, however, association into polymer

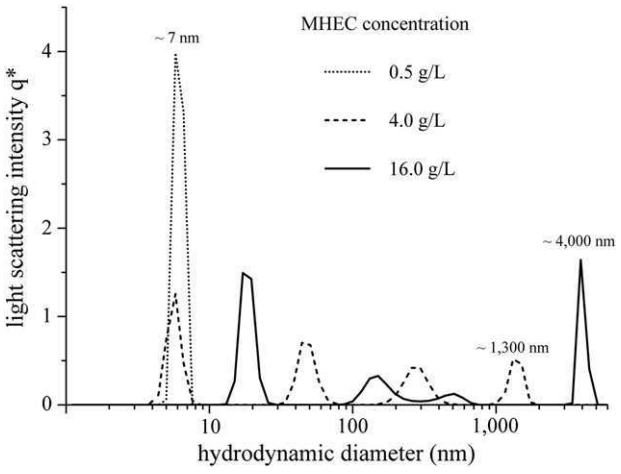

Fig. 6. Hydrodynamic diameter of MHEC molecules dissolved in cement pore solution, as measured by dynamic light scattering.

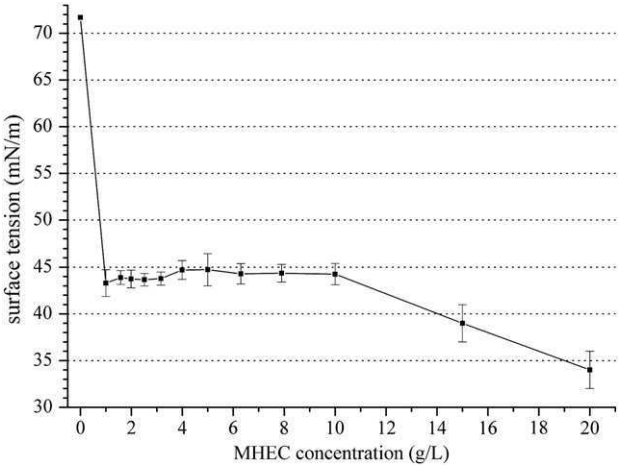

Fig. 7. Surface tension of cement pore solution in dependence of MHEC concentration, measured at 25 °C.

networks starts to occur and progresses rapidly once a specific concentration (the so-called "overlapping" concentration) is exceeded [34].

To further prove the concept of association of MHEC molecules, the surface tension of aqueous MHEC solutions was measured. Generally, cellulose ethers are macrotensides which always exhibit surface activity. The reduction in surface tension of water depends on their anionic charge amount. The higher the anionic charge, the lower the surface activity. The MHEC sample tested here is practically non-ionic (see Section 3.1). Therefore, it can be expected to show strong surface activity. This behavior was confirmed, as shown in Fig. 7. According to this data, at only 1 g/L of MHEC dissolved in cement pore solution, surface tension decreases to ~44 mN/m and remains constant until an MHEC concentration of ~10 g/L is reached. Beyond this value which is in the region of the "overlapping" concentration, a further decrease of the surface tension begins (e.g. to 34 mN/m at 20 g/L). This effect can be ascribed to progressing association of polymer molecules. Such process is commonly known to result in lower surface tension [35].

4. Conclusions

The working mechanism of MHEC as water retention agent in cement relies on two separate effects: first, its water sorption capacity and second the formation of hydrocolloidal associated 3D polymer networks. At low MHEC concentrations ($\leq$6 g/L which corresponds to a dosage of 0.32% bwoc), water sorption presents the main mechanism for water retention while above this concentration, the first mechanism is supplemented by the formation of associated polymer networks which are highly effective in retaining water within the cementitious matrix.

The experiments also demonstrate that potential adsorption of MHEC on cement plays no role with respect to its water-retention capability. This way, the working mechanism of MHEC at low dosages differs from those established for HEC and CMHEC, but is consistent with them at higher dosages.

Acknowledgments

The authors wish to thank H. Klehr from SE Tylose GmbH, Wiesbaden, for generously providing the cellulose ether sample.

References

[1] H. Lutz, R. Bayer, Dry mortars, Ullmann's Encyclopedia of Industrial Chemistry, Wiley-VCH Verlag GmbH & Co. KGaA, Weinheim, 2010, pp. 1–41.
[2] J.A. Grover, Methylcellulose and its derivatives, in: R.L. Whistler, J.N. BeMiller (Eds.), Industrial Gums, Academic Press, San Diego, 1993, pp. 475–504.
[3] L. Lilienfeld, Alkyl ethers of cellulose and process of making the same, US 1,188,376 (1916).
[4] O. Leuchs, Verfahren zur Darstellung von Cellulosederivaten, DE 322,586 (1912).
[5] H. Dreyfus, Procédé pour la fabrication d'éthers cellulosiques et de leurs produits de transformation, FR 462,274 (1912).
[6] J. Plank, Applications of biopolymers in construction engineering, in: A. Steinbüchel (Ed.), Biopolymers, Wiley-VCH, Weinheim, 2003, pp. 29–95.
[7] I. Müller, D. Schweizer, W. Hohn, D. Bosbach, A. Putnis, H. Weyer, B. Schmitt, Influence of cellulose ethers on the kinetics of early Portland cement hydration, GDCh-Monogr. Band 36 (2006) 3–10.
[8] J. Pourchez, P. Grosseau, B. Ruot, Current understanding of cellulose ethers impact on the hydration of C_3A and C_3A-sulphate systems, Cem. Concr. Res. 39 (2009) 664–669.
[9] H. Thielking, M. Schmidt, Cellulose ethers, Ullmann's Encyclopedia of Industrial Chemistry, Wiley-VCH Verlag GmbH & Co. KGaA, Weinheim, 2006, pp. 1–18.
[10] R. Dönges, Non-ıonic cellulose ethers, Br. Polym. J. 23 (1990) 315–326.
[11] A. Jenni, L. Holzer, R. Zurbriggen, M. Herwegh, Influence of polymers on microstructure and adhesive strength of cementitious tile adhesive mortars, Cem. Concr. Res. 35 (2005) 35–50.
[12] L. Patural, P. Marchal, A. Govin, P. Grosseau, B. Ruot, O. Devès, Cellulose ethers influence on water retention and consistency in cement-based mortars, Cem. Concr. Res. 41 (2011) 46–55.
[13] J. Pourchez, A. Peschard, P. Grosseau, R. Guyonnet, B. Guilhot, F. Vallée, HPMC and HEMC influence on cement hydration, Cem. Concr. Res. 36 (2006) 288–294.
[14] J. Pourchez, B. Ruot, J. Debayle, E. Pourchez, P. Grosseau, Some aspects of cellulose ethers influence on water transport and porous structure of cement-based materials, Cem. Concr. Res. 40 (2010) 242–252.
[15] D. Schweizer, The role of cellulose ethers in gypsum machine plaster, ConChem-International Exhibition & Conference — Conference Proceedings, Verlag für chemische Industrie, H. Ziolkowsky GmbH, Düsseldorf, 1997, pp. 277–284.
[16] D. Schweizer, G. Dewald, Rheological evaluation of mortars containing cellulose ethers, in: C.A. Finch (Ed.), Industrial Water Soluble Polymers, Royal Society of Chemistry, Manchester, 1996, pp. 42–51.
[17] H. Yammamuro, T. Izumi, T. Mizunuma, Study of non-adsorptive viscosity agents applied to self-compacting concrete, 5th CANMET/ACI International Conference on Superplasticizers and Other Chemical Admixtures in Concrete, ACI SP-173, Detroit, 1997, pp. 427–444.
[18] A. Jenni, M. Herwegh, R. Zurbriggen, T. Aberle, L. Holzer, Quantitative microstructure analysis of polymer-modified mortars, J. Microsc. 212 (2003) 186–196.
[19] A. Jenni, R. Zurbriggen, M. Herwegh, L. Holzer, Changes in microstructures and physical properties of polymer-modified mortars during wet storage, Cem. Concr. Res. 36 (2006) 79–90.
[20] J. Desbrières, Cement cake properties in static filtration: Influence of polymeric additives on cement filter cake permeability, Cem. Concr. Res. 23 (1993) 347–358.
[21] J. Desbrières, Cement cake properties in static filtration. On the role of fluid loss control additives on the cake porosity, Cem. Concr. Res. 23 (1993) 1431–1442.
[22] C. Fringant, J. Desbrières, M. Milas, M. Rinaudo, C. Joly, M. Escoubes, Characterisation of sorbed water molecules on neutral and ionic polysaccharides, Int. J. Biol. Macromol. 18 (1996) 281–286.
[23] D. Bülichen, J. Plank, Formation Of colloidal polymer associates from hydroxyethyl cellulose (HEC) and their role to achieve fluid loss control ın oil well cement, SPE International Symposium on Oilfield Chemistry, The Woodlands/TX, SPE paper, 141182, 2011.
[24] D. Bülichen, J. Plank, Mechanistic study on carboxymethyl hydroxyethyl cellulose as fluid loss control additive in oil well cement, J. Appl. Polym. Sci. 124 (2012) 2340–2347.
[25] B. Franke, Bestimmung von Calciumoxyd und Calciumhydroxyd neben wasserfreiem und wasserhaltigem Calciumsilikat, Z. Anorg. Allg. Chem. 247 (1941) 180.
[26] L. Picton, L. Merle, G. Muller, Solution behavior of hydrophobically associating cellulosic derivatives, Int. J. Polym. Anal. Charact. 2 (1996) 103–113.
[27] J. Plank, B. Sachsenhauser, Experimental determination of the effective anionic charge density of polycarboxylate superplasticizers in cement pore solution, Cem. Concr. Res. 39 (2009) 1–5.
[28] Standard DIN 18555–7, Testing of Mortars Containing Mineral Binders; Part 7: Determination of Water Retentivity of Freshly Mixed Mortar by the Filter Plate Method, Deutsches Institut für Normung, 2000.
[29] EN 459–2, Building Lime — Part 2: Test Methods, European Committee for Standardization, 2010.
[30] American Petroleum Institute, API Recommended Practice 10B-2, 1st ed. American Petroleum Institute, Washington, 2005.
[31] W. Burchard, Static and dynamic light scattering from branched polymers and biopolymers, Adv. Polym. Sci. 48 (1983) 1–124.
[32] L. Schulz, W. Burchard, Lösungsstruktur verschiedener Cellulose-Derivate, Das Papier 47 (1993) 1–10.
[33] W. Burchard, Solubility and solution structure of cellulose derivatives, Cellulose 10 (2003) 213–225.
[34] P.G. de Gennes, Scaling Concepts in Polymer Physics, Cornell University Press, Ithaca, New York, 1979.
[35] H.-G. Elias, Macromolecules. Volume 3: Physical Structures and Properties, Wiley-VCH, Weinheim, Germany, 2008.

Publikation 4

Water Retention Capacity and Working Mechanism of Methyl Hydroxypropyl Cellulose (MHPC) in Gypsum Plaster – Which Impact has Sulfate?

Bülichen, D., Plank, J.

Cement and Concrete Research

accepted on 29th of January 2013

Water Retention Capacity and Working Mechanism of Methyl Hydroxypropyl Cellulose (MHPC) in Gypsum Plaster – Which Impact has Sulfate?

D. Bülichen, J. Plank*

Technische Universität München
Chair for Construction Chemicals
85747 Garching, Lichtenbergstrasse 4
Germany

*: Corresponding author
Tel.: +49 (0)89 289 13151
Fax.: +49 (0)89 289 13152
E-mail address: sekretariat@bauchemie.ch.tum.de (J. Plank).

Abstract

The water retention effectiveness of a commercial methyl hydroxypropyl cellulose (MHPC) sample (DS_{methyl} ~ 1.6, $MS_{hydroxypropyl}$ ~ 0.2, M_w = 419,000 g/mol) in cement paste and in a gypsum plaster was compared utilizing the filter paper test. It was found that the water retention capacity decreased significantly in the calcium sulfate system. Thus, higher dosages of MHPC were required in gypsum plaster to attain water retention values comparable to those in cement. This effect is well known from practical application.

To understand the impact of calcium sulfate on effectiveness and working mechanism of MHPC, its solubility, dynamic viscosity in cement and gypsum plaster pore solution, and the formation of MHPC associates as a function of sulfate concentration were analyzed. It was found that sulfate anions hinder the formation of colloidal associates which presents the key process to achieve water retention. This observation explains the higher dosages required in $CaSO_4$ systems.

Key words:

Water Retention (A), Calcium Sulfate (D), Admixture (D), Cement (D), Cellulose Ether

1. Introduction

In modern building products, water retention admixtures play an important role, particularly in dry-mix mortars such as e.g. wall renders and plasters based on mineral binders including lime, cement or gypsum [1]. Their main function is to prevent uncontrolled water loss into porous substrates such as brick, limestone and foamed concrete. Cellulose ethers dominate the market for water retention admixtures because of their favourable cost effectiveness and their environmental compatibility [2]. Major current applications of cellulose ethers include wall renders and plasters, joint compounds for gypsum wall boards, cementitious tile adhesives (CTAs), water-proofing membranes, floor screeds, self-levelling underlayments (SLUs) and self-compacting concrete [3]. In dry mortars, cellulose ethers serve to provide water retention, viscosity, anti-settling and sometimes air entraining properties, whereby some types can retard Portland cement hydration severely [4, 5]. Some studies investigated the effect of cellulose ethers on cement hydration in detail. One of the main findings was that the degree of substitution represents the key parameter relative to cement hydration, because it impacts the time period at which portlandite precipitation occurs [6, 7].

The most frequently used cellulose ethers are methyl hydroxyethyl cellulose (MHEC, also referred to as HEMC) and methyl hydroxypropyl cellulose (MHPC, also referred to as HPMC) [8-10]. MHEC is applied in self-levelling flooring compounds (SLCs) and cementitious tile adhesives (CTAs) while MHPC, because of its air-entraining effect stemming from the hydrophobic hydroxypropyl groups, is often used in wall renders and plasters [1]. Application dosages of cellulose ethers may range between 0.02 - 1.5 % by weight of binder, depending on the desired properties and the binder system. Remarkably, dosages in gypsum based formulations are commonly higher than in cementitious binder systems [3].

In recent studies we have already investigated the working mechanisms for water retention of methyl hydroxyethyl cellulose (MHEC), hydroxyethyl cellulose (HEC) and carboxymethyl hydroxyethyl cellulose (CMHEC) in cementitious systems [11-13]. It was found that at low dosages, MHEC achieves water retention by intramolecular sorption of water and concomitant swelling. The enormous water-binding capacity of polysaccharides in general has been described in an earlier study. By using a sorption balance and a microcalorimeter it was found that at the saturation level, neutral polysaccharides (e.g. amylose and amylopectin) can bind up to four water molecules per anhydroglucose unit [14]. However, at higher dosages, MHEC molecules agglomerate into large hydrocolloidal microgel particles ($d > 1$ µm) which effectively plug the pores in the mortar matrix [11]. Furthermore, the working mechanism of HEC relies on a dual effect, namely its enormous intramolecular water sorption (binding) capacity and a concentration dependent formation of hydrocolloidal associated polymer networks [12]. Contrary to this, the working mechanism of CMHEC changes with dosage. At low dosages (up to ~ 0.3 % by weight of cement), adsorption presents the predominant mode of action, whereas above a certain threshold concentration (the "overlapping" concentration), formation of associated polymer networks is responsible for its effectiveness [13]. Due to its comparable structure, chemical behavior and characteristic properties such as e.g. anionic charge or molecular weight, the working mechanism of MHPC in principle should resemble that of MHEC.

In the present study, the impact of sulfate on the effectiveness of MHPC as water retention admixture was investigated. More specifically, the concept for the working mechanism of methyl celluloses previously established in cementitious systems was checked for its validity in a gypsum binder system where elevated sulfate concentrations occur. For this purpose, the water retention effectiveness of MHPC in neat cement paste was compared with that in an industrial gypsum plaster. Moreover, to probe on the specific impact of sulfate, a cement paste

was dosed with additional amounts of alkali sulfate (Na_2SO_4) and the effects were studied. Furthermore, the solubility of MHPC in high sulfate environments and its dynamic viscosity in cement and gypsum plaster pore solution were measured. Finally, sulfate concentration-dependant hydrodynamic diameters (molecular sizes) of solved MHPC macromolecules were measured with the aim to clarify the working mechanism of MHPC as water retention agent under the influence of sulfate.

2. Materials and methods

2.1. Cement

This study was conducted using a CEM I 52.5 N sample ("Milke®" from HeidelbergCement AG, Geseke plant, Germany). Its properties are presented in Table 1. Composition of the cement was obtained by quantitative X-ray diffraction (Q-XRD) using a Bruker axs D8 Advance instrument (Bruker, Karlsruhe/Germany) with Bragg-Brentano geometry. Topas 4.0 software was employed to quantify the amounts of individual phases present in the sample by following *Rietveld's* method of refinement. The amounts of gypsum ($CaSO_4 \cdot 2\ H_2O$) and hemi-hydrate ($CaSO_4 \cdot 0.5\ H_2O$) were measured by thermogravimetry (STA 409 PC/PG from Netzsch, Selb/Germany). Free lime (CaO) was 0.1 wt.% as quantified following the extraction method established by Franke [15]. Using a Blaine instrument (Toni Technik, Berlin/Germany), the specific surface area was found at 3,316 cm^2/g. Specific density of the cement was 3.16 kg/L, as measured by Helium pycnometry (Ultrapycnometer® 1000 from Quantachrome Instruments, Boynton Beach, FL/USA). Particle size distribution was determined utilizing a laser-based particle size analyzer (CILAS 1064 instrument from Cilas, Marseille/France). Average particle size (d_{50} value) was 10 µm.

2.2. Gypsum plaster

A commercial industrial gypsum plaster (HASIT 130 Leichtglättputz, batch 03/2012, from Kissing plant) supplied by HASIT Trockenmörtel GmbH, Freising, Germany was used. The plaster was based on beta hemi-hydrate, hydrated lime, fine sand and a lightweight aggregate. To obtain a practical workability period of > 50 minutes, the plaster contained 2R, 3R-tartaric acid as retarder. Furthermore, for our study it was custom made without any water retention admixture (methyl cellulose) and anti-settling agent like e.g. modified guar ethers, xanthan

gum or polyacrylamides. This base render allowed us to incorporate MHPC as necessary and to study its effectiveness and working mechanism in a practical system. Note that most gypsum plaster formulations contain hydrated lime which was the reason for its selection here.

2.3. Methyl hydroxypropyl cellulose (MHPC)

A commercial sample of methyl hydroxypropyl cellulose (Tylose® MO 60016 P4, supplied by SE Tylose GmbH & Co KG, Wiesbaden, Germany) exhibiting a degree of substitution (DS_{methyl}) of ~ 1.6 and a molar degree of substitution ($MS_{hydroxypropyl}$) of ~ 0.2 was used (DS and MS terminology and values are supplier information). This sample was chosen for its performance characteristics (excellent water retention capability, immediate high viscosity development, and air-entraining effect) and because of its widespread use in the industry. Its characteristic properties are shown in Table 2. Particle size measurement produced a d_{50} value of 73 µm for the dry MHPC powder.

For determination of molar masses (M_w and M_n), polydispersity index and molecular size in solution ($R_{h(z)}$), size exclusion chromatography (Waters Alliance 2695 instrument) equipped with RI detector 2414 from Waters, Eschborn, Germany and an 18 angle dynamic light scattering detector (Dawn EOS from Wyatt Technology, Santa Barbara, CA/USA) was utilized. Prior to application on the columns, the 2 g/L MHPC solution was filtered through a 5 µm filter and separated on a precolumn and two Aquagel-OH 60 columns (Polymer Laboratories, distributed by Varian, Darmstadt, Germany). Eluent was 0.2 M aqueous $NaNO_3$ solution (adjusted to pH 9.0 with NaOH) pumped at a flow rate of 1.0 mL/min. The value of dn/dc used to calculate M_w and M_n was 0.159 mL/g (value for hydroxyethyl cellulose) [16].

155 The specific anionic charge amount of the polymer in cement pore solution was determined at
156 room temperature using a PCD 03 pH apparatus (BTG Mütek GmbH, Herrsching, Germany).
157 Charge titration was carried out according to a literature description employing a 0.001 N
158 solution of laboratory grade poly(diallyl dimethylammonium chloride) from BTG Mütek
159 GmbH, Herrsching, Germany as cationic polyelectrolyte [17]. The value presented is the
160 average obtained from three different measurements. Deviation of this method was found to
161 be ± 2 C/g.

162 Dynamic viscosities of cement and gypsum plaster pore solutions containing dissolved
163 MHPC polymer were determined on an Ubbelohde viscometer using 501 10/I, 501 20/II, 501
164 30/III, and 501 40/IV capillaries supplied by Schott Instruments, Mainz, Germany. 15 mL of
165 individual solutions were filled into the reservoir of the viscometer and the flow time was
166 measured. From this, the kinematic viscosity of the solution was calculated according to
167 equation 1.

168 $$\upsilon = K\,(t - \zeta) \qquad \text{equation 1}$$

169 Where K is the viscometer constant (0.1004 mm^2/s^2), t is the flow time and ζ is the flow time
170 dependant Hagenbach-Couette correction term which is provided in the instrument instruction
171 sheet. Multiplying the value for the kinematic viscosity with the specific density of the
172 solution produced the value for the dynamic viscosity η_{dyn}, as is expressed by equation 2.

173 $$\eta_{dyn} = \upsilon \cdot \rho \qquad \text{equation 2}$$

174 Hydrodynamic diameters (d_{50} value) of the MHPC polymer associates were measured in
175 aqueous Na_2SO_4 solution using a dynamic light scattering particle size analyzer (LB-550 from
176 Horiba, Irvine, CA/USA).

177

178

2.4. Preparation of binder pastes

For the water retention tests, cement and gypsum plaster pastes were prepared using Milke® cement CEM I 52.5 N and gypsum plaster, respectively, and deionized water. The pastes were mixed at water-to-binder ratios of 0.35, 0.53, and 0.7, respectively, using a blade type laboratory Waring blender (Torrington/CT, USA). 700 g of the binder and the respective amount of MHPC powder were dry-blended and homogenized. Within 15 seconds, the binder/polymer blend was added to the respective amount of DI water placed in the cup of the Waring blender and was mixed for 35 seconds at "low" speed (4,000 rpm). If present, sodium sulfate (anhydrous, fine powder, Ph.Eur., VWR International bvba/sprl, Leuven, Belgium) was dissolved prior to mixing in the DI mixing water. To ensure homogeneous consistency, all pastes were stirred and homogenized for 20 minutes at 25 °C in an atmospheric consistometer (Model 1250, Chandler Engineering, Broken Arrow/OK, USA).

2.5. Water retention test

Water retention effectiveness was determined using a modified version of the filter paper method which is specified in EN 495-2 (former DIN 18555-7) [18, 19]. In a typical experiment, 15 half-folded filter papers (size 240 mm x 105 mm from Einzinger, Munich, Germany) were covered with a tissue (Delicarta S.p.A., Porcari, Italy). Next, Vicat cone (70 x 80 x 40 mm) was placed on top of the stack, with the smaller diameter facing the bottom [11]. To establish the value for water retention, a paste was prepared using the procedure from section 2.4., filled into the Vicat cone exactly to the rim and levelled with a spatula. After a test period of 7.5 minutes during which water is sucked from the paste by the filter papers, both the Vicat cone holding the paste and the tissue were removed carefully from the stack of filter papers. The amount of water absorbed (w_{abs}) was determined from the difference in

weight between the stack of paper after and before exposure to the paste. From this, the value for water retention in % was calculated relative to the amount of mixing water contained in the paste placed in the Vicat cone (w_0), as presented in equation 3.

$$\text{water retention (\%)} = \left(1 - \frac{w_{abs}}{w_0}\right) \cdot 100 \qquad \text{equation 3}$$

2.6. Sulfate analysis

Sulfate concentrations present in cement and gypsum plaster pore solutions at a water-to-binder value of 0.53 were measured using ion chromatography (ICS-2000 apparatus from Dionex, Idstein, Germany). Here, the alkaline pore solutions were adjusted to pH 7 by adding 0.1M HCl.

2.7. Solubility of MHPC

The concentration of dissolved MHPC was determined via total organic carbon analysis using a High TOC II apparatus (Elementar, Hanau, Germany) equipped with a CO_2 detector. The amount of polymer in the supernatant was quantified after centrifugation. Maximum deviation of the concentration was found to be ± 0.1 g/L.

3. Results and discussion

3.1. Characteristic properties of MHPC sample

The representative chemical structure of a MHPC exhibiting a DS (methyl) of 2.0 and an MS (hydroxypropyl) of 0.5 is presented in Fig. 1. Size exclusion chromatography (SEC) produced molar masses of $4.2 \cdot 10^5$ g/mol (M_w) and of $2.6 \cdot 10^5$ g/mol (M_n), respectively (Table 2). Using static light scattering, a hydrodynamic radius $R_{h(z)}$ of 26.6 nm and a radius of gyration $R_{g(z)}$ of 87 nm were found for this polymer. From this data, the Burchard parameter $\rho = R_{g(z)} / R_{h(z)}$ which describes the solved conformation of macromolecules was calculated [20, 21]. According to this, a value of 3.3 which corresponds to a polymer architecture of stiff chains was obtained [22]. In alkaline cement pore solution (pH ~ 12.8), the MHPC sample exhibited an almost negligible specific anionic charge amount of – 8 ± 2 C/g, as measured by charge titration employing polyDADMAC as cationic counter polymer [17]. According to this value, MHPC is practically non-ionic in cement pore solution.

3.2. Performance in cement and gypsum plaster

3.2.1. Cementitious system

At increasing dosages of MHPC, water retention of neat cement pastes exhibiting a water-to-binder ratio of 0.53 was measured at 25 °C. Increased amounts of MHPC produce higher water retention, as is shown in Fig. 2. At a dosage of only 0.2 % bwoc (by weight of cement), MHPC achieved a water retention of 98.5 % which is considered adequate for cement-based renders. Water retention converges asymptotically to ~ 99.8 % at a dosage of 0.6 % bwoc of MHPC. There, the cement paste becomes too viscous to apply.

3.2.2. Gypsum plaster

Next, effectiveness of MHPC in an industrial gypsum plaster paste was examined and compared with that from the neat cement paste. At the beginning, comparable water retention values for the neat cement and gypsum plasters (no MHPC present) were adjusted by selecting the appropriate w/b ratios for each system, as shown in Table 3. Thus, to obtain initial water retention values between 86 and 88 %, the w/b value required for the cement paste was 0.35, while for the gypsum plaster 0.7 was found. Subsequently, both systems were tested with respect to their water retention capacity at MHPC additions of 0.1 – 0.6 % by weight of binder (bwob) as presented in Fig. 3.

The cementitious system immediately showed strong response to MHPC addition. High water retention values of 98.2 % at 0.1 % bwob of MHPC and 98.8 % at 0.2 % bwob were achieved. Contrary to this, in the gypsum plaster a dosage of 0.1 % bwob of MHPC produced a water retention of 90.9 % only. To obtain acceptable values, a dosage of 0.2 % bwob (water retention: 98.4 %) is required in the gypsum plaster. This signifies that at MHPC dosages of $\leq$ 0.2 % bwob, its water retention capacity is less in gypsum plaster than in cement. While at a dosage of 0.3 % bwob, both systems attained values of > 99 % and thus became comparable.

These findings demonstrate that in a sulfate-based binder system, higher amounts of MHPC are needed to attain comparable effectiveness. Gypsum plaster is based on highly soluble beta hemi-hydrate binder and therefore can be expected to exhibit a significantly higher sulfate concentration in its pore solution than the cement paste. To ascertain this, the concentrations of dissolved sulfate present in both systems were determined at a constant water-to-binder (w/b) ratio of 0.53 using ion chromatography. Following this method, a sulfate concentration of 4.29 g/L was obtained for the cement pore solution while 5.83 g/L were found in the gypsum plaster pore solution. This result signifies that in the gypsum plaster, the

concentration of dissolved sulfate is ~ 30 % higher than in the cementitious system. From this data it was hypothesized that sulfate ions may negatively impact the performance of MHPC. To investigate, effectiveness of MHPC in a sulfate-enriched cement paste was probed as a next step.

3.3. Impact of sulfate on MHPC

3.3.1. Effectiveness in sulfate-enriched cement paste

To determine the impact of sulfate on MHPC performance in cement, its water retention effectiveness at 0.1 % bwoc MHPC in the presence of increased amounts of Na_2SO_4 was measured. Cement pastes holding 0 – 9.65 g/L of sulfate were tested at 25 °C applying the filter paper test. To establish conditions comparable to those in the gypsum plaster, a w/c ratio of 0.70 was chosen.

The results are presented in Fig. 4. They clearly demonstrate the negative impact of sulfate on MHPC effectiveness. Additions of only 2.4 g/L of sulfate significantly decreases the water retention capacity of MHPC from ~ 95 to ~ 92 %. Note that this additional amount of sulfate roughly corresponds to the differences in the SO_4^{2-} concentrations occurring in cement paste (~ 4.3 g/L) and gypsum plaster (~5.8 g/L). At further increased sulfate concentrations, water retention continues to decline and attains a minimum value of 90.7 % at 4.8 g/L of sulfate added. Thereafter, a slight increase occurred whereby a final value of ~ 91 % water retention capacity is measured at ~ 10 g/L of sulfate. The results confirm that sulfate can perturb the effectiveness of MHPC as water retention agent.

3.3.2. Working mechanism in $CaSO_4$ systems

As shown in an earlier study, the working mechanism of methyl hydroxyethyl cellulose as water retention agent in cement relies (a) on its water sorption capacity and (b) on the formation of hydrocolloidal associated 3D polymer networks [11]. MHPC is assumed to behave similarly, whereby the formation of associated polymer networks above a certain threshold ("overlapping") concentration is most important. The associates are critical for effective water retention in the binder matrix [23].

The negative impact of sulfate on MHPC performance might be owed to a solubility problem of MHPC in the pore solution loaded with electrolytes. In particular, sulfate may decrease the water solubility of MHPC which constitutes a non-ionic polymer. For this purpose, solubility of MHPC in the presence of sulfate ions was probed. 3.77 g/L MHPC (this concentration corresponds to a dosage of 0.2 % bwob at a w/b value of 0.53) were dissolved in water and a total organic carbon content of 1.8 g/L was measured. When this solution was contaminated with sodium sulfate, a white precipitate occurred at concentrations beyond ~ 30 g/L of sulfate. Based on TOC analysis, the precipitate was identified as MHPC. Thus, MHPC clearly becomes less soluble at very high sulfate concentrations.

Nevertheless, this precipitation phenomenon cannot explain the decreased effectiveness of MHPC since a sulfate concentration of 30 g/L is ~ five times higher than that occurring in an actual gypsum plaster pore solution. To probe further into the impact of sulfate on the working mechanism of MHPC, dynamic viscosities in cement and gypsum plaster pore solution as well as the occurrence of MHEC associates in the presence of sulfate were determined.

3.3.2.1. Dynamic viscosity

Generally, cellulose ethers viscosify aqueous or mineral binder pore solutions in dependence of their concentration. Their effectiveness strongly depends on the molecular weight, chain length and stiffness of the polymer. The MHPC sample selected for this study was a type which develops high viscosity very rapidly, as would be required for a machinery plaster.

Here, the dynamic viscosities of cement and gypsum plaster pore solutions containing increasing concentrations (0.5 – 8 g/L) of MHPC were measured at 25 °C. The results are presented in Fig. 5. At low MHPC concentrations (≤ 4 g/L), for both systems a comparable minor increase in viscosity was observed. For example, at 4 g/L MHPC the dynamic viscosity of the cement pore solution was 53 mPa·s and 59 mPa·s in the gypsum plaster pore solution. However, beyond this concentration, in cement pore solution the dynamic viscosity increased more rapidly than in the $CaSO_4$ system, e.g. at 6 g/L MHPC to 254 mPa·s vs. 129 mPa·s in the gypsum system. This signifies that in cement pore solution, the critical threshold concentration (designated as "overlapping" concentration 1 in Fig. 5) which signifies the beginning formation of polymer associates from MHPC has been reached. Opposite to this, in the gypsum plaster pore solution, higher concentrations of MHPC were necessary to initiate polymer association. The most significant viscosity change occurs between 6 and 8 g/L ("overlapping" concentration 2 in Fig. 5) where the dynamic viscosity increases from 129 to 623 mPa·s. In a control experiment, 1.5 g/L sulfate were dosed to the cement pore solution, to adjust the SO_4^{2-} concentration present in the gypsum pore solution which holds ~ 6 g/L of sulfate. There, the dynamic viscosity of the cement pore solution dropped to 135 mPa·s which is practically the same value as in the $CaSO_4$ pore solution (129 mPa·s). This experiment demonstrates that the sulfate concentration determines viscosity, and not the type of binder from which the pore solution was produced.

The results indicate that in cement and gypsum based systems, MHPC molecules associate and develop 3D networks at significantly different concentrations. In $CaSO_4$ systems, higher MHPC dosages were required to achieve association. This effect can be assigned to the higher sulfate concentration present in the gypsum plaster pore solution. It infers that MHPC is hindered by sulfate in its early associative behavior and thus requires higher dosages to become effective in water retention.

3.3.2.2. Polymer association

To proof whether MHPC association is in fact hindered, sulfate dependent hydrodynamic diameters (molecular sizes) of MHPC macromolecules in the "overlapping" region were determined at 25 °C, using dynamic light scattering technique. Fig. 6 exhibits only the portion of large MHPC particles present in aqueous solutions of 4 and 6 g/L MHPC containing 2, 4, 6, 8, 12 and 14 g/L of sulfate. In all measurements, smaller particles were found as well but were not included here due to the fact that only large particles are indicative for MHPC association. The complete curves are shown in the appendix to this paper.

Generally, the largest particles detected in this experiment possessed a hydrodynamic diameter of ~ 300 nm which is typical for beginning overlapping of the molecules [12]. In a 4 g/L MHPC solution (this dosage was found to achieve 98 % water retention in cement), relatively low sulfate concentrations of 2 and 4 g/L do not change the size of the MHPC associates much. Note that 4.3 g/L was the sulfate concentration found in the cement pore solution. However, when the sulfate concentration was increased to 6 and 8 g/L, a significant decrease in particle size to very small diameters (~ 10 nm) occurred. While at 6 g/L MHPC (this corresponds to ~ 0.3 % bwob in the gypsum plaster) the particle size was only marginally affected by sulfate concentrations up to 8 g/L. However, particle size decreased

374 rapidly when the sulfate concentration was higher at 10 – 14 g/L. Note that in the gypsum
375 plaster, the SO_4^{2-} concentration was ~ 6 g/L only. Consequently, this experiment signifies that
376 when sulfate is present, higher concentrations of MHPC are required to form those large
377 associates. These particles are responsible for the water retention capacity of MHPC. The
378 result explains why higher dosages of MHPC are required in $CaSO_4$-based systems.

379 A potential explanation for the decreased association is a decrease in hydrogen bridging
380 between MHPC strains. In aqueous solution, cellulose ethers have been shown to attain the
381 conformation of "fringed micelles" whereby parts of the molecule are amorphous, hydrated
382 and dissolved as individual strains while in other parts, the strains are aligned parallel via
383 hydrogen bridging and form micellar subunits [22]. Here, one can assume that the increased
384 electrolyte content owed to the presence of larger amounts of sulfate decreases the polarity in
385 the OH groups present in the cellulose ether as a result of the higher ionic strength of the
386 solution. In such case, hydrogen bridging will be reduced and association of the cellulose
387 ether molecules will require higher MHPC dosages to achieve a sufficient bonding strength.
388 Similar observations were made for poly(ethylene oxide) and poly(vinyl alcohol) in the
389 presence of 0.5 – 2.0 M NaCl. There, a significant decrease in viscosity of the polymer
390 solutions was found which was attributed to partial disruption of hydrogen bonds [24, 25].

391

392 **4. Conclusion**

393

394 From previous research it is known that the working mechanism of methyl cellulose is based (a)
395 on its water sorption capacity and (b) on the formation of hydrocolloidal associated 3D networks
396 above the "overlapping" concentration. High water retention effectiveness is only achieved at
397 cellulose ether dosages at which these 3D networks are formed.

Cement or gypsum release different amounts of sulfate into their respective pore solutions. Those different sulfate concentrations influence the effectiveness of MHPC considerably. It was found that in a gypsum plaster, MHPC requires higher dosages to achieve the same water retention as in a cement-based system. Thus, at ~ 4 g/L of sulfate (this represents the SO_4^{2-} concentration in cement paste), only 0.2 % bwob of MHPC are required whereas in the $CaSO_4$ plaster (sulfate concentration ~ 6 g/L), 0.3 % bwob of cellulose ether are needed to achieve the same water retention value. The underlying mechanism is that sulfate ions hinder the formation of large colloidal associates from MHPC which effectively plug the pores in the binder matrix and thus achieve water retention. The mechanism behind this interaction is hindrance of the association of MHPC strains, possibly owed to higher ionic strength in the pore solution. This model is supported by the observation that NaCl also reduces the water-retention capacity of the MHPC sample, although on a comparable molar basis, its effect is less than that from Na_2SO_4. This suggests that ionic strength is the main parameter here. Consequently, higher dosages of MHPC are required to form a sufficient amount of associates which can provide the desired effect.

Sulfate is known to perturb the fluidizing effect of polycarboxylates which present an important group of concrete admixtures. There, the effect is owed to competitive adsorption between sulfate and polycarboxylate whereby both anionic species attempt to occupy the surfaces of hydrating cement. Here, it is shown that sulfate also negatively impacts the performance of another group of admixtures, the cellulose ethers. Surprisingly, this divalent anion can impact admixtures even stronger than the divalent Ca^{2+} cation.

The results reported here were developed using a specific MHPC sample in a common plaster formulation. However, two additional industrial MHPC products obtained from different suppliers experienced a similar negative impact from sulfate. Also, when using the MHPC sample studied here in another gypsum plaster received from a second source, again a large influence of sulfate on MHPC performance was detected. Those findings confirm that the trend observed for the MHPC product chosen here can be generalized.

More generally, the study demonstrates that relatively simple parameters (here: the concentration of dissolved sulfate) can severly perturb the effectiveness of costly additives. The reason behind is that those admixtures work on molecular level. Any factor which impacts e.g. their molecular conformation, steric size, ionic charge, solubility, etc. can interfere with their working mechanism and decrease their performance.

Acknowledgments

The authors wish to thank H. Klehr from SE Tylose GmbH, Wiesbaden, for generously providing the cellulose ether sample and T. Lipp from HASIT Trockenmörtel GmbH for producing the gypsum plaster.

436 **References**

437

438 [1] H. Lutz, R. Bayer, Dry Mortars, in: Ullmann's Encyclopedia of Industrial Chemistry,
439 Wiley-VCH Verlag GmbH & Co. KGaA, Weinheim, 2010, pp. 1-41.

440 [2] J.A. Grover, Methylcellulose and its derivatives, in: R.L. Whistler, J.N. BeMiller (Eds.)
441 Industrial Gums, Academic Press, San Diego, 1993, pp. 475-504.

442 [3] J. Plank, Applications of Biopolymers in Construction Engineering, in: A. Steinbüchel
443 (Ed.) Biopolymers, Wiley-VCH, Weinheim, 2003, pp. 29-95.

444 [4] I. Müller, D. Schweizer, W. Hohn, D. Bosbach, A. Putnis, H. Weyer, B. Schmitt,
445 Influence of Cellulose Ethers on the Kinetics of Early Portland Cement Hydration, GDCh-
446 Monographie Band 36 (2006) 3-10.

447 [5] J. Pourchez, P. Grosseau, B. Ruot, Current understanding of cellulose ethers impact on the
448 hydration of C_3A and C_3A-sulphate systems, Cem Concr Res, 39 (2009) 664-669.

449 [6] J. Pourchez, A. Peschard, P. Grosseau, R. Guyonnet, B. Guilhot, F. Vallée, HPMC and
450 HEMC influence on cement hydration, Cem Concr Res, 36 (2006) 288-294.

451 [7] J. Pourchez, B. Ruot, J. Debayle, E. Pourchez, P. Grosseau, Some aspects of cellulose
452 ethers influence on water transport and porous structure of cement-based materials, Cem
453 Concr Res, 40 (2010) 242-252.

454 [8] H. Thielking, M. Schmidt, Cellulose Ethers, in: Ullmann's Encyclopedia of Industrial
455 Chemistry, Wiley-VCH Verlag GmbH & Co. KGaA, Weinheim, 2006, pp. 1-18.

456 [9] R. Dönges, Non-Ionic Cellulose Ethers, Brit Polym J, 23 (1990) 315-326.

457 [10] A. Jenni, L. Holzer, R. Zurbriggen, M. Herwegh, Influence of polymers on
458 microstructure and adhesive strength of cementitious tile adhesive mortars, Cem Concr Res,
459 35 (2005) 35-50.

460 [11] D. Bülichen, J. Kainz, J. Plank, Working Mechanism of Methyl Hydroxyethyl Cellulose
461 (MHEC) as Water Retention Agent, Cem Concr Res, 42 (2012) 953-959.

462 [12] D. Bülichen, J. Plank, Role of Colloidal Polymer Associates for the Effectiveness of
463 Hydroxyethyl Cellulose as a Fluid Loss Control Additive in Oil Well Cement, J Appl Polym
464 Sci, 126 (2012) E25–E34.

465 [13] D. Bülichen, J. Plank, Mechanistic Study on Carboxymethyl Hydroxyethyl Cellulose as
466 Fluid Loss Control Additive in Oil Well Cement, J Appl Polym Sci, 124 (2012) 2340-2347.

467 [14] C. Fringant, J. Desbrières, M. Milas, M. Rinaudo, C. Joly, M. Escoubes, Characterisation
468 of sorbed water molecules on neutral and ionic polysaccharides, Int J Biol Macromol, 18
469 (1996) 281-286.

470 [15] B. Franke, Bestimmung von Calciumoxyd und Calciumhydroxyd neben wasserfreiem
471 und wasserhaltigem Calciumsilikat, Z Anorg Allgem Chem, 247 (1941) 180.

472 [16] L. Picton, L. Merle, G. Muller, Solution Behavior of Hydrophobically Associating
473 Cellulosic Derivatives, Int J Polym Anal Ch, 2 (1996) 103-113.

474 [17] J. Plank, B. Sachsenhauser, Experimental determination of the effective anionic charge
475 density of polycarboxylate superplasticizers in cement pore solution, Cem Concr Res, 39
476 (2009) 1-5.

477 [18] DIN 18555-7, Testing of Mortars Containing Mineral Binders; Part 7: Determination of
478 Water Retentivity of Freshly Mixed Mortar by the Filter Plate Method, Deutsches Institut für
479 Normung, 2000.

480 [19] EN 459-2, Building lime - Part 2: Test methods, European Commitee for
481 Standardization, 2010.

482 [20] W. Burchard, Static and Dynamic Light Scattering from Branched Polymers and
483 Biopolymers, Adv Polym Sci, 48 (1983) 1-124.

484 [21] L. Schulz, W. Burchard, Lösungsstruktur verschiedener Cellulose-Derivate, Das Papier,
485 47 (1993) 1-10.

[22] W. Burchard, Solubility and Solution Structure of Cellulose Derivatives, Cellulose, 10 (2003) 213-225.

[23] P.G. de Gennes, Scaling concepts in polymer physics, Cornell University Press, Ithaca, New York, 1979.

[24] B. Briscoe, P. Luckham, S. Zhu, Rheological Study of Poly(ethylene oxide) in Aqueous Salt Solutions at High Temperature and Pressure, Macromol, 29 (1996) 6208-6211.

[25] B. Briscoe, P. Luckham, S. Zhu, The effects of hydrogen bonding upon the viscosity of aqueous poly(vinyl alcohol) solutions, Polym, 41 (2000) 3851-3860.

Table 1: Phase composition (Q-XRD, Rietveld), specific density, specific surface area (Blaine) and d_{50} value of cement sample CEM I 52.5 N.

C_3S (wt. %)	C_2S (wt. %)	C_3A_c (wt. %)	C_3A_o (wt. %)	C_4AF (wt. %)	free CaO (wt. %)	$CaSO_4 \cdot 2\ H_2O$ (wt. %)	$CaSO_4 \cdot 0.5\ H_2O$ (wt. %)	$CaSO_4$ (wt. %)	specific density (kg/L)	specific surface area Blaine (cm^2/g)	d_{50} value (µm)
62.9	20.4	3.9	3.3	2.3	0.1	3.5 *	2.0 *	2.1	3.16	3,316	10 ± 1.0

***** measured by thermogravimetry.

Table 2: Characteristic properties of the MHPC sample.

molar masses (g/mol)		polydispersity index (M_w/M_n)	hydrodynamic radius $R_{h(z)}$ (nm)	radius of gyration $R_{g(z)}$ (nm)	specific anionic charge amount ε (C/g)*
M_w	M_n				
419,000	258,000	1.6	27	87	8 ± 2

***** measured in cement pore solution

Table 3: Comparison of the water retention capacity of MHPC in cement and gypsum plaster.

binder and admixture system	water-to-binder ratio	water retention capacity (%)
cement	0.35	86.5
cement + 0.1 % bwob MHPC	0.35	98.2
cement + 0.2 % bwob MHPC	0.35	98.8
cement + 0.3 % bwob MHPC	0.35	99.3
gypsum plaster	0.7	88.8
gypsum plaster + 0.1 % bwob MHPC	0.7	90.9
gypsum plaster + 0.2 % bwob MHPC	0.7	98.4
gypsum plaster + 0.3 % bwob MHPC	0.7	99.2

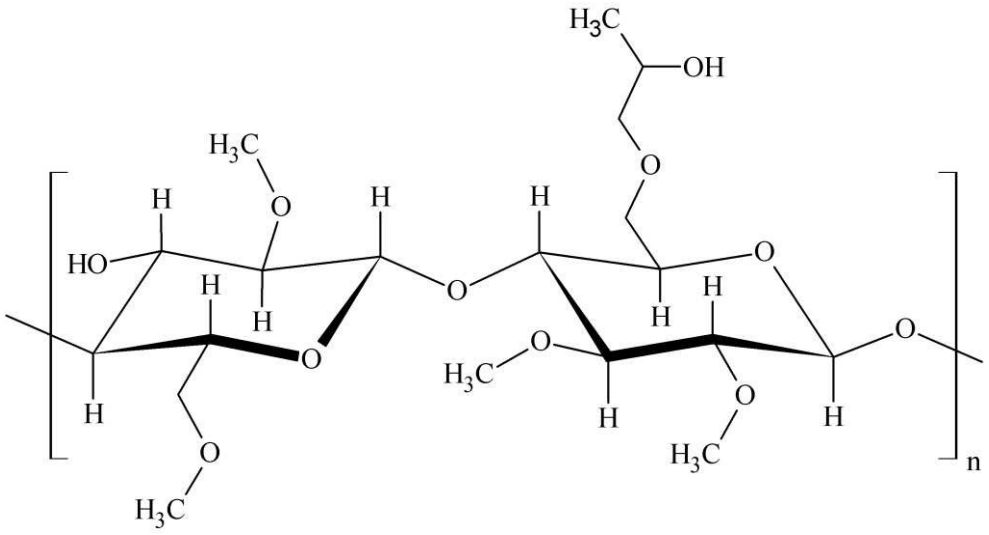

Fig. 1. Chemical structure of methyl hydroxypropyl cellulose exhibiting a DS (methyl) of 2.0 and an MS (hydroxypropyl) of 0.5.

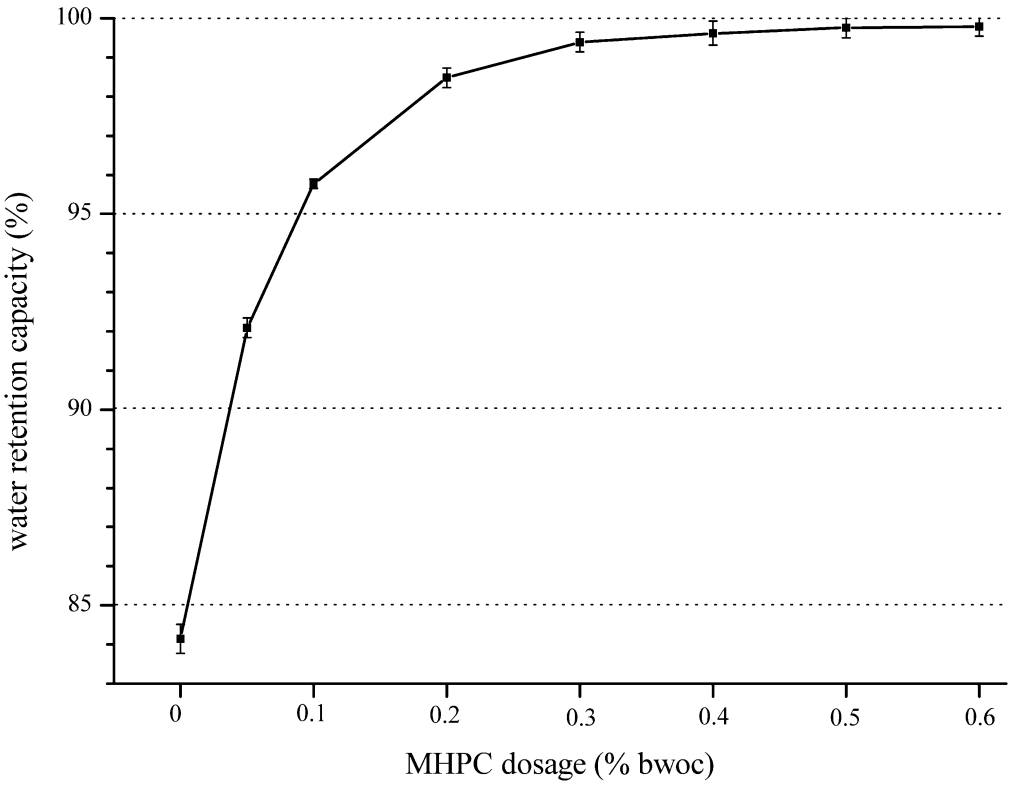

Fig. 2. Water retention capacity of MHPC in cement (w/c = 0.53) as a function of polymer dosage.

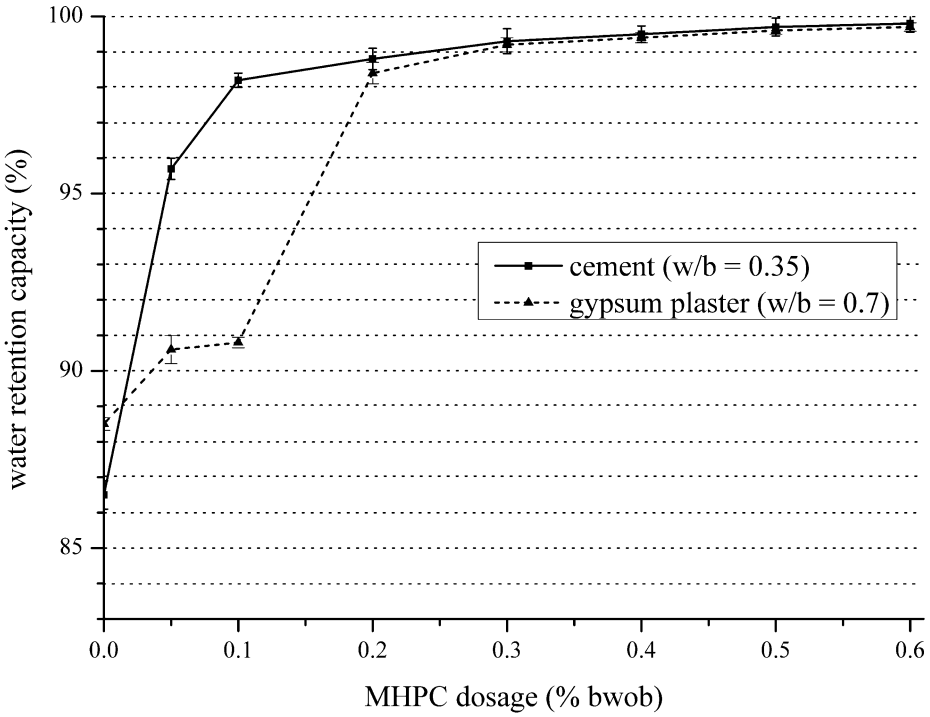

510

511 **Fig. 3.** Water retention capacity of MHPC in cement and gypsum plaster at water-to-binder

512 ratios of 0.35 (cement) and 0.7 (gypsum plaster) as a function of polymer dosage.

513

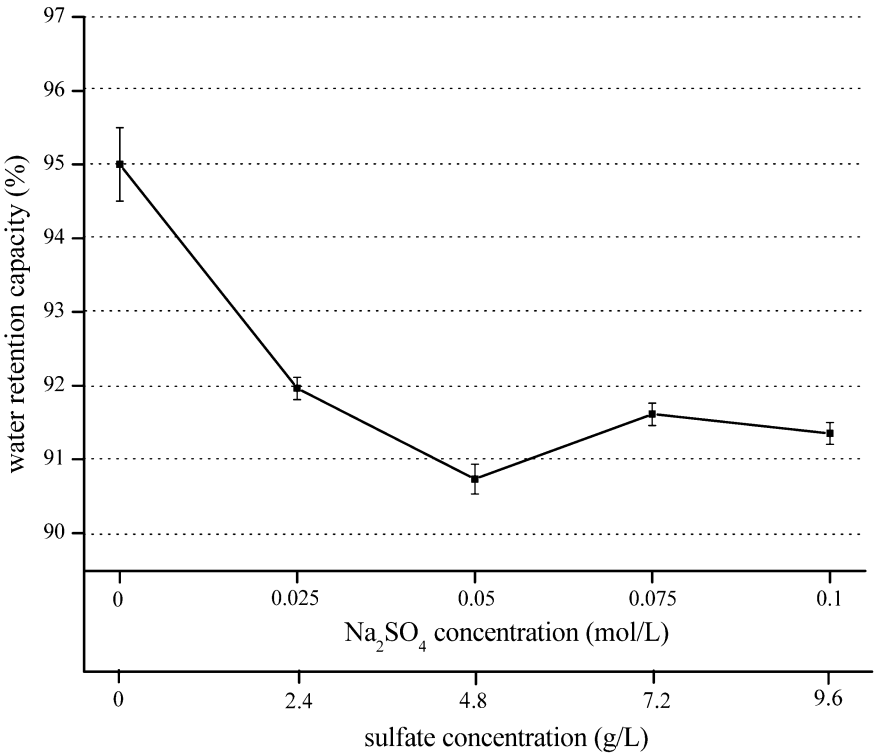

514

515 **Fig. 4.** Water retention capacity of 0.1 % bwoc of MHPC in cement paste (w/c = 0.7) as a

516 function of the amount of sodium sulfate added.

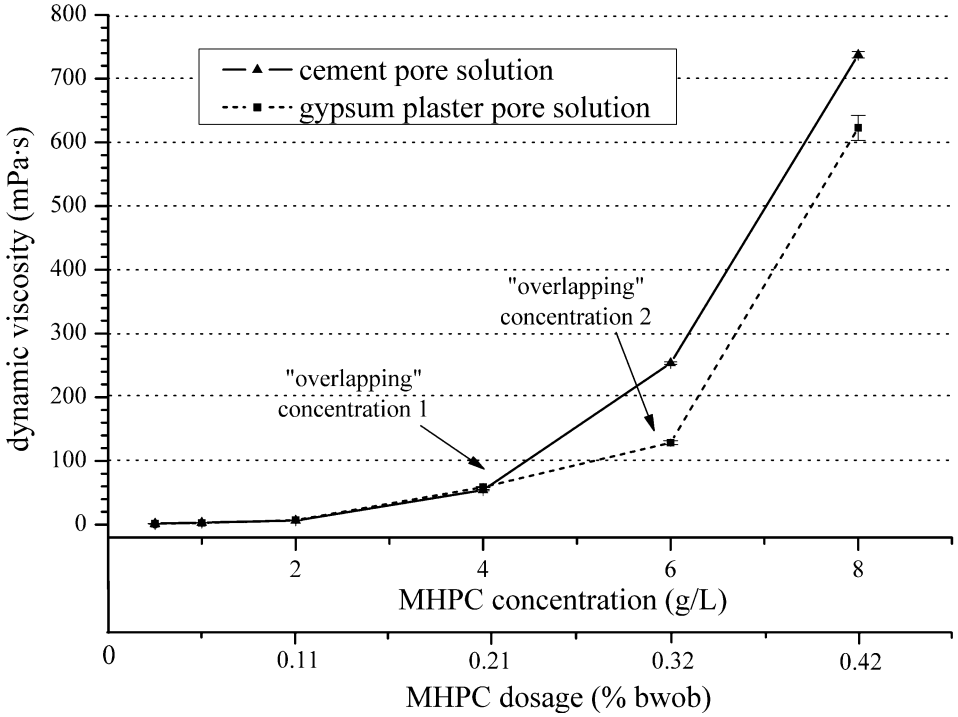

517

518 **Fig. 5.** Dynamic viscosity of pore solutions from cement and gypsum plaster, respectively,

519 containing different additions of MHPC.

520

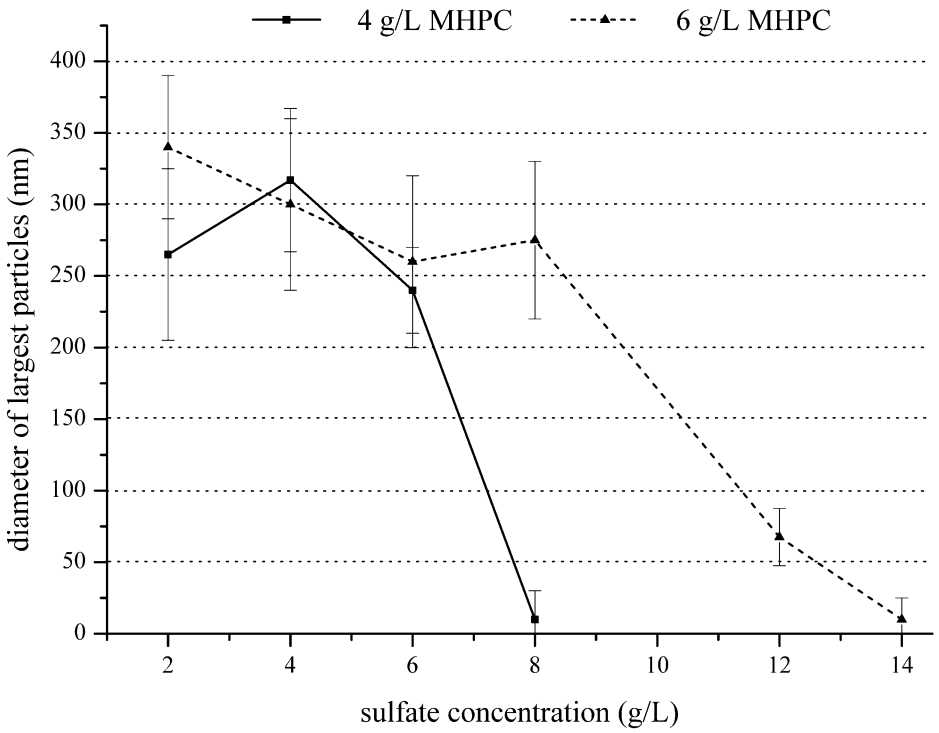

521

522 **Fig. 6.** Hydrodynamic diameter of the portion of large MHPC particles present in DI water at

523 different sulfate concentrations, as measured by dynamic light scattering.

524 **Appendix**

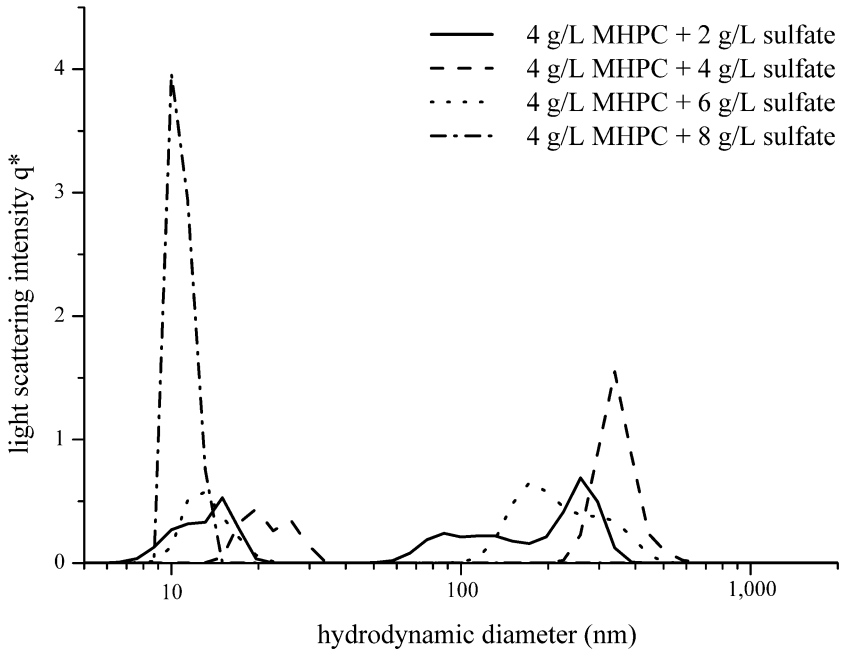

525

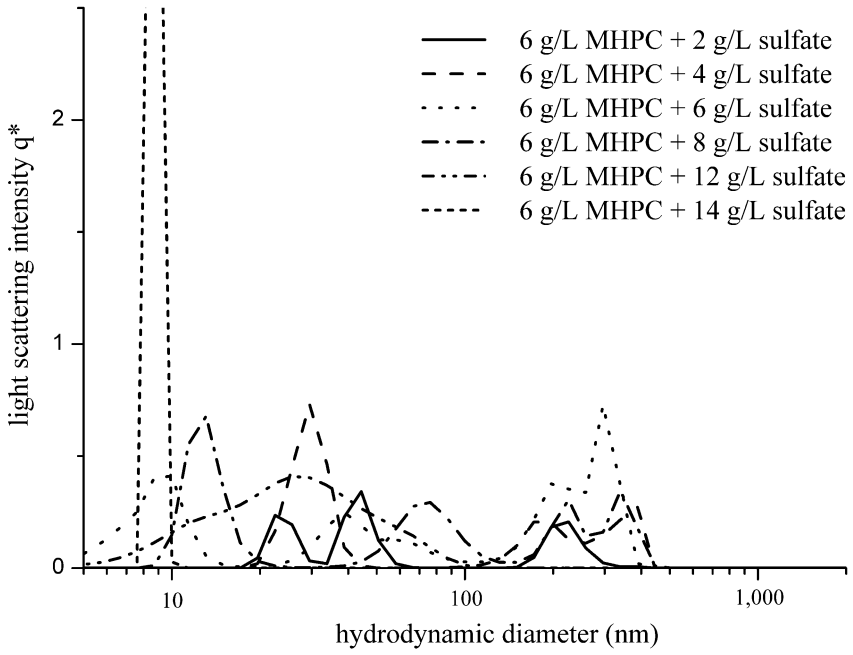

526

527 Profiles of hydrodynamic diameters of MHPC particles present in DI water at different

528 MHPC and sulfate concentrations, as measured by dynamic light scattering.